T-PM-Sym-1 THE STRUCTURE OF NUCLEIC ACID DUPLEXES IN SOLUTION. Brian Reid, Dept. of Chemistry, University of Washington, Seattle, WA 98195.

T-PM-Sym-2 DETERMINATION OF PROTEIN AND PEPTIDE CONFORMATIONS IN SOLUTION. Peter E. Wright, Department of Molecular Biology, Research Institute of Scripps Clinic, 10666 North Torrey Pines Road, La Jolla, California 92037.

It is now possible to determine three-dimensional solution structures for proteins of 100 or more amino acids from constraints derived from two-dimensional NMR spectroscopy. A prerequisite to structure determination is assignment of the ^1H NMR spectrum of the protein. It is desirable that proton assignments be as complete as possible if high quality structures are to be obtained. We have devised an integrated assignment strategy which relies upon both relayed coherence transfer and multiple quantum spectroscopy to yield complete proton assignments. Constraints on interproton distances are obtained from 2D NOE spectra and dihedral angle constraints are obtained from coupling constants, both for backbone and sidechains. Three-dimensional structures are calculated using distance geometry methods and are optimized using energy minimization and restrained molecular dynamics. For larger proteins, not all of the resolved cross peaks in NOESY spectra can be unambiguously identified because of spectral overlap. Many of the ambiguities can be resolved by back calculation from the initial three-dimensional structures. Factors which affect the quality of NMR structures, including the importance of stereospecific assignments, will be discussed. Examples of structure determination for plastocyanin (99 residues) and thioredoxin (108 residues) will be presented. Two-dimensional NMR experiments also provide a powerful approach to determination of the conformational preferences of linear peptide fragments of proteins in aqueous solution. Folded structures, in rapid dynamic exchange with unfolded states, have now been identified in several linear peptides. Such structures are believed to play an important role in initiation of protein folding and in induction of protein-reactive antipeptide antibodies.

T-PM-Sym-3 INTERNAL MOTIONS AND PROTEIN CONFORMATION AS STUDIED BY NMR, Gerhard Wagner, University of Michigan

During the last couple of years two-dimensional NMR procedures have been developed which allow determination of protein conformations in solution. These techniques require nearly complete assignments of the proton spectrum and collection of a large number of conformational parameters, such as distance constraints and dihedral angle constraints. Molecular models that are consistent with these constraints are then constructed with suitable distance geometry algorithms. The resulting structures show a certain variability which is usually expressed root mean square distance (rmsd). This variability may be due to imprecise data, to an incomplete data set and to internal mobility, respectively. We have concentrated on these three aspects of structure analysis and developed methods for precise measurements of intramolecular distances, we have applied novel techniques to get access to new classes of conformational constraints, and we have developed techniques to characterize internal mobility. The latter techniques include measurements of individual relaxation times for all backbone CH carbons, and various two-dimensional heteronuclear experiments for characterization of multiple conformations. Using these methods we have detected, for example, that there are multiple conformations localized around the reactive site of a protease inhibitor.

T-PM-Sym-4 ISOTOPE-FILTERED PROTON NMR OF MACROMOLECULES. Alfred G. Redfield, Departments of Physics and Biochemistry, Brandeis University, Waltham MA 02254. Modern molecular biology permits facile production of biopolymers enriched at classes of sites with 15N, 13C, or deuterons. The latter can be observed directly, used as a negative proton label, or be used to improve resolution by general partial enrichment. 13C and 15N can also be observed directly, but newer methods use 15N, for example, to observe 15NH (amide) groups by detecting proton signals directly while using 15N as a perturbant via spin-spin interaction with the attached proton. This interaction is about 10x larger than proton-proton spin spin interactions, making these methods feasible in larger molecules, perhaps up to 100 kDa. NOE can be wedded to these methods, as 1D to 3D experiments, to retain NOE's only from protons on 15N. This, together with the dispersion provided by 2D to separate resonances, makes assignments and distance estimates possible in these larger systems, and clarifies other experiments such as proton solvent exchange, by decreasing the density of the data set. Proteins up to 20 kDa may be fully assignable by these methods, but for larger molecules local sites of interest can be targeted without full identification, using multiple labels and mutants. Examples will be presented from work on T4 lysozyme in collaboration with L. McIntosh and F. Dahlquist and others, and on N-ras p21 protein by S. Campbell Burk.

T-PM-Min-1 HORMONAL REGULATION OF ION CURRENTS VIA G PROTEINS. Paul Sternweis, Dept. of Pharmacology, University of Texas Health Science Center, Dallas, TX 75235-9040.

T-PM-Min-2 REGULATION OF M CURRENT IN SYMPATHETIC GANGLION CELLS BY G PROTEIN-COUPLED RECEPTORS. Bertil Hille, Paul J. Pfaffinger, Mark D. Leibowitz, Martha M. Bosma. Dept. of Physiology and Biophysics, University of Washington, Seattle, WA 98195.

The M-current is a K current that is suppressed by muscarinic agonists and by LHRH and substance P (SP) (Adams and Brown, Br. J. Pharmacol. 68:353, 1980; Adams et al., Br. J. Pharmacol. 79:330, 1983). In frog lumbar sympathetic ganglion cells under whole-cell clamp these three agonists suppress M-current and induce an overrecovery (rebound) of the M-current, and the two peptides induce homologous desensitization of their receptors. We have been interested in the G-protein(s) and possible second messengers underlying these effects. AlF_4^- and GTPγS in the pipette can suppress M-current spontaneously, and with low concentrations of GTPγS, agonists suppress M-current irreversibly (Pfaffinger, J. Neurosci. 8:3343, 1988). The G protein is not pertussis toxin sensitive. Agonists do induce phosphoinositide turnover and intracellular Ca transients; however these seem not to be important for the electrophysiological actions on M-current (Pfaffinger et al., Neuron 1:477, 1988). A modest decrease of M-current and a fast desensitization of SP receptors can be induced with phorbol esters and diacylglycerol analogs; nevertheless, both M-current suppression and homologous peptide receptor desensitization are readily induced by agonists when protein kinase C is inhibited by H7, staurosporine, or a regulatory-site directed peptide. We therefore do not believe that Ca, IP_3, or protein kinase C are essential intermediates in coupling these receptors to M-current or in homologous desensitization of the peptide receptors. Supported by NS08174, GM07170, MDA, and FESN. MDL is a FESN scholar in "Transduction of Neuronal Signals."

T-PM-Min-3 REGULATION OF ION CHANNELS BY G-PROTEINS IN CARDIAC MYOCYTES. Gabor Szabo, Department of Physiology & Biophysics, University of Texas Medical Branch, Galveston, TX 77550.

T-PM-Min-4 AGONIST-DEPENDENT AND AGONIST-INDEPENDENT REGULATION OF G PROTEIN-K^+ CHANNEL SYSTEM IN HEART. Y. Kurachi, T. Nakajima, H. Itoh and T. Sugimoto. The 2nd Department of Internal Medicine, University of Tokyo, Tokyo 113, Japan

Molecular mechanisms underlying acetylcholine (ACh)-activation of cardiac K^+ channel were examined in single atrial myocytes of guinea pig. Electrophysiological studies using patch clamp techniques revealed that G proteins, whose functions are inhibited by pertussis toxin, couple muscarinic ACh and adenosine receptors to a K^+ channel in the cardiac cell membrane. Activation of G proteins by intracellular GTP analogues has an absolute requirement for intracellular Mg^{2+}. During activation with GTP and Mg^{2+}, G proteins may be dissociated into their subunits (α-GTP,$\beta\gamma$). Reconstitution experiments using purified subunits from brain showed that both subunits can activate the K^+ channel. Activation model of the K^+ channel by G protein subunits will be discussed.

Recently, we found that lipoxygenase metabolites of arachidonic acid stimulate the G protein-K^+ channel system in the absence of agonist-binding to the receptors. This agonist-independent pathway to activate the G protein-K^+ channel system may be important in various physiological and pathophysiological conditions of the heart.

T-PM-Min-5 EFFECTS OF ISOPROTERONOL AND INTRACELLULARLY APPLIED PROTEASES ON CARDIAC L-TYPE CHANNELS. W. Trautwein, II. Physiologisches Institut, 6650 Homburg/Saar, F.R.G.

In guinea pig ventricular myocytes beta-adrenergic agonists increase the amplitude of the L-type Ca current 3-4 fold by increasing the open probability of the Ca channel due to phosphorylation by the cAMP-dependent protein kinase. The intracellular cascade involved can be traced by intracellular administration of cAMP or catalytic subunit of the kinase. Ca channels (Dihydropyridine binding sites) reconstituted in bilayers do also increase their open probability when phosphorylated by C subunit of the kinase. Interventions which block the cascade like intracellular application of protein kinase inhibitor or Rp cAMPS suppress the response of the agonist. Also intracellular dialysis of non-hydrolizable ATP-analogues do strongly depress the current. In the absence of beta-adrenergic stimulation cell dialysis with ATPγS or endogenous phosphatase inhibitor or occadaic acid (a phosphatase inhibitor) increase the Ca current. These agents do also amplify the effect of low agonist concentrations. Phosphatase I and IIa, intracellularly applied, abolish the effect of Isoproterenol on the Ca current.
Effects very similar to those of beta-adrenergic stimulation are observed on intracellular application of Trypsin or Carboxypeptidase. Both enzymes increase the amplitude of the Ca current by a factor of 3-4 without a change in threshold and apparent reversal potential. Later in the course of the experiment, Trypsin, but not Carboxypeptidase, does also prolong the inactivation of the current. We assume that Endopeptidases or Carboxypeptidase cleave from the C terminus the regulatory site of the channel and thereby open the gate permanently. A similar effect could be achieved by a conformational change of the regulatory site due to phosphorylation.

T-PM-Min-6 G PROTEINS, THEIR RECEPTORS AND EFFECTORS. L. Birnbaumer, A. Yatani, R. Mattera, A. VanDongen, R. Graf, Z. Zhou and A. M. Brown. Departments of Cell Biology, Physiology and Molecular Biophysics, and Medicine, Baylor College of Medicine, Houston, Texas 77030.

About 80 receptors for neurotransmitters, peptide and protein hormones, and auto- and paracrine factors are coupled to effector systems by G proteins. Until recently effector systems were few: adenylyl cyclase, phospholipase C and A_2 and phosphodiesterases, and all were concerned with regulation of an also small number of "classical" second messengers: cyclic nucleotides, inositol polyphosphates and diacylglycerol. Everything followed from there. The discovery in late 1986 that ionic channels could also be under direct regulation by G proteins has increased the number of effector systems, first by one, the inward rectifying K^+ channels of heart and endocrine cells, and then by a second, the dihydropyridine-sensitive Ca^{2+} channels of heart and skeletal muscle. This indicated that membrane potential has to be added as a primary target of G protein regulation and should be treated as a second messenger system. Using both purified G proteins activated with GTPγS and recombinant α subunits (rG.'s) made in bacteria we concentrated recently on four questions raised by previous studies: 1. are K^+ channels specific for one G_i; 2. are there more ionic channels under direct G protein control? 3. can we confirm using rGα's the results obtained with biochemically resolved Gα's and continue ascribing the regulatory effector to this part of the $\alpha\beta\gamma$ holo-G protein? and 4. can we confirm that a single G., $G_s\alpha$ in this case, is able to affect more than one type of effector function? We found $G_i\alpha$'s are isoforms, that there are G_i-insensitive, G_o reponsive K^+ channels and that Gα's can be multifunctional. Thus, a single receptor will elicit cellular responses that will depend on the endogenous G protein as well as the type of effector function expressed in it.

Tu-PM-A1 Tetrodotoxin Blocks Late Na^+ Currents in Early Embryonic Chick Ventricular Myocytes, by I.R. Josephson and N. Sperelakis, Dept. of Physiology and Biophysics, Univ. of Cincinnati College of Medicine, Cincinnati, OH 45267. Single ventricular myocytes were dissociated from 3-day-old embryonic chick hearts and maintained in culture for 9-21 hr. The whole-cell patch voltage clamp method was used to record membrane current. The density of the tetrodotoxin (TTX)-sensitive fast Na^+ current recorded at this early stage of development was about 10 times smaller than that of older embryonic or adult heart. The peak Na^+ current recorded at -20 mV ranged from 10 to 70 $\mu A/cm^2$. The current-voltage relationship, steady-state inactivation, and time course of the Na^+ currents were similar to the older embryonic (and adult) hearts. One feature found in the early embryonic Na^+ current was that, at more negative potentials, a significant component decayed very slowly, resulting in a steady-state or late Na^+ current. The origin of the late Na^+ current was revealed through the examination of single Na^+ channel currents recorded in outside-out membrane patches. The single Na^+ channel conductance was 20 pS. It was found that an unusually high percentage of the trials (~ 16%) displayed multiple re-openings of a single Na^+ channel, resulting in bursts of current lasting for $\geq$ 150 msec. The frequency distributions of the Na^+ channel open-times were bi-exponential. The burst mode of Na^+ channel activity, which underlies the slowly-or non-inactivating currents recorded macroscopically, was more sensitive to block by TTX, compared to the early current. The results suggest that a TTX interaction with the channel leading to its closure is enhanced when the Na^+ channel protein conformation is in the bursting mode. Supported by an NIH grant to N.S. and an AHA grant (Southwest Chapter) to I.J.

Tu-PM-A2 VOLTAGE- AND pH-DEPENDENCE OF RECOVERY FROM USE-DEPENDENT BLOCK OF Na CHANNELS BY LOCAL ANESTHETICS. Jay Z. Yeh and Joëlle Tanguy. Dept. of Pharmacol., Northwestern Univ. Med. Sch., Chicago, IL 60611 and Lab Neurobiologie Ecole Normale Superieure, Paris, France.

The physico-chemical properties of the channel-bound tertiary amine drugs were investigated by comparing the effect of changing external or internal pH on the recovery at rest from use-dependent block of Na channels caused by repetitive depolarizing pulses in the presence of quaternary (RAC 421) and tertiary amine (RAC 109) enantiomers internally applied to voltage-clamped squid axons. With RAC 421s, changing external pH(pH_o) did not appreciably affect the time constant of recovery (τ_r) or its voltage dependence (V_{rec}), suggesting that external H^+ ion does not titrate the receptor site for the applied drug. RAC 421-I had τ_r 5-6 times larger than RAC 421-II while both exhibited an identical V_{rec}: 12-13 mV hyperpolarization caused an e-fold increase in τ_r. In contrast, pH_o strongly affected τ_r and its V_{rec} with RAC 109s. As pH_o was increased from 6.8 to 9.5, the τ_r became smaller, with τ_r for RAC 109-I being 5-6 times larger than RAC 109-II at -80 mV. At $pH_o <$ 7, RAC 109s (pK_a = 9.4) exist virtually in the cationic form, yet their V_{rec} was less steep than that of RAC421s. If the difference in τ_r at low pH_o is to reflect the dissociation of the cationic drug molecule from the channel through the hydrophilic pathway as with RAC421s, the pK_a of the channel-bound RAC 109s might be different from that in the bulk solution. At $pH_o > 8.5$, V_{rec} of RAC 109-I disappeared whereas that of RAC 109-II remained the same. This difference in τ_r at high pH_o is interpreted to reflect mainly the difference in the dissociation of neutral molecule from the channel through a hydrophobic pathway. Internal pH changes had minimal effect on τ_r, suggesting that internal H^+ ion does not gain access to the channel-bound drug molecule as easily as the external H^+ ion. Supported by NIH grant GM-24866.

Tu-PM-A3 BLOCK OF SINGLE CARDIAC Na CHANNELS BY LIDOCAINE AND QUINIDINE. **Paul B. Bennett,** Department of Pharmacology, Vanderbilt University, Nashville, TN.

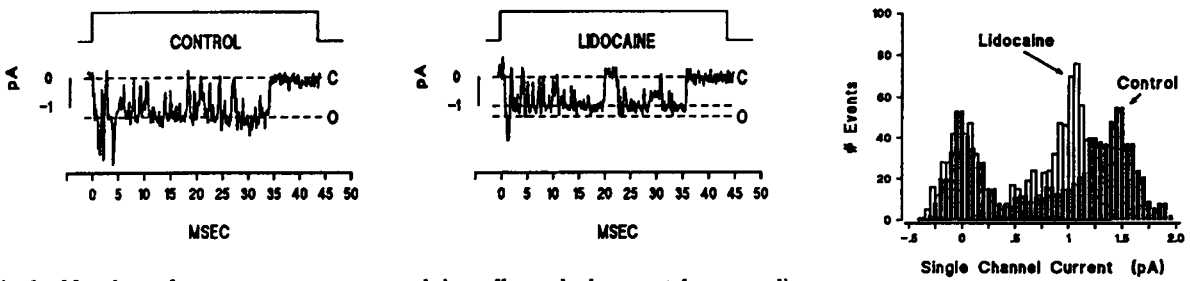

Single Na channel currents were measured in cell-attached neonatal rat cardiocytes using standard patch clamp methods. Pipettes contained (mM) : 140 NaCl, 5 CsCl, 2 4 AP, 5 TEA-Cl, 2 $CaCl_2$, 10 HEPES. Cell resting membrane potentials were eliminated with 140 mM external KCl. Na channels exhibited multiple modes of gating : mostly channels opened briefly (τ_{open}=0.6 msec) and inactivated; occasionally they failed to inactivate and flickered for prolonged periods (> 10 msec; mode 0). Neither quinidine nor lidocaine (L) reduced the single channel current (i) of the normal brief openings. L (30 μM) could reduced i of the mode 0 openings, but this was not observed in every case, suggesting that lidocaine may only block open Na channels if they spend sufficient time in an open state, and if lidocaine is available to bind when the channel enters mode 0.

Tu-PM-A4 MODULATION OF CARDIAC Na CHANNELS BY β-ADRENORECEPTORS AND THE G-PROTEIN, G_s. B. Schubert‡*, A.M.J. VanDongen‡, G.E. Kirsch‡ and A.M. Brown‡. ‡Department of Physiology and Molecular Biophysics, Baylor College of Medicine, One Baylor Plaza, Houston, TX 77030; *Division of Cellular and Molecular Cardiology, Central Institute for Cardiovascular Research, Academy of Sciences of the GDR, Berlin-Buch, GDR.

The action of the β-adrenergic agonist Isoproterenol (ISO) on Na^+ channels was studied in single ventricular myocytes of neonatal rat using the gigaseal patch clamp technique. ISO at 40 μM had no effect on whole-cell Na^+ currents when the holding potential (HP) was -90 mV. However, at HP of -60 mV ISO decreased Na^+ current amplitude by about 50%. The inhibition was greatly diminished when the patch pipette contained 2 mM GDPβS instead of 500 μM GTP, indicating the involvement of a guanine nucleotide binding (G) protein. In cell-free inside-out patches addition of the non-hydrolyzable GTP analog, GTPγS at 40 μM to 400 μM decreased averaged single channel Na^+ currents. The G Protein G_s, the stimulatory regulator of adenylyl cyclase purified from human erythrocytes and preactivated with GTPγS (G_s^*) at 100 pM, mimicked the inhibitory effects of GTPγS. The effect was specific since neither human erythrocyte G_k^*, the activator of muscarinic K^+ channels, nor a partially purified preparation of bovine brain G_o^* produced inhibition. We conclude that ISO inhibits cardiac Na^+ channels via G_s and that G_s may act directly (membrane delimited) and/or indirectly by cytoplasmic second messengers. The results are relevant to arrhythmias during myocardial ischemia when cells are partially depolarized due to an increased extracellular K^+ concentration and catecholamine concentration is increased. (Supported by NIH grants HL36930 and HL37044.) Sponsored by A.E. Lacerda.

Tu-PM-A5 ANGIOTENSIN II AND PHORBOL ESTER MODULATE CARDIAC SODIUM CHANNELS IN NEONATAL RAT. J.R. Moorman, G.E. Kirsch, A.M. Brown. Dept. of Medicine, University of Texas Medical Branch, Galveston TX; Dept. of Physiology and Molecular Biophysics, Baylor College of Medicine, Houston, TX.

We examined the effects of angiotensin II (AII) and the protein kinase C (PKC) activating phorbol ester 12-O-tetradecanoylphorbol-13-acetate (TPA) on Na^+ channels in neonatal rat ventricular myocytes. We studied single channel Na^+ currents in cell-attached patches to avoid loss of intracellular substances required for response (Lacerda et al., Nature 335, 1988). K^+-depolarization was used to set the membrane potential to near 0 mV, and hyperpolarizing prepulses were used to remove resting inactivation. AII at 250 nM and TPA at 200 nM increased the peak probability of channel opening and decreased the frequency of late reopenings, resulting in increased and more rapidly decaying average Na^+ currents. Drugfree patches showed no significant change with time in either peak average current or decay time constant. 4α phorbol, which does not activate PKC, had no effect on peak current or decay time constant (n=4). Pretreatment with TPA at 200 nM but not 4α phorbol at 100 nM blocked the response to AII (n=4 each). At saturating concentrations, AII increased the peak average current by about 2-fold at test potential -50 mV. Single channel conductance and mean open time were unchanged, and latency to first opening fell after AII. TPA produced a 50% or greater increase in current in 2 of 6 experiments and faster current decay in all experiments. We conclude AII and TPA modulate cardiac Na^+ channels via second messengers. This kind of Na^+ channel modulation may be important in genesis and treatment of cardiac arrhythmias associated with chronic congestive heart failure syndromes. Supported by KL01858 and the Sealy Endowment (JRM), AHA 876197 (GEK), HL36930 and 37044 (AMB).

Tu-PM-A6 STEREOSPECIFICITY OF A LOCAL ANESTHETIC RECEPTOR IN BTX-ACTIVATED NA CHANNELS. G.K. Wang, Dept. of Anesthesia Research Labs, Harvard Medical School and Brigham and Women's Hospital, Boston, MA 02115

The stereochemical property of a local anesthetic (LA) receptor in skeletal muscle BTX-activated Na channels was examined in planar bilayers using 200 mM NaCl symmetrical conditions. Both the on-rate and off-rate kinetics were measured when the LA drugs had a dwell time of more than 30 ms. Otherwise, the averaged current amplitude was determined. The results show that the structure of the LA receptor appears highly stereospecific. For example, cocaine(-) has a dissociation constant (K_d) of 80 μM at +50 mV whereas cocaine(+) has a K_d of 3.2 mM. Unlike cocaine(-), which induces long lasting block with a dwell time of ~400 ms at +50 mV, cocaine(+) elicits an apparent current noise in a manner similar to that produced by QX-314. The dwell time of cocaine(+) was estimated to be less than 30 ms at +50 mV. Consistent with this result, the structure of the LA receptor appears to differentiate all the stereoisomers that we tested, including bupivacaine(+,-), mepivacaine(+,-), RAC109(I,II) and RAC421(I,II). Preliminary data indicate that this stereospecificity of the LA receptor in BTX-activated Na channels is also preserved in other Na channel preparations. Both the brain and cardiac BTX-activated Na channels exhibit similar stereochemical properties, thus suggesting that the structure of the LA receptor is conserved in various types of Na channels. **Supported by NIH-GM35401.**

Tu-PM-A7 PURIFIED, MODIFIED NA CHANNELS ARE ACTIVE IN PLANAR BILAYERS IN THE ABSENCE OF BTX

S. Shenkel, E. C. Cooper, W. S. Agnew and F. J. Sigworth. Dept. of Cellular & Molecular Physiology, Yale Univ. School of Medicine, New Haven, CT 06510.

The effects of certain proteases and chemical agents on purified-reconstituted Na channels have previously been studied with a combination of radiotracer flux assays and SDS/PAGE (Cooper et al., 1987. PNAS 84). Here, aliquots of vesicles containing Na channels purified from E. electricus electroplax were incubated with trypsin (5ug/ml; 5 min) or NBS (5uM; 10 min) and fused with decane/phospatidylethanolamine (25 mg/ml) bilayers in the absence of batrachotoxin (BTX). The most prominent conductance was about 40pS (400mM NaCl). Channels were not seen without prior exposure to trypsin or NBS. The figure shows records (400mM Na cis/100mM Na trans) at three different pulse potentials (mV). Openings occurred in bursts separated by closed intervals lasting many seconds. The fraction of time spent open within a burst was a function of voltage with increasing P_o with stronger depolarizations. Saxitoxin (300nM) appears to block the 40pS channel events, as does QX-314 (50% block at 300uM and 95% at 1mM; +95mV) when applied to the opposite ("intracellular") surface of the protein.

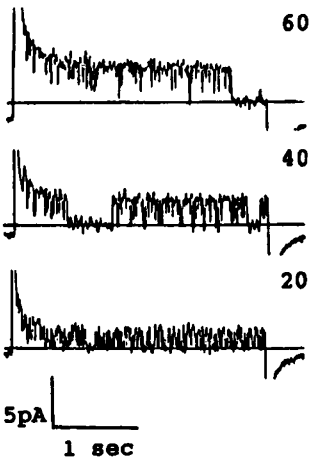

Tu-PM-A8 FUNCTIONAL EXPRESSION OF A CLONED RAT SKELETAL MUSCLE Na CHANNEL IN Xenopus OOCYTES

J.Zhou,[2] J.S.Trimmer, W.S.Agnew, M.B.Boyle[1], S.S.Cooperman[2], R.H. Goodman[2], G.Mandel[2] & F.J.Sigworth. Dept. of Cellular and Molecular Physiology, Yale Sch. of Med., New Haven, CT 06510; [1]Dept. Physiol. and Biophys., Univ. of Iowa; and [2]Division of Molecular Medicine, Tufts-New England Medical Center.

Messenger RNAs synthesized from two distinct full-length cDNA clones (top Fig.) encoding a denervated rat skeletal muscle Na channel were injected into Xenopus oocytes. Our initial two-microelectrode voltage clamp experiments show Na-dependent, voltage-gated currents expressed from each clone. Although the cDNAs were isolated from a tissue which expresses toxin-resistant Na channels, these currents are blocked by low concentrations of TTX ($k_{1/2}$ = 10nM) and μ-conotoxin ($k_{1/2}$ = 8nM). The rates of activation and inactivation (τ_h = 7.4 ms at -10 mV, 20°C; bottom Fig.) are slower than those of currents in oocytes injected with rat skeletal muscle poly-A^+ mRNA and than those reported for rat brain Na channel II.

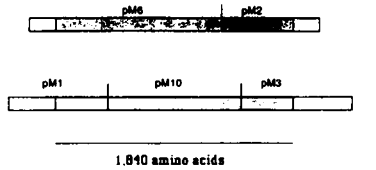

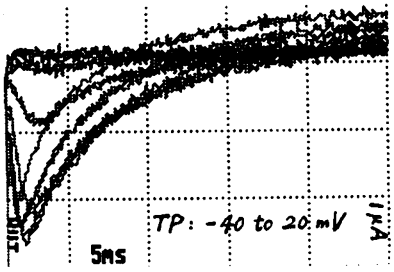

Tu-PM-A9 STRUCTURAL MODELS OF VOLTAGE-ACTIVATED POTASSIUM, SODIUM, AND CALCIUM CHANNELS

H. Robert Guy and G. Raghunathan, Lab. Math. Biology, NCI, NIH, Bethesda, MD 20892

Earlier models of the sodium channel (Guy and Seetharamulu 1986 PNAS 83:508) have been modified and extended to include the type A potassium (Temple, et al. 1987 Science 237:770) and dihydropyridine receptor calcium channels (Tanabe, et al. 1987 Nature 328:313). All homologous repeating units of our models have similar backbone structures for the transmembrane regions. A cross-sectional view of the model we currently favor is shown below. Circles are transmembrane α helices labeled S1 - S6 according to Noda et al.(1984 Nature 312:121). Short segments SS1 and SS2 span only part of the membrane. These correspond to S6 and S7 of Guy and Seetharmulu (1986) and F and G helices of the Greenblatt et al. (1985, FEBS Letters 193:125) sodium channel models, and H5 of the Temple et al. (1987) potassium channel model. In our scheme negatively charged SS2 β strands (in black) form the selectivity filter. SS's are well conserved among channels of the same type (e.g., sodium channels) but are poorly conserved among homologous repeats or channel types. Most residues that differ among sodium channels and between fly and rat potassium channels are on the exterior where they can be in contact with lipid. Charges of the putative gating domain formed by S1-S4 are well conserved among all homologous repeats and channel types. We have developed a computer graphics representation of the potassium channel model and are using the CHARMM program to obtain an energy refined version of this model.

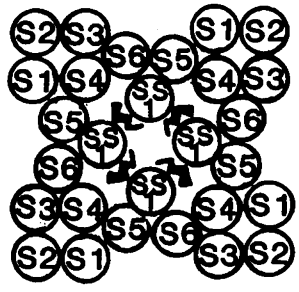

Tu-PM-A10 IDENTIFICATION OF PHOSPHORYLATION SITES ON THE EEL SODIUM CHANNEL BY DIRECT AMINO ACID SEQUENCING OF TRYPTIC PHOSPHOPEPTIDES. M.C. Emerick and W.S. Agnew (intr. by W.H.Martin) Dept. of Cellular and Molecular Physiology, Yale School of Medicine. New Haven, CT 06510

The sodium channel of *Electrophorus electricus* is a substrate for cyclic-AMP-dependent protein kinase (PKA) (Emerick & Agnew [1988] *Biophys. J. 53*, 539a). Brief exposure of purified sodium channels to PKA and [^{32}P]-ATP, followed by exhaustive trypsin cleavage and separation of the resulting tryptic peptides by reverse-phase HPLC revealed seven phosphopeptides. Each of the three major phosphopeptides was separated from contaminating species on a second reverse-phase HPLC dimension, and direct sequence determination by automated Edman degradation using an Applied Biosystems gas-phase sequencer showed them to be derived from regions close to the terminal domains of the channel protein: two amino-terminal (Ser-6 and Thr-17) and one carboxy-terminal (Ser-1776). The C-terminal region has been shown by immunostaining to be cytoplasmic (Gordon, *et al.* [1987] *PNAS, USA 84*, 308) and the N-terminus is predicted to be so based on the absence of a signal peptide (Noda, *et al.* [1984] *Nature, 312*, 121). Our results contrast with studies of rat brain sodium channels, which have been shown to be phosphorylated at multiple but as yet unidentified sites within a 190-amino acid region between homology domains I and II (Rossie, *et al.* [1987] *JBC, 262*, 17530). such a region, which contains five consensus PKA phosphorylation sites, is not present in the electroplax channel. Conversely, the electroplax sequence has three such consensus PKA sites on the amino terminus, two shown here to be good substrates for the enzyme, which are absent in the homologous brain channel sequences. These differences between sodium channels from different sources, in the clustering of consensus phosphorylation sites and in the pattern of phosphorylation, may reflect differences in the role of phosphorylation in regulating the expression and/or function of the two types of sodium channels.

Tu-PM-B1 BINDING OF PROTEOLYTIC FRAGMENTS OF CALDESMON TO MYOSIN AND TROPOMYOSIN. Eisaku Katayama*, Kurumi Y. Horiuchi* and Samuel Chacko, Faculty of Medicine, University of Tokyo, and University of Pennsylvania, Philadelphia, PA 19104.

Caldesmon binding to actin in the absence of Ca^{2+}-calmodulin inhibits the actin-activated ATPase of phosphorylated smooth muscle myosin. Recent studies have shown that the tropomyosin and heavy meromyosin also bind to caldesmon. In this investigation, we studied the binding of chymotryptic fragments of caldesmon to tropomyosin and myosin. Effects of fragments which bound to tropomyosin or myosin affinity columns on the actin-activated myosin ATPase were determined. The molecular weight of the major component of the caldesmon fragment bound to tropomyosin and myosin affinity columns were 80 k dalton. Small amounts of fragments of 60 k and lower molecular weights were also bound to these affinity columns. However, the C-terminal fragment (40k or its break down products) which has been shown to bind to actin and calmodulin did not bind to either tropomyosin or myosin affinity columns. This fragment bound to actin and actin-tropomyosin and it inhibited the actin-activated ATPase in the presence or absence of tropomyosin. Fragments which bound to tropomyosin, myosin or heavy meromyosin affinity columns failed to bind to actin-tropoymosin and they had no effect on the ATPase. Based on these data, we propose that the caldesmon exerts its effect on actomyosin ATPase through the binding of the C-terminal region to actin filaments. Supported by NIH grants HL 22264 and DK 3970.

Tu-PM-B2 STRUCTURE AND EXPRESSION OF MYOSIN HEAVY CHAIN GENE IN SMOOTH MUSCLE. Muthu Periasamy, Philip Babij and Ryozo Nagai, (Intr. by D. Maughan) Dept. of Physiology and Biophysics, Univ. of Vermont.

We previously reported the characterization of a rabbit uterus cDNA clone (SMHC-29) which encoded part of the light meromyosin (LMM) of smooth muscle myosin heavy chain (Nagai et al, Proc. Natl. Acad. Sci. USA (1988) 85:1047-51). We have now characterized a second cDNA clone (SMHC-40) which also encodes part of the LMM but differs from SMHC29 in the following respects. Nucleotide sequence analysis demonstrates that the two MHC mRNA's are identical over 1422 nucleotides but differ in part of the 3' carboxyl coding region and a portion of the 3' non-translated sequence. Specifically, SMHC40 cDNA encodes a unique stretch of 44 amino acids at the carboxyl terminus, whereas SMHC 29 cDNA contains a shorter carboxyl terminus of 10 unique amino acids which is the result of a 39 nucleotide insertion. Recent peptide mapping of smooth muscle myosin heavy chain identified two isotypes with differences in the light meromyosin fragment and were designated as SM1 (205 KDa) and SM2 (200 KDa) type myosin (Eddinger and Murphy, Biochemistry (1988), 27:3807-3811). Our results indicate that SMHC40 cDNA and SMHC29 cDNA resemble SM1 and SM2 type myosin respectively. Based on nucleotide sequence information of SMHC40 and SMHC29 cDNAs, we propose that the two smooth muscle MHC mRNA isotypes are the products of a single gene. The two types of SMHC mRNAs are coexpressed in all types of smooth muscle cells from vascular and nonvascular tissues so far examined.

Tu-PM-B3 MONOCLONAL ANTIBODIES DETECT AND STABILIZE CONFORMATIONAL STATES OF SMOOTH MUSCLE MYOSIN. Kathleen M. Trybus, Larry Henry and Susan Lowey. Rosenstiel Basic Medical Sciences Research Center, Brandeis University, Waltham, MA 02254.

Monoclonal antibodies directed against epitopes both in the head region and along the rod of avian smooth muscle myosin have been isolated and characterized. Two antibodies distinguish between the folded and extended conformational states of smooth muscle myosin. Anti-rod antibody 5D11, localized to the HMM/LMM hinge, binds approximately 100-fold more strongly to myosin in the folded than the extended state as determined by solution competition ELISA. Complementary behavior is shown by the anti-S2 antibody 6C11.2, which reacts preferentially with myosin in the extended state. The effect of the antibodies on myosin filament assembly was also determined. 2E8.1 IgG, which binds to the tip of the tail, depolymerizes filaments in the absence of nucleotide. Three antibodies that localize to the central region of the rod (1A6.1, 3H9.1, and 6C11.2) bind to synthetic filaments with a 14 nm periodicity, and prevent disassembly to the folded conformation upon addition of MgATP. These antibodies allow one to investigate the relationship between enzymatic activity and phosphorylation for a given conformational state without changing solvent conditions. The ATPase activity of antibody-stabilized dephosphorylated filaments could therefore be determined in the steady state and by single-turnover experiments. The results suggest that when both dephosphorylated and phosphorylated myosin are filamentous, a high degree of regulation of the actin-activated ATPase activity can be obtained by changes in light chain phosphorylation. (Supported by NIH grants HL38113 and AR17350.)

Tu-PM-B4 KINETICS OF CONTRACTION IN TONIC AND PHASIC SMOOTH MUSCLE INITIATED BY FLASH PHOTOLYSIS OF CAGED ADENOSINE TRIPHOSPHATE, K. Horiuti, A.V. Somlyo, Y.E. Goldman & A.P. Somlyo, PA Muscle Institute & Dept. of Physiology, Univ. of PA Medical School, Phila., PA 19104 and Dept. of Physiology, Univ. of Virginia, Charlottesville, VA 22908.

Laser flash photolysis of caged adenosine triphosphate (ATP) was used to examine the time course of isometric force development from rigor states in glycerinated tonic (rabbit trachealis) and phasic (guinea-pig ileum and portal vein) smooth muscles (Somlyo et al., 1988, J Gen Physiol 91, 165). Photolytic liberation of ATP from caged ATP initiated force development, at 20°C, with half-times of 5.4s in trachealis and 1.2-2.2s in the phasic muscles. Prior to the photolysis, some muscles were phosphorylated with ATP plus okadaic acid (an inhibitor of myosin light-chain phosphatase; Bialojan et al., 1988, J Physiol 398, 81) or thiophosphorylated with ATP$_\gamma$S in order to fully activate the regulatory system before turning on the contractile apparatus. In these pre-phosphorylated muscles, force development following caged ATP photolysis was more rapid than in the unphosphorylated muscles, but the half-time for trachealis (0.8-1.0s) was still longer than for ileum and portal vein muscles (0.20-0.25s). The results suggest that the contractile machinery and the regulatory system are slower in the tonic than in the phasic smooth muscles. Supp. by grant HL15835 to PA Musc Inst.

Tu-PM-B5 EFFECTS OF ENDOTHELIN ON VASCULAR SMOOTH MUSCLE CONTRACTION AND ON THE PHOSPHORYLATION OF MYOSIN REGULATORY LIGHT CHAIN AND CALDESMON. L.A. Milio, L. P. Adam, J. R. Haeberle, and D. R. Hathaway. Department of Medicine, Indiana University School of Medicine, Indianapolis, IN 46202.

The precise mechanisms underlying force maintenance in vascular smooth muscle are unknown and may involve a combination of both myosin regulatory light chain (LC_{20}) and caldesmon phosphorylation. In order to study how the phosphorylation of LC_{20} and caldesmon each individually contribute to the overall contractile response we have previously shown that KCl, histamine, ouabain, and phorbol esters all cause sustained contractions with elevated levels of caldesmon phosphorylation and low levels of LC_{20} phosphorylation. We now present data on the effects of a recently discovered and potent endothelium-derived contracting factor, endothelin, on vascular smooth muscle function. In porcine carotid arterial strips, we used KCl to stimulate muscles, allowed them to relax and then determined endothelin dose-response curves. Endothelin caused a contraction of the muscle that reached a peak level of 68% of the KCl contraction (EC_{50}=10 nM). With prolonged stimulation by 50 nM endothelin, contraction was phasic, reaching a peak at 15 min and subsequently declining. In KCl (110 mM) stimulated muscles, LC_{20} phosphorylation increased from basal levels to a level of 0.42 mol/mol at 2 min and subsequently declined. The level of LC_{20} phosphorylation, in response to stimulation by endothelin (50 nM), increased during the course of contraction reaching 0.29 mol/mol at 10 min. In response to endothelin stimulation, the levels of caldesmon phosphorylation were not different from control at 10 min (0.30 mol/mol), even though the force of contraction was maximal at this point, and the levels were only slightly elevated at 60 min (0.45 mol/mol). This contrasts with data of caldesmon phosphorylation in response to stimulation by KCl where the levels approached 1.0 mol/mol within 60 min. We conclude that endothelin acts to contract vascular smooth muscle by a mechanism that is different than that of other commonly used agonists such as KCl, histamine, ouabain, and phorbol esters.

Tu-PM-B6 PHOSPHORYLATION AND DEPHOSPHORYLATION OF DISTINCT SITES OF THE 20,000-DALTON MYOSIN LIGHT CHAIN IN ARTERIAL SMOOTH MUSCLE. K. Bárány, F. Erdődi, A. Rokolya and M. Bárány, College of Medicine, University of Illinois, Chicago, IL 60612.

In a 1-min K^+-contracted artery, the phosphate content of the 20,000-dalton myosin light chain (LC) is about 0.7 mol/mol LC and is distributed on five peptides, labelled A through E. In isolated LC, the extent of phosphorylation may be four-fold and an additional phosphopeptide, F, is found. We have shown (Arch. Biochem. Biophys., in press) that MLCK phosphorylated serine residues in peptides A and B, and predominantly threonine residues in peptides C and D, while protein kinase C phosphorylated serine and threonine residues in peptides E and F, respectively. The differences in LC phosphorylation between *in vivo* and *in vitro* may be attributable to the action of phosphatases. Two types of myosin light chain phosphatase from aortic smooth muscle extract were separated by chromatography on heparine-agarose. The phosphatase which appeared in the flow-through fractions had low activity on actomyosin, its apparent molecular mass was 260,000 dalton and upon ethanol treatment it generated a 38,000-dalton catalytic subunit. The phosphatase retained by heparine-agarose had high activity on actomyosin, its apparent molecular mass was 150,000 dalton and it contained a 40,000-dalton catalytic subunit. The 38,000-dalton phosphatase preferentially dephosphorylated peptide F over A,B,C,D and E in both isolated LC and actomyosin. The 40,000-dalton phosphatase could effectively dephosphorylate all sites in isolated LC, whereas it was less effective on dephosphorylation of peptide E in actomyosin. It seems that the protein phosphatases present in artery modulate the extent of LC phosphorylation as well as the sites on the LC which are phosphorylated. (Supported by American Heart Association and by NIH, AR 34602).

Tu-PM-B7 ESTIMATING THE LATCHBRIDGE DISSOCIATION RATE CONSTANT IN ARTERIAL SMOOTH MUSCLE.
Steven P. Driska, Physiology Department, Temple University School of Medicine, Philadelphia, PA 19140

Mathematical models of the regulation of smooth muscle contraction by myosin light chain phosphorylation (S.P. Driska, Prog. Clin. Biol. Res. 245:387–398, 1987; Hai & Murphy, Am. J. Physiol. 254:C99–C106, 1988) are very dependent on the rate constant chosen for the dissociation of latchbridges from the actin filament to form free, unphosphorylated myosin. If the rate constant for the dissociation of latch bridges (k_d) is very low, then the relationship between steady–state force maintenance and light chain phosphorylation is very interesting because only a low level of phosphorylation is needed to support maximum force production, in agreement with experiment. On the other hand, higher values of k_d give a force–phosphorylation relationship that is more nearly linear (and not as interesting). The isometric relaxation rate seemed to be a measurable parameter which could provide an estimate of k_d, but complications arising from variable myosin light chain kinase (MLCK) inactivation rates and alternate pathways raised questions about the utility of this approach. To resolve these questions, simulations were performed for both instant and gradual inactivation of MLCK, starting from both high (90%) and moderate (25%) phosphorylation levels. Starting from high phosphorylation levels, inactivation of MLCK caused a transient increase in the number of latchbridges. In simulations starting from lower levels of phosphorylation, where substantial numbers of latchbridges exist, MLCK inactivation did not cause a pronounced increase in the number of latchbridges. However, in all cases examined, the decay of force could be superimposed on the decay of the latchbridge population. Thus, the rate constant for latchbridge dissociation, k_d, can be estimated by fitting the latter part of the isometric relaxation time course. Values of k_d obtained in this way for hog carotid artery are in the range of $0.01 - 0.02\ s^{-1}$, and support a model where about 80% of the maximum force is developed with only about 20% phosphorylation. Supported by NIH grant HL24881 & RCDA 01198.

Tu-PM-B8 CYTOSOLIC pH MEASURED SIMULTANEOUSLY WITH ISOMETRIC TENSION IN CANINE TRACHEAL SMOOTH MUSCLE : EFFECT OF EXTRACELLULAR ACIDOSIS. Ingrid K. Krampetz and Ratna Bose. Dept. of Pharmacology, Univ. of Manitoba, Winnipeg, Canada. R3E 0W3.

We have previously shown that addition of acid to the bathing solution of a tracheal muscle strip which was contracted with either carbachol or potassium, induced a transient relaxation (J. Pharmacol. Exper. Therap., 246: 641 - 648 (1988). The recovery of tension in an acidic environment could be prevented with the addition of 100 uM amiloride. Magnitude of relaxation observed with acid addition was significantly greater for carbachol-induced contractions. In order to elucidate the effects of extracellular acidosis, we have measured cytosolic pH along with isometric tension. The pH sensitive fluoroprobe BCECF (2'7'-bis-(2-carboxyethyl) 5 and 6 carboxy fluorescein) was used in its permeant form as its tetra acetoxy methyl ester. Tissue strips were incubated for 30 minutes with 2 uM BCECF-AM, in oxygenated Krebs Hensleit solution, at 37°C. Autofluoresence corresponded to less than 10% of the dye signal. Calibration of the pH signal was done with 7 uM hydrogen/potassium ionophore, nigericin in potassium rich HEPES buffered physiological salt solution. Predetermined amount of either acetic acid or hydrochloric acid was used for lowering th pH of the bathing medium. Extracellular acidosis decreased the cytosolic pH both in the unstimulated and stimulated muscle. Activation with either carbachol (1uM) or potassium depolarization (80 mM) resulted in rapid acidification. Intracellular pH in an active muscle strip could be further decreased with extracellular acidification and was associated with relaxation. The magnitude of relaxant action and intracellular pH changes in response to extracellular acid was significantly greater in carbachol-contracted muscle when compared to potassium-depolarized strips.

(Supported by Man. Health Res. Council and Man. Lung Foundation).

Tu-PM-B9 X-RAY DIFFRACTION STUDIES ON LIVING AND SKINNED SMOOTH MUSCLE PREPARATIONS FROM THE RECTOCOCCYGEUS OF THE RABBIT. Anders Arner* and John S. Wray**. Dept. of Physiology and Biophysics, Lund University, Sweden, **Max Planck Inst. fur Med. Forschung, F.R.G.

Smooth muscle from the rectococcygeus of the rabbit was studied with x-ray diffraction. Living relaxed muscles were investigated in physiological salt solutions of normal osmolarity. On the meridian a clear reflection at 144 A, presumably from myosin was observed, suggesting that organized myosin filaments are present under these conditions. The reflection was stronger at 4°C than at 37°C, possibly reflecting changes in the myosin filament assembly/disassembly process or in the conformation of the heads. On the equator a strong reflection at 120 A from regular clusters of actin filaments was observed. Chemical skinning was performed with Triton X-100. If 7.5% dextran T-500 was included during skinning and observation, the skinned preparations revealed an equatorial spacing corresponding to that in the living muscle and a strong meridional reflection from myosin. Electron microscopy showed that the skinning caused disruption of cell membranes but left the appearance and distribution of dense bodies and contractile filaments little changed from the living state. The equatorial actin spacing in the skinned muscle could be influenced by varying dextran. Compared to the living muscle the intensity of the myosin signal showed less temperature dependence. In ATP-free solution the myosin reflection was greatly weakened and a distinct layer line appeared at about 370 A. These results provide diffraction evidence for a change in myosin filament structure and cross-bridge attachment to actin in ATP-free rigor solutions.

Tu-PM-B10 THE EFFECT OF TISSUE LENGTH ON AGONIST-INDUCED INTRACELLULAR [Ca^{2+}] CHANGES IN ARTERIAL SMOOTH MUSCLE. C.M. Rembold and R.A. Murphy. Division of Cardiology, Departments of Internal Medicine and Physiology, University of Virginia School of Medicine, Charlottesville, VA 22908.

The effect of tissue length on myoplasmic [Ca^{2+}] was evaluated by measuring aequorin-estimated myoplasmic [Ca^{2+}] and force production in swine carotid media. Tissues were equilibrated at their optimal length for force production (L_o). Step increases in tissue length to 1.2 L_o were associated with transient rises in intracellular [Ca^{2+}]. After twenty minutes, [Ca^{2+}] returned to near basal levels. Stimulation with 10 μM histamine at 1.2 L_o was associated with changes in intracellular [Ca^{2+}] that were similar to that observed at 1.0 L_o. Step decreases in tissue length to 0.7 L_o were not associated with changes in resting [Ca^{2+}]. However, at 0.7 L_o tissues stimulated with histamine had smaller sustained increases in [Ca^{2+}] than at 1.0 L_o. Isotonic shortening from L_o at very low loads was also associated with smaller histamine-induced increases in [Ca^{2+}]. Oscillations in tissue length (0.95 to 1.05 L_o at 1 Hz) were not associated with significant changes in resting or histamine stimulated increases in [Ca^{2+}]. These results suggest that tissue length affects myoplasmic [Ca^{2+}] and contractile system activation in the swine carotid media. Supported by Markey Trust 025, 5 PO1 HL19242 and RO1 HL39818.

Tu-PM-B11 PARTICIPATION OF CALCIUM CURRENTS IN COLONIC ELECTRICAL SLOW WAVE ACTIVITY. P.D Langton, E.P Burke, and K.M Sanders. University Nevada Medical School, Reno, NV 89557.
Single canine circular colonic myocytes were studied with the whole-cell patch clamp technique. In media containing physiological concentrations of Ca^{2+} inward currents could evoked by depolarizing test pulses. Inward current activated positive to -50 mV, reached a maximum at approximately -10 mV, and reversed at approximately +50 mV. Decay of peak current was fit by a double exponential function. Inward current was potentiated by high $[Ca^{2+}]_o$ and BAYk8644 and decreased by low external Ca^{2+}, nifedipine, and Mn^{2+} indicating that the current was carried by Ca^{2+} ions. The voltage dependence of activation and inactivation were characterized and indicated a "window current" range in which inward current might may be sustained for long durations. The window current range corresponded to the same potentials achieved during the plateau phase of electrical slow waves recorded from cells in intact syncytia. Voltage clamp protocols were designed to simulate physiological depolarizations and were found to elicit inward currents lasting for several secs. Maximum changes in intracellular Ca^{2+} that might result from sustained inward currents were calculated. These estimates suggested that depolarizations to the level of slow wave plateau potentials increased cell Ca^{2+} sufficiently to couple excitation to contraction. The data support the hypothesis that electrical slow waves in colonic smooth muscle are due, in part, to inward Ca^{2+} current. This current appears to be of sufficient magnitude to explain the previously documented relationship between slow waves and contractions, thus providing a mechanism for the mechanical threshold in colonic muscles. Supported by NIADDKD grant DK38717 and Career Development Award to KMS DK01209.

Tu-PM-C1 PHOSPHOINOSITIDE KINASE AND PHOPSHOLIPASE C ACTIVITIES IN T-TUBULE MEMBRANE VESICLES OF FROG SKELETAL MUSCLE

N. Lagos and J. Vergara, Department of Physiology, UCLA, Los Angeles, CA 90024.

The cleavage of L-α-phosphatidylinositol 4,5 bisphosphate (PIP_2) by phospholipase C results in the formation of the second messengers inositol (1,4,5)-trisphosphate ($InsP_3$), which functions to mobilize Ca^{2+} from intracellular stores in several tissues, and 1,2-diacylglycerol (DAG), an activator of protein kinase C. We have investigated the presence of this enzyme in an isolated T-tubule membrane preparation obtained from frog skeletal muscle and studied its activity by directly following the synthesis and catabolism of its endogenous substrate (PIP_2) and the occurrence of $InsP_3$. The experimental procedures included the use of HPTLC separation of phospholipids in the organic phase and simultaneously HPLC separation of nucleotides and inositol phosphates in the aqueous phase. We found that, in this T-tubule vesicle preparation, the synthesis of PIP_2 and its further cleavage to $InsP_3$ and DAG, are limited by the availability of ATP. This nucleotide is competitively hydrolysed by the ubiquitous Mg^{2+}-ATPase at a rate of 5.1±0.3 μmoles/mg protein/min in its initial rapid phase. Experimental manipulations that guarantee an adequate supply of ATP to the kinases result in a marked increase in PIP, PIP_2, and $InsP_3$. Conversely, the disappearance of ATP from the incubating medium is followed by a rapid breakdown of PIP_2, evidencing a significant phospholipase C activity in the T-tubule membrane. Supported by NIH, MDA and NSF grants. N.L. is a recipient of an AHA-GLAA postdoctoral fellowship.

Tu-PM-C2 INACTIVATED STATE RATHER THAN TRANSVERSE TUBULE DEPOLARIZATION INCREASES PEELED SKELETAL MUSCLE FIBER SENSITIVITY TO INOSITOL TRISPHOSPHATE. Sue K. Donaldson, University of Minnesota, Minneapolis, MN 55455 USA.

Single rabbit adductor magnus fibers were mechanically skinned (peeled) to remove the sarcolemma and then mounted in transducers for continuous monitoring of isometric force. Following loading of internal fiber stores with Ca^{2+} from the bath, inositol trisphosphate ($InsP_3$) was microinjected (1nl) through a glass pipette into the myofilament lattice of the peeled fiber in oil. This stimulated the sarcoplasmic reticulum to release Ca^{2+} which was measured as the peak force of the $InsP_3$-induced tension transient. The $InsP_3$ concentration in the pipette was 0.5μM (with peeled fiber bathing solution as solvent). We recently reported that the sensitivity of the peeled fiber to $InsP_3$ stimulation of Ca^{2+} release was enhanced by transverse tubule (TT) depolarization (Donaldson et al., 1988, PNAS, 85:5749-5753). This effect might be the result of inactivation or the TT membrane voltage. To separate these two parameters, peeled fibers were stimulated with $InsP_3$ under the polarizing bathing solution conditions (i.e., 4mM Cl^-, 66mM K^+) associated with low sensitivity to $InsP_3$. With the TTs polarized, the fibers were microinjected with $InsP_3$ in the absence of drugs (i.e., primed state) and in the presence of D600 (i.e., inactivated state). D600 was demonstrated to block the SR Ca^{2+} release in response to TT depolarization in each fiber tested. In paired data tests, $InsP_3$ stimulation of polarized, D600-inactivated peeled fibers yielded Ca^{2+} releases which were larger than those for fibers under polarized/primed conditions. These data suggest that the inactivated state rather than TT voltage determines sensitivity to $InsP_3$. (Supported by NIH grant AR 35132.)

Tu-PM-C3 TEMPORAL APPEARANCE AND DISTRIBUTION OF THE 1,4-DIHYDROPYRIDINE RECEPTOR (DHPR) IN DEVELOPING RABBIT SKELETAL MUSCLE. S. Yuan*, W. Arnold*, K.P. Campbell+, A. Leung+ and A.O. Jorgensen*, *Department of Anatomy, University of Toronto, Toronto, Canada, M5S 1A8 and +Department of Physiology and Biophysics, University of Iowa, Iowa City, IA 52242.

Immunoelectron microscopical studies have shown that the DHPR is densely distributed in transverse tubules (TTs) of adult rabbit skeletal muscle. To determine the distribution of the DHPR in developing skeletal muscle, transverse cryosections of fetal and neonatal rabbit gracilis muscle were stained with antibodies to the DHPR, the ryanodine receptor (RR) and cavulin. Cavulin is a protein which, like the 1,4-DHPR, is also densely distributed in the TT but absent from the sarcolemma, as determined by double immunofluorescence labeling. TTs start to form on day 17 of fetal development and extend halfway towards the center of the myotube by day 24. One to two days after birth TTs extend throughout the cytosol of the myofibers. During these stages of development, the DHPR and the RR are present in discrete foci throughout the cytosol. The intensity of these foci increase with development. In contrast, specific labeling of cavulin was present in distinct foci or short rods at the periphery of the myotubes on day 17. On day 24, cavulin appears to be distributed as wavy strands originating from the sarcolemma and reaching approximately halfway towards the center of the myotube. One-two days after birth, it is distributed in a chicken wire pattern throughout the cytosol. Assuming that the distribution of cavulin represents the distribution of the forming TTs, the results presented are consistent with the idea that the DHPR is incorporated into the TT membranes subsequent to the formation of the TTs.

Tu-PM-C4 A FOUR GAP VOLTAGE CLAMP IMPROVES MEASUREMENTS OF EC COUPLING EVENTS IN FROG SKELETAL MUSCLE. E. Ríos, G. Pizarro and G. Brum. Rush University, Chicago, IL.

Studies of EC coupling at the cellular level often use 1, 2 or 3 Vaseline gap clamps of cut fibers. In these devices the current is measured with error, due to substantial contributions from regions of membrane under the Vaseline seals. These regions should be less polarized and respond more slowly to imposed voltage steps (W.K. Chandler, personal communication). A new device, with four seals separating five aqueous compartments around a cut fiber, solves the problems. As in the double gap, the end compartments measure intracellular voltage (1) and pass current (5). Of the three central compartments the lateral ones (2 and 4) are "guards" connected to ground, and the middle one (3) goes to virtual ground on a current–measuring circuit. The diagram shows the solution of the cable equation when the measuring pool is at –100 mV. The membrane of all three central compartments is clamped to a similar voltage; current that flows through the membrane in 2 and 4 and under the lateral seals goes to ground via the guards; only the membrane current flowing in the middle compartment is measured.

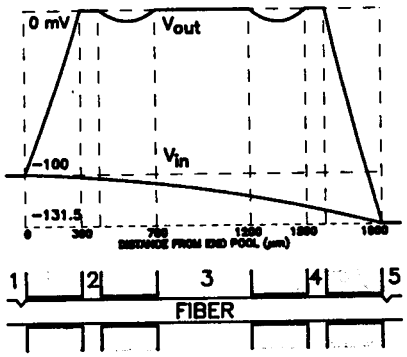

Results 1. Charge movement transients were much faster, therefore better defined. 2. Charge 2 had similar magnitude (Q_{max} = 42 ± 4 nC/μF, n = 8) but a steeper voltage dependence (K = 14.6 ± 1.1 mV) than in double gap measurements. 3. Charge 2 was reduced 30–60% upon steady polarization to –90 mV. Charge 1 increased by the same or a slightly greater amount. These results strengthen the view that charges interconvert upon polarization.

Tu-PM-C5 TETRACAINE AND PATHWAYS OF Ca^{2+} RELEASE IN SKELETAL MUSCLE. G. Pizarro, L. Csernoch, I. Uribe and E. Ríos. Dept. of Physiology, Rush University, Chicago, Illinois 60612.

Tetracaine is known to suppress the delayed phase of intramembrane charge movement ($Q\gamma$). We used cut fibers in a double gap to study its effects on myoplasmic Ca^{2+} transients. 0.2 mM tetracaine abolished $Q\gamma$, reduced $Q\beta$ and substantially altered the size and time course of the Ca^{2+} transients elicited by depolarizing pulses. $[Ca^{2+}]_i$ rose steadily during the pulse (Fig.); it reached a plateau at 500 ms (not shown); Ca release flux was derived from the transients (Melzer et al. 1987): instead of the normal peak followed by decay to a low plateau, it had constant or steadily increasing time course. The decaying phase of release (attributed by Simon & Schneider to inactivation by Ca^{2+}) was absent, even though $[Ca^{2+}]_i$ and $d[Ca^{2+}]_i/dt$ reached levels that caused inactivation before exposure to the drug (Figure).

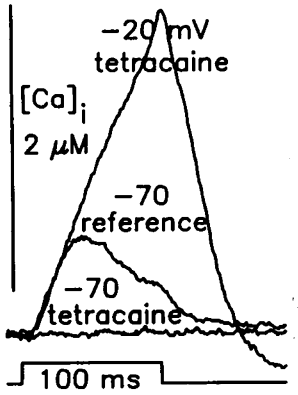

The experiments were repeated at pH 5.8. Tetracaine (fully protonated) still reduced charge movement but the Ca^{2+} transients were only scaled down, corresponding to a Ca release flux with normal peak and inactivation. This suggests that the drug has two targets: the T membrane carrier of charge movement and an intracellular Ca release channel. Acting extracellularly, the drug reduces charge movement and Ca release is scaled down. Intracellularly, it abolishes the inactivating peak component of Ca release and spares a non–inactivating one. These two components may correspond to separate pathways of release. Alternatively, they could be due to a common carrier, that loses its inactivation when altered by tetracaine. Supported by NIH and MDA.

Tu-PM-C6 FLICKERY BLOCK OF THE PURIFIED RYANODINE RECEPTOR BY RUTHENIUM RED, TETRAAMMINE PALLADIUM AND TETRAAMMINE PLATINUM. Jianjie Ma, C. Michael Knudson, Kevin P. Campbell, and Roberto Coronado. Dept. of Physiology & Molecular Biophysics, Baylor College of Medicine, Houston, TX, and Dept. of Physiology & Biophysics, Iowa University School of Medicine, Iowa City, Iowa.

We studied the mechanism of block of the 450 KDa purified ryanodine receptor by ruthenium red (RR), a well known blocker of Ca release and two related compounds, $Pd(NH_3)_4Cl_2$ (4APd) and $Pt(NH_3)_4Cl_2$ (4APt). In channels held open by 200 nM ryanodine, RR induced an all-or-none block (flickery block) when added to the myoplasmic side. Open channel probability vs RR concentration showed a strong voltage dependence. Blockade of the 500 pS open state could be fit by a Hill coeff. of approximately 2 and and a dissociation constant Kd= 0.2 μM, 0.35 μM, and 0.6 μM at +100 mV, +80 mV, and +60 mV, respectively (cis-positive potentials). Entry and exit rates of RR from the receptor were extracted from single channel records. "On" and "off" rate constants for RR blockade at +80 mV were K_{on} = 3.93 μM^{-1} ms^{-1}, K_{off} = 1.37 ms^{-1}. In the 250 pS open state of the receptor, RR had a Kd = 0.7 μM at +100 mV which is about three times larger than for the 500 pS state. Two compounds related to RR, 4APd and 4APt induce the same flickery blockade when added to the myoplasmic side. Approximate Kds are 150 μM for 4APd and 560 μM for 4APt at +80 mV. The analogs displayed a Hill coeff. of approximately 1. Analogs of RR that are not dyes, such as 4APd and 4APt, may prove more useful in cellular studies. Supported by NIH, MDA, and AHA.

Tu-PM-C7 MECHANISM OF RYANODINE ACTIVATION IN THE PURIFIED RYANODINE RECEPTOR CHANNEL. Jianjie Ma, C. Michael Knudson, Kevin P. Campbell, and Roberto Coronado. (Intr. by W. Schilling). Department of Physiology & Molecular Biophysics, Baylor College of Medicine, Houston, TX, and Department of Physiology and Biophysics, Iowa University School of Medicine, Iowa City, Iowa.

The purified ryanodine receptor forms Ca release channels regulated by Ca, pH, and voltage (Ma et al., Science 1988). Ryanodine transforms the kinetics of the receptor from a fast (60 μs open time) to a slow (10 ms open time) gating and drives the channel into a quasi-permanent open state. At pH 7.0, 10 μM free Ca, HP +80 mV, ryanodine (50 nM) increases open probability from p=0.03 to p=0.8. The channel modified by ryanodine shows three conductances, 500 pS, 250 pS, and 125 pS in 0.25 M KCl. Conductance states depend on free Ca in solution. At 50 nM Ca, the predominant conductance is 500 pS; from 10 μM to 100 μM Ca the predominant conductance is 250 pS, and at 3.5 mM Ca the channel only exist in the low conductance state of 125 pS. Ryanodine can bind to the closed conformation of the receptor since 200 nM ryanodine opens the channel to a probability p>0.6 under the following conditions where the receptor channel is known to exist in the closed state with p<0.001: 1) pH 6.5, 10 μM Ca; 2) pH 7.4, 50 nM Ca; and 3) pH 7.4, 3.5 mM Ca. Given that the receptor is a homotetramer of the 450 kDa subunit, it is likely that the subconductance states associated with changes in Ca may reflect changes in subunit assembly of the tetrameric receptor complex. Supported by NIH, MDA and AHA.

Tu-PM-C8 NON-LINEAR T-SYSTEM VOLTAGE CHANGES DETECTED OPTICALLY UNDER 'LINEAR' CHARGE MOVEMENT RECORDING CONDITIONS, Judith A. Heiny and De-Shien Jong, Dept. of Physiology & Biophysics and Dept. of Physics, University of Cincinnati, Cincinnati, OH 45267.

Charge movement currents and T-system voltage changes were recorded simultaneously from single voltage-clamped skeletal muscle fibers, perfused internally and externally with typical charge movement recording solutions designed to eliminate all ionic currents. T-system voltage changes were recorded optically using potentiometric dyes. In response to hyperpolarizing voltage-clamp steps, the T-system voltage reaches a constant level in approximately 5 ms at 5°C. In response to depolarizing steps, the T-system voltage takes approximately 20 ms to reach a steady level; in addition, the steady-state amplitude exceeds that recorded in response to the equivalent hyperpolarizing pulse. This finding was not expected as it is normally assumed that the T-system membrane should be entirely linear under these conditions. The non-linearities cannot be accounted for by unblocked voltage-dependent ionic currents. Neither do they result from residual calcium-activated ionic currents as they remain after both calcium currents and SR calcium release have been blocked. Additionally, they do not seem to be dye- related artifacts. Rather, they appear to reflect a T-system membrane phenomenum. We propose that the dye senses both local electrostatic potentials and the potential of bulk solution whereas the voltage-clamp responds only to the bulk or Nernst potential. These data are consistent with the hypothesis that, upon depolarization, a transient local electrostatic potential is generated at the T-system membranes. (Supported by NSF Grant 8508305, M.D.A. and A.H.A.)

Tu-PM-C9 ORIGIN OF THE NON-LINEAR T-SYSTEM POTENTIAL CHANGES: A POSSIBLE ASSOCIATION WITH E-C COUPLING? De-Shien John and Judith A. Heiny (Intr. by J. Suszkiw). Dept. of Physics and Dept. of Physiology & Biophysics, University of Cincinnati, Cincinnati, OH 45267.

Non-linear T-system voltage changes were detected optically under standard charge movement recording conditions (Heiny & Jong, Biophys. J., 1989, these proceedings). If the hyperpolarizing light signal is used as a control and subtracted from the corresponding depolarizing signal, a "difference light signal" is revealed which rises to a steady level after a delay. With increasing depolarization, the delay decreases and the amplitude increases, until both reach a limiting value at large positive potentials. These steady-state differences were plotted versus the command voltage applied across the surface membrane. They occur at voltages positive to about -50 mV and increase in a sigmoid manner, saturating at large positive potentials. The difference light signals disappear over this same voltage range when the fiber is pulsed instead from a holding potential of 0 mV, a potential at which charge movement is largely inactivated. Perchlorate, which shifts charge movement to more negative potentials and lowers the mechanical threshold, shifts the difference light curve in parallel. Similarly, Dantrolene Na, a drug which elevates mechanical threshold, shifts the difference light curve to the right. Ruthenium Red, at concentrations that block Ca release, does not eliminate the difference light signal, indicating that this signal is not a consequence of Ca release. We propose that these voltage changes may reflect some early step associated with excitation-contraction coupling. (Supported by NSF Grant 8508305, M.D.A. and A.H.A.)

Tu-PM-C10 EFFECTS OF TETRACAINE AND MAINTAINED DEPOLARIZATION ON CHARGE MOVEMENT COMPONENTS IN FROG CUT TWITCH FIBERS. Wei Chen and Chiu Shuen Hui, Department of Physiology and Biophysics, Indiana University Medical Center, Indianapolis, IN 46223.

Charge movement was measured from cut fiber segments of semitendinosus muscles from R. temporaria using the double vaseline-gap voltage clamp under conditions identical to those of Hui and Chandler (Biophys. J. 53: 646a, 1988). Q_{off} after a single test pulse can be separated into Q_β and Q_γ components by fitting the Q-V curve with two Boltzmann's terms. The more steeply voltage-dependent component (Q_γ) can be blocked by tetracaine whereas the other one (Q_β) cannot. If test pulses are followed by a constant post-pulse to -60 mV, the final Q_{off} when plotted against V shows a sigmoidal Q_γ component which is also sensitive to tetracaine. In typical experiments, 0.2 mM tetracaine blocks roughly 70% of Q_γ. 0.5 mM blocks more but the blockage is still incomplete. Most fibers cannot tolerate 1 mM tetracaine. Of those that survive long enough, Q_γ seems to be completely blocked. This shows that Q_γ isolated in cut fibers by the method of Hui and Chandler can be identified with the tetracaine-sensitive component observed in intact fibers. The two charge components in cut fibers also respond differently to maintained depolarization. When holding potential is shifted in the depolarizing direction, a larger fraction of Q_γ is immobilized than Q_β. At around -50 mV, Q_γ is completely immobilized whereas some Q_β can still move. This is a direct demonstration that the inactivation curve for Q_γ in cut fibers has a steeper voltage-dependence than that for Q_β. (Supported by NS-21955 and a grant from MDA).

Tu-PM-C11 TWITCH TENSION IN FROG SKELETAL MUSCLE DURING D600 PARALYSIS AND REVIVAL. Chiu Shuen Hui, Department of Physiology and Biophysics, Indiana University Medical Center, Indianapolis, IN 46223.

When frog twitch fibers were paralyzed by D600 after conditioning depolarization at low temperature, both components of charge movement disappeared. When paralyzed fibers were warmed, its ability to give K-contracture was recovered and Q_β was reprimed concomitantly, but Q_γ sometimes could not be reprimed. Information about twitch tension in those revived fibers was lacking. Experiments were performed on single intact fibers of semitendinosus muscles of R. temporaria. It was found that when paralyzed fibers were warmed, their twitch tension could recover to various extent and sometimes not at all, even though they could still give full size K-contractures. This is parallel to the variable repriming of Q_γ and is consistent with the hypothesis that Q_γ is closely associated with contractile activation. The rate and extent of revival of twitch tension is steeply temperature-dependent, with the optimal temperature for the highest revival rate within 8-15°C. Revived twitch tension can be re-suppressed when temperature is brought above or below that range. Conversely, by using a solution with 60 mM K^+ for conditioning depolarization, fibers can be brought to partially paralyzed states with twitch tension reduced but not completely suppressed. The partially paralyzed or partially revived states are highly unstable, as they are affected by the amount of D600 present in the bathing solution and by stimulating the fiber. (Supported by NS-21955 and a grant from MDA).

Tu-PM-C12 DIFFERENTIAL SENSITIVITY TO RYANODINE IN SKINNED FIBERS OF FETAL AND ADULT RAT HEART. J.Y. Su, Dept. of Anesthesiology, RN-10, University of Washington, Seattle, WA 98195

Ryanodine, an SR Ca^{2+} channel blocker, produces a negative inotropic effect on adult mammalian heart but its effect on fetal heart is much less potent. This resistance of fetal heart to ryanodine (Pflügers Arch 347:173, 1974) has been attributed to an underdeveloped T system. In the skinned papillary muscle of the adult rabbit, I have previously shown that ryanodine, in a dose-dependent manner (IC_{50} = 50 nM), decreases caffeine-induced tension transient of the subsequent control (Pflügers Arch 411:132, 1988). The aim of this study was to test whether there is a difference in sensitivity to ryanodine between fetal and adult heart at the SR. Accordingly, I studied the effects of ryanodine on skinned myocardial fibers from fetal (20 days) and adult rat. Ventricular muscles were skinned by homogenization as described previously (J Appl Physiol 39: 1052, 1975). Fiber bundles were dissected from the homogenate. One end was attached to a photodiode force transducer. The skinned fibers were immersed in bathing solutions to load Ca^{2+}. The Ca^{2+} was then released from the SR with 25 mM caffeine, resulting in a tension transient (Pflügers Arch 380:29, 1979). The area of the tension transient was used as an estimate of the amount of calcium released from the SR. Ryanodine (0.3 nM - 1 μM), present in the releasing solution (containing 25 mM caffeine), decreased the tension transient of the subsequent control in a dose-dependent manner, for both fetal and adult hearts (IC_{50} = 56 nM and 2.6 nM, respectively). Thus, SR Ca^{2+} channels in the skinned fibers from fetal heart are about 20-fold less sensitive to ryanodine than those of the adult. In the adult rat heart the potency of ryanodine in skinned fibers is comparable to that observed in isolated intact papillary muscle. (Supported by NIH HL 20754)

Tu-PM-D1 ACTINOMYCIN D INDUCED DNase I CLEAVAGE ENHANCEMENT CAUSED BY SEQUENCE SPECIFIC PROPAGATION OF AN ALTERED DNA STRUCTURE. Yao-Qi Huang[1], Robert P. Rehfuss[1], Steven R. LaPlante[2], Eilis Boudreau[2], Philip N. Borer[2] and Michael J. Lane[1] (Intr. by Jeffrey C. Freedman); [1]Departments of Medicine and Microbiology, State University of New York at Syracuse, Syracuse, NY 13210 [2]Department of Chemistry and NIH Resource for NMR and Data Processing, Syracuse, NY 13244.

Two DNA hexadecamers containing one central 5'-GC-3' base step have been examined by footprinting methodology in the presence and absence of actinomycin D. The results of these studies, coupled with imino proton NMR measurements indicate that the antitumor drug causes a change in DNA conformation at a distance from actinomycin intercalation site in a molecule of sequence d(ATATATAGCTATATAT) that does not occur in d(AAAAAAAGCTTTTTTT). The experiments demonstrate that DNase I rate enhancements associated with actinomycin D binding are caused by ligand alteration of equilibrium DNA structure. Further, the susceptibility of d(AT)n sequences to unwinding suggests that unwinding caused by actinomycin intercalation at the GC core of d(ATATATAGCTATATAT) is propagated into the d(AT)n sequences. Given this suggestion we have studied the rate of cleavage of two series of DNA molecules by the restriction enzyme Alu I (5'-AGCT-3'). The first series, (AT)nAGCT(AT)n (where n = 2, 3, 4), is cleaved consistently faster by the enzyme than the congeners in the second series, (AA)n AGCT(TT)n (where again n = 2, 3, 4). Our results are consistent with the notion that the (AA)nAGCT(TT)n DNA molecules are resistant to unwinding. (Supported by NCI grant CA45698 [MJL], and by GM 35069 and RR01317 [PNB and GCLevy]).

Tu-PM-D2 DIRECT EVIDENCE FOR LEFT-HANDED Z-DNA CONFORMATION IN A SUPRAMOLECULAR ASSEMBLY OF POLYNUCLEOTIDES. T.J. Thomas, Department of Medicine, Division of Rheumatology, UMDNJ-Robert Wood Johnson Medical School, New Brunswick, New Jersey 08903.

Multivalent ions like $Co(NH_3)_6^{3+}$ and $Ru(NH_3)_6^{3+}$ are known to provoke the B-DNA to Z-DNA transition in poly(dG-dC).poly(dG-dC) and poly(dG-m^5dC).poly(dG-m^5dC) under very low counterion concentrations. At higher concentration (>50 uM) of these counterions, however, Z-DNA transforms to the ψ-DNA, a twisted tightly packed assembly of DNA. Since the ψ-DNA form is associated with a 25- to 100-fold increase in the molar ellipticity of DNA, circular dichroism spectroscopy provides no information on the helical handedness of ψ-DNA. In order to circumvent this difficulty, we used a recently developed enzyme immunoassay technique to probe the conformation of -DNA. A highly specific monoclonal anti-Z-DNA antibody was used in this study. This antibody bound strongly to ψ-DNA immobilized on a microtiter plate, thereby providing direct evidence for the presence of a left-handed ψ-DNA. We also found that several other counterion, including the ethylene diamine complexes of Co, Ru and Rh were capable of altering the conformation of polynucleotides. Supramolecular organizations like the ψ-DNA are believed to play a role in the compaction of DNA in virus heads and chromatin. Therefore, our results suggest that blocks of potential Z-DNA forming sequences in the genome may assume a left-handed conformation under favorable ionic conditions. We will also compare these results with that obtained under physiologically compatible conditions, including the presence of natural polyamines.

This work was partly supported by research grants from the Arthritis Foundation, Atlanta, GA and the National Institutes of Health (RO1 AR 39020).

Tu-PM-D3 EQUILIBRIUM AND COVALENT BINDING OF AFLATOXINS WITH DNA. Michael P. Stone, Thomas M. Harris, Steven W. Baertschi, Suzanne Byrd, S. Gopalakrishnan, and Kevin D. Raney. Department of Chemistry and Center in Molecular Toxicology, Vanderbilt University, Nashville, TN 37235.

Aflatoxin B_1 (AFB1) is metabolically activated in vivo to the electrophilic species AFB1-8,9-epoxide, which reacts exclusively at the N^7 position of guanine to form the cationic adduct 8,9-dihydro-8-(N^7-guanyl)-9-hydroxy-AFB1. This adduct can (1) undergo subsequent rearrangement to the FAPY derivative in which the imidazole ring of guanine is opened, (2) undergo depurination by scission of the glycosyl linkage, or (3) be removed from the DNA with formation of AFB1 dihydrodiol. The AFB1 moiety in the cationic adduct could be intercalated or located in the major groove of B-DNA. Equilibrium binding studies of AFB1 and related mycotoxins with a variety of nucleic acids and oligodeoxynucleotides support intercalative association with B-DNA. The equilibrium with the self-complementary oligodeoxynucleotides $d(ATGCAT)_2$ and $d(ATCGAT)_2$ is rapid on the NMR time scale and dependent upon maintenance of the B-DNA duplex. Increased shielding is observed for AFB1 protons in the non-covalent complex, and increased spin-lattice relaxation rates are observed for the adenine H2 protons which are located in the minor groove. The intercalative agents actinomycin D and ethidium bromide both displace AFB1 from $d(ATGCAT)_2$. Titration of negatively supercoiled plasmid pBR322 with AFB1 as monitored by gel electrophoresis results in progressive unwinding of the plasmid; titration of closed circular relaxed plasmid results in introduction of positive supercoils. We have synthesized, isolated, and carried out chemical and spectroscopic characterization of AFB1-8,9-epoxide, the ultimate carcinogenic species of AFB1. The epoxide readily reacts both with DNA and with guanine-containing oligodeoxynucleotides to yield the cationic adduct 8,9-dihydro-8-(N^7-guanyl)-9-hydroxy-AFB1. We have successfully prepared and characterized cationic adducts of AFB1 with $d(ATGCAT)_2$ and $d(ATCGAT)_2$; these adducts are double-stranded and sufficiently stable to allow conformational analysis by NMR. Supported by USPHS grants ES-03755 and ES-00267.

Tu-PM-D4 G:C AND A:T DOMAINS IN B-DNA ARE DISTINGUISHED BY DIFFERENCES IN SOLVENT ACCESSIBILITY AT PURINE EXCHANGEABLE (8CH) SITES: DISCRIMINATION BY RAMAN OPTICAL MULTICHANNEL ANALYSIS.
Renee Becka, Om Lamba and George J. Thomas, Jr., Division of Cell Biology and Biophysics, School of Basic Life Sciences, University of Missouri-Kansas City, Kansas City, MO 64110.

The sensitivity of the Raman spectrum to DNA conformation serves as a basis for distinguishing A, B and Z forms in oligomer crystals and in solutions of large DNA molecules. The Raman spectrum of B-DNA also contains evidence for subtle differences in phosphodiester geometries of G:C and A:T domains of the macromolecule (1). To investigate further the specific conformational features of G:C and A:T domains of aqueous B-DNA, we have developed a Raman dynamic probe which is diagnostic of solvent accessibility along the major groove (2). Our methodology exploits deuterium exchange of purine 8C-H groups as a sensitive indicator of D_2O solvent access to 7N-8C loci. Using Raman optical multichannel analysis, we have measured separately the rates of deuterium exchanges of guanine and adenine 8C-H groups in calf thymus DNA and in the lambda operator sequences O_L1 and O_R3. The results show that adenine 8C-H groups suffer more significant retardation of exchange than guanine 8C-H groups, consistent with more restricted access of solvent molecules to regions of the major groove which are richer in A:T pairs. Implications of these results for recognition by DNA binding proteins will be discussed. (Supported by N.I.H.)

(1) Thomas, G. J., Jr. et al. (1986) Biomolecular Stereodynamics 4, 227-253 (Adenine Press, NY).
(2) Benevides, J. M. and Thomas, G. J., Jr. (1985) Biopolymers 24, 667-682.

Tu-PM-D5 A SPECIFIC QUADRILATERAL SYNTHESIZED FROM DNA BRANCHED JUNCTIONS,
Jung-Huei Chen, Neville R. Kallenbach and Nadrian C. Seeman, Department of Chemistry, New York University, NY, NY 10003.

It has been suggested that nucleic acid branched junctions can serve as the vertices of N-connected stick figures and networks. Previously, we have shown that 3-arm and 4-arm junctions are flexible, because macrocycles containing 3, 4, 5 or more monomers form when an individual junction containing two complementary cohesive ends is covalently oligomerized. Here, we demonstrate that greater control may be gained over the construction process if unique cohesive ends are used for each junction. Four different 3-arm branched DNA junctions have been synthesized and linked together in a prescribed arrangement to form a macrocycle of previously specified sequence. One end of each individual junction is closed by a hairpin loop. Each open arm of the four junctions terminates in a unique single-stranded cohesive ('sticky') end; there are four pairs of complementary sticky ends among the eight arms, two pairs with 3' overhangs, and two pairs with 5' overhangs. The junctions which associate in this fashion have been enzymatically joined together by T4 DNA ligase. The final product is a "quadrilateral" the sides of which are each 16 nucleotide pairs long, approximately 1.5 turns of DNA. The quadrilateral is designed to be composed of two hextuply linked circles of DNA. Each of the two circles contains a unique restriction site on an exocyclic arm; these sites facilitate the analysis of the products of the ligation reaction.
This research has been supported by grants GM-29554 and CA-24101 from the NIH.

Tu-PM-D6 T4 ENDONUCLEASE VII CLEAVES THE CROSSOVER STRANDS OF HOLLIDAY CROSSOVER ANALOGS.
John E. Mueller[1], Borries Kemper[2], Richard P. Cunningham[1], Neville R. Kallenbach[3] and Nadrian C. Seeman[3]. [1]Dept. of Biology, SUNY/Albany, NY 12222, [2]Institute of Genetics, University of Köln, FRG, [3]Dept. of Chemistry, New York University, NY, NY 10003.

We have formed 4-arm branched DNA junctions from oligonucleotides which contain no more than a single base pair of branch migratory freedom. These junctions have two-fold symmetric hydroxyl radical protection patterns in solution: Relative to double helix, two opposite strands of an immobile junction show extensive protection in the vicinity of the branch point, while the other pair of opposite strands is virtually as susceptible as double helix. The same result is seen in a monomobile junction closely related to the immobile junction. A second monomobile junction has the opposite protection pattern. These patterns suggest that a crossover-isomer bias exists in these molecules, and that the protected strands form the crossover between helices. We have examined the cleavage pattern of T4 endonuclease VII, a well-characterized enzyme capable of resolving Holliday junctions, on these branch point structures. Junctions have been formed from a single shamrock-shaped molecule, which contains 5', 3', or internal labels. The enzyme shows a preference for cleaving these modified junctions at sites near those protected from hydroxyl radical cleavage. This result suggests that only crossover strands in a Holliday junction are cleaved, and thus an odd number of crossover isomerizations must occur when flanking markers are exchanged.
This research has been supported by NIH grants GM-29554, CA-24101 and GM-33346.

Tu-PM-D7 FAR-INFRARED EVIDENCE FOR THE METASTABILITY OF POLY(dA)POLY(dT). Glenn Edwards, Steve Morgan, and Enrique Silberman. Department of Physics and Astronomy, Vanderbilt University, Nashville, Tennessee and Department of Physics, Fisk University, Nashville, Tennessee. We report on experiments using two complementary spectroscopic techniques that probe far-infrared vibrational modes of DNA. Low-frequency Raman and Fourier transform infrared techniques are used to measure resonant features in the 20 to 200 wavenumber range. Measurements of random sequenced DNA and various polynucleotides demonstrate that poly(dA)poly(dT) is a metastable structure. These results are consistent with recent structural and CD investigations of the propeller twist structure of poly(dA)poly(dT).

Tu-PM-D8 DNA SEQUENCES WHICH ARE ATTACKED BY THE CARCINOGEN N-ACETOXY-N-ACETYL-2-AMINO-FLUORENE. Stephen A. Winkle, Marta Bascoy, and James Brown, Department of Chemistry, Florida International University, Miami, FL 33199, Michael A. Mallamaci, Biochemistry Department, Rutgers University, New Brunswick, NJ 08903, and Richard D. Sheardy, Department of Chemistry, The Pennsylvania State University-Hazleton, Hazleton, PA 18201.

Restriction enzyme inhibition studies and lambda exonuclease studies in our laboratory have suggested that the carcinogens 4-nitroquinoline-oxide (NQO) and N-acetoxy-N-acetyl-2-amino-fluorene (AAAF) bind to bases within the same set of eight sequences on pBR322. When these sequences are moved from their native locations to regions on pBR322 which do not possess binding sites in the native plasmid, new binding sites for AAAF are created at the insertion site. Insertion of the synthetic oligomer shown below, which contains the characteristics of this set of sequences, into pBR322 also creates a new AAAF binding site.

G-T-C-A-G-C-T-C-T-T-G-C-T-G-C-G
C-A-G-T-C-G-A-G-A-A-C-G-A-C-G-C

Insertion of this oligomer into other plasmids, e.g. IBI24, creates AAAF binding sites at the insertion sites. Restriction enzyme inhibition studies suggest that AAAF binds preferentially to sequences on ØX174 and SV40 that are similar to the eight preferred binding sites on pBR322. These studies provide insight as to the possible sequence features which are attractive to carcinogens.

This work supported by NCI grant 34762 (SAW) and NSF grant DBM-8616358 (RDS).

Tu-PM-D9 CONSTRUCTION AND PRELIMINARY CHARACTERIZATION OF A SYNTHETIC DNA DUMBBELL CONTAINING A B-Z JUNCTION AT HIGH SALT. Richard D. Sheardy, Department of Chemistry, The Pennsylvania State University-Hazleton, Hazleton, PA 18201 and Albert S. Benight, Department of Chemistry, The University of Illinois at Chicago, Chicago, IL 60680. Supported by NSF grant DMB-8616358 (to RDS).

We wish to report the construction of a DNA dumbbell of specific sequence and its preliminary characterization by gel electrophoretic, CD and UV spectroscopic techniques. The DNA dumbbell, shown below, was constructed from hairpins with sticky ends (the dashed line separates the two hairpins).

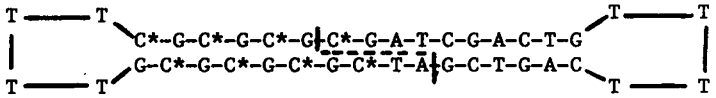

The hairpins were kinased and ligated together using standard techniques. The final dumbbell was obtained in high purity and yield via preparative scale HPLC. Control molecules were also synthesized in which only one of the hairpins was kinased, giving rise to a dumbbell with a "nick" on either the upper strand or lower strand. Gel electrophoresis studies indicated great differences in mobility through acrylamide gels between the individual hairpins, the closed dumbbell, and the nicked dumbbells. CD studies indicated that the closed dumbbell is a right handed double helix at low salt and undergoes a conformational transition as the salt concentration is increased. The CD spectra at high salt indicate that the molecule has both left and right handed regions and thus a B-Z junction separating them. Finally, temperature dependent UV studies indicate that the molecule has a Tm of over 100°C in low salt and around 88°C in high salt (5M NaCl).

Tu-PM-D10 Molecular Mechanics of $d(N_2A_4T_4N_2)_2$, $d(N_2T_4A_4N_2)_2$, and $d(C_2A_6C_2).d(G_2T_6G_2)$: An Explanation for Curved DNA

Chang-Shung Tung and Angel E. García

T10 MS K710, Los Alamos National Laboratory, Los Alamos, New Mexico. 87545

We have performed unconstrained molecular mechanics (energy minimization) of ideal B-DNA structures for the oligomers $d(C_2A_4T_4G_2)_2$, $d(G_2A_4T_4C_2)_2$, $d(C_2T_4A_4G_2)_2$, $d(G_2T_4A_4C_2)_2$, and $d(C_2A_6C_2).d(G_2T_6G_2)$. Without any *a priori* constraints, starting from standard B-DNA geometries, the energy minimized structures of all five molecules show bifurcated H-bonds between adjacent A and T bases on different strands. The bifurcated H-bond seems to be a structural signature of *A-tracts*. To avoid fictitious end effects, only the central 10 basepairs (8 basepairs for $d(C_2A_6C_2).d(G_2T_6G_2)$) are considered in the detailed study of the energy minimized structures. By themselves, none of the five oligomers show significant bending. However, when these oligomers are joined together, the resulting concatemers are very different in shape. These concatemers have curved structures in qualitative agreement with the experimental data.

Tu-PM-D11 Theoretical Study of the Stability and Dynamics of a B-Z Junction

Goutam Gupta and Angel E. García

T10 MS K710, Los Alamos National Laboratory, Los Alamos, New Mexico. 87545

We have constructed a stereochemical model for the B-Z junction for the oligomer d(TTTTCGCG).d(CGCGAAAA). In this model the junction is formed via a single base pair step. The stacking of the bases at the junction is different from that in the B and Z DNA. The two neighboring stacked bases in the helical array(right of left) can be exactly superimposed on each other by rotation and translation. However the two stacked bases in each chain at the junction are flipped with respect to each other. This type of stacking (called inverted stacking) has been observed in the crystal structure of bases, nucleosides and nucleotides.

We will report molecular mechanics and normal mode analysis for this oligomer in the B and the B-Z junction conformations. We will examine the structural stability, harmonic dynamics and the thermodynamic stability of the model.

Tu-PM-D12 THE ROLE OF WATER AND IONS IN DETERMINING THE CONFORMATION OF THE DNA DOUBLE-HELIX, W.Fuller, A.Mahendrasingam, V.T.Forsyth, Department of Physics, University of Keele, Keele, Staffs. ST5 5BG (IUPAB Council Member, Introduced by L.D. Peachy).

Neutron fibre diffraction combined with D_2O/H_2O isotopic replacement has been used to determine the location of water around the D-form of the synthetic polynucleotide poly (d(A-T)). poly (d(A-T)) and the A-form of natural DNA. These studies at the Institut Laue Langevin, Grenoble complement experiments at the SERC Daresbury Laboratory Synchrotron Radiation Source (SRS) in which the variation in the x-ray fibre diffraction pattern has been recorded during structural transitions within the DNA double-helix induced by varying its degree of hydration. Fibre diffraction patterns were recorded in these experiments in $\sim$ 10 seconds using the FAST detector. The transitions studied include the D to B and A to B transitions in poly (d(A-T)).poly (d(A-T)) and the S to B transition in poly (d(G-C)).poly (d(G-C)). Isotopic replacement and anomalous scattering studies at the SRS have been used to investigate the location of ions around the D form of poly (d(A-T)).poly (d(A-T)). Information from x-ray fibre diffraction studies on the influence of the degree of hydration and the ionic content of the fibre on the conformation assumed by DNA shows the recent proposal by Saenger, Hunter and Kennard[1] that "hydration economics determines DNA conformation" is incorrect.

[1]Nature 324 385-388 (1986)

Tu-PM-E1 **MECHANICAL TRANSDUCTION IN GLIAL CELLS: SACS AND SICS.** J.P. Ding, C.L. Bowman, M. Sokabe, and F. Sachs. Biophysical Sciences, SUNY-Buffalo, Buffalo, NY 14214.

Rat astrocytes in primary cell culture exhibit four kinds of mechanically sensitive ion channels: three stretch-actvated (SACS) and one stretch-inactivated channel (SIC). The SACs have three different conductance levels, large, medium and small. The SIC may represent an entirely different gating mechanism from the SACs. SACs can be turned on by applying positive or negative hydrostatic pressure to the patch implying that membrane tension is the important variable. The SIC, on the otherhand, will inactivate with negative pressures, but not with positive pressure suggesting that membrane curvature may be the important variable controlling SIC gating.

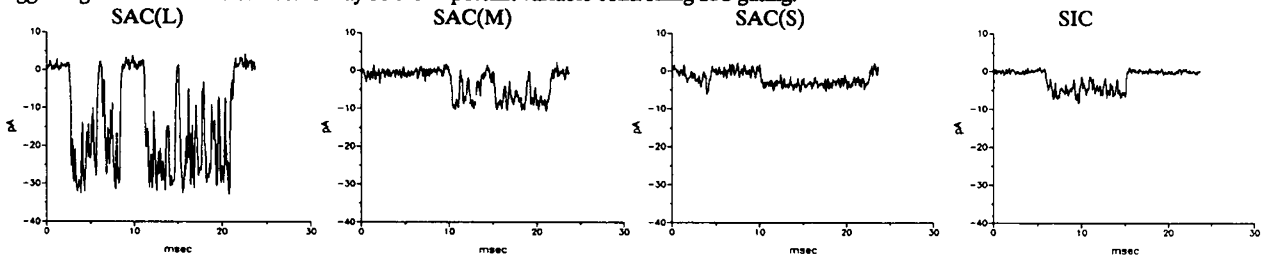

Supported by NIH NS-24891 (CB), DK-37792(FS) and USARO 22560-LS (FS).

Tu-PM-E2 *Zn^{++} AND H^+ INHIBIT Cl EFFLUX IN DEPOLARIZED FROG SKELETAL MUSCLE AT DIFFERENT SITES.* B.C. Spalding, P. Taber, J.G. Swift and P. Horowicz, Department of Physiology, University of Rochester Medical Center, Rochester, NY 14642.

It has been suggested that H^+ and Zn^{++} inhibit Cl channels in skeletal muscle by binding to the same site. We have measured the Cl efflux from depolarized frog sartorius muscles in solutions designed to examine this hypothesis. In all solutions tested, the dependence of Cl efflux rate coefficient on H^+ or Zn^{++} is fitted by a Hill equation of the form:

$$\text{rate coeff} = \frac{\text{constant}}{(1+(c[x])^n)}$$

where [x] is the external concentration of Zn^{++} or H^+. The results may be summarized as follows.

1. Increasing external H^+ enhanced inhibition by low Zn^{++} concentrations (<2 mM). When external pH was changed from 7.5 to 6.5, the enhancement at low concentrations was largely explained by a decrease in n from -1 to -0.5. The half-inhibition Zn^{++} concentration ($Zn_{1/2}$=1/c) was also slightly decreased ($Zn_{1/2}$≈1-2 mM).
2. Increasing external Cl^- at constant V_i protected against Zn^{++} inhibition. At pH 6.5, when [Cl^-] was increased from 135 to 390 mM, $Zn_{1/2}$ increased by an order of magnitude and n increased from -0.5 to -2.
3. An identical 3-fold increase in [Cl^-] had negligible effect on inhibition by H^+ (apparent pK_a of -6.5 was unchanged, n decreased slightly).

We conclude that H^+ and Zn^{++} inhibit Cl channels by different mechanisms, since H^+ enhances inhibition by Zn^{++}, while Cl^- protects against Zn^{++} inhibition but does not significantly affect H^+ inhibition.

(Supported by grants from the USPHS and the MDA.)

Tu-PM-E3 *NO_3^- DOES NOT PASS THROUGH pH-DEPENDENT Cl^- CHANNELS IN FROG SKELETAL MUSCLE.* B.A. Kotsias, and P. Horowicz, Department of Physiology, University of Rochester Medical Center, Rochester, NY 14642.

Hutter and Warner (1968) have reported that in frog muscle NO_3^- permeability is greater than Cl^- permeability at acid pH while Cl^- permeability is greater than NO_3^- permeability at alkaline pHs. Experiments were done to further examine this issue.

Membrane potential changes were measured in response to quick solution changes in single fibers initially equilibrated in isotonic, high K_2SO_4 solutions. The solutions were first changed to ones containing either Cs_2SO_4 or Rb_2SO_4 to replace the external K^+ and then to solutions containing either NO_3^- or Cl^- to replace SO_4^{2-}. The hyperpolarizations produced by external Cl^- depend on external pH, being smaller in acid then in alkaline solutions. Hyperpolarizations produced by external NO_3^- were independent of external pH over the range from 5.5 to 9.0.

In other experiments, voltage clamp studies were made on short toe muscle fibers. These were initially equilibrated in isotonic solutions containing mainly K_2SO_4 plus Na_2SO_4. To these solutions either KCl or KNO_3 were added. When equilibrated in these solutions the fibers had the same volume they had in the sulfate solutions before the additions. Constant hyperpolarizing voltage pulses of 0.5 to 1.0 sec duration were applied when all external K^+ was replaced by TEA^+. Under these conditions, inward currents flowing during the pulses were largely carried by Cl^- or NO_3^- depending on the final equilibrating solution. Cl^- currents during voltage pulses were both external pH and time dependent. By contrast, NO_3^- currents were independent of both external pH and time.

From these results we conclude that NO_3^- does not pass through the external pH, time dependent Cl^- channels but rather passes through a different class of channels.

REFERENCE: Hutter, O.F. and Warner, A.E. (1968). *J. Physiol. (Lond.)* 194: 61P-62P.

(Supported by grants from the USPHS and MDA).

Tu-PM-E4 A cAMP-REGULATED CHLORIDE CHANNEL IN T-LYMPHOCYTES WHICH IS AFFECTED IN CYSTIC FIBROSIS
P. Gardner*, J. Chen, and H. Schulman. Dept. of Medicine and Pharmacology, Stanford University, Stanford, CA 94305.

A defect in cAMP-dependent regulation of chloride (Cl^-) channels appears to be the molecular basis for cystic fibrosis (CF). Using patch clamp recording, we have demonstrated that the CF Cl^- channel is present in both T- and B-lymphocyte cell lines. When membrane patches are excised from cells into media containing sufficient free calcium ($>10^{-8}$M) and depolarized, Cl^- channels with an outwardly rectifying I-V relation and slope conductance of 40 pS at 0 mV, were activated in approximately 50% of patches. The channel could be activated on-cell infrequently by sustained strong depolarization or frequently by exposure of the cell to 8-bromo-cAMP (10^{-4}M). The regulatory effect of cAMP was further investigated by exposing the cytoplasmic surface of inside-out patches to catalytic subunit of cAMP-dependent protein kinase (C-subunit) plus ATP (1 mM). C-subunit plus ATP activated Cl^- channels with properties identical to those activated on-cell by 8-bromo-cAMP, implying a phosphorylation event. Importantly, cAMP-dependent protein kinase regulation of transformed B-cells from CF patients is defective. We have further noted that calcium ionophore A23187 (10^{-7}M) activates Cl^- in on-cell patches from both normal and CF cells. Alternative phosphorylation pathways which are preserved in CF are currently being investigated. We conclude that lymphocytes may serve as an accessible source of CF tissue for study of this defect and for cloning of the chloride channel complex.

Tu-PM-E5 IONOMYCIN ACTIVATES A POTASSIUM-SELECTIVE CONDUCTANCE IN HUMAN T LYMPHOCYTES.
Stephan Grissmer and Michael Cahalan, Department of Physiology & Biophysics, UC Irvine, CA 92717.

In the human T-cell-derived cell line Jurkat E6-1 we investigated the effect of the Ca^{2+}-ionophore ionomycin on the conductance properties measured between -90 mV and -50 mV. To measure the ionomycin effect under physiological conditions, we used the perforated-patch method (Horn and Marty, *J. Gen. Physiol.* 92:145-159). An example of original ramp current traces is shown in the left side of the figure. The traces are recorded in normal Ringer (trace 1), K-Ringer (2,5), and K-Ringer + 100 nM ionomycin (3,4). The slope conductance measured by fitting a line through the ramp current trace between -90 mV and -50 mV is about doubled in K-Ringer (trace 2) compared to normal Ringer (trace 1); transiently increased about 10-fold (trace 3) compared to K-Ringer after application of 100 nM ionomycin; reached a plateau in K-Ringer + ionomycin about 4 times that in K-Ringer (trace 4); and recovered almost completely after washing out the ionomycin (trace 5). The time course of these changes is best seen on the right side of the figure, where the slope conductance g is plotted at different times. The numbers correspond to the traces shown at the left side. Measurements with the Ca^{2+}-indicator Fura-2 showed that $[Ca^{2+}]_i$ increased after application of 100 nM ionomycin, reached a peak and decreased again to above resting levels. Thus the induction of the slope conductance could parallel the increase in $[Ca^{2+}]_i$, indicating a Ca^{2+}-activated conductance. Supported by the DFG (Gr 848/2-2) and by NIH grants NS14609 and AI21808.

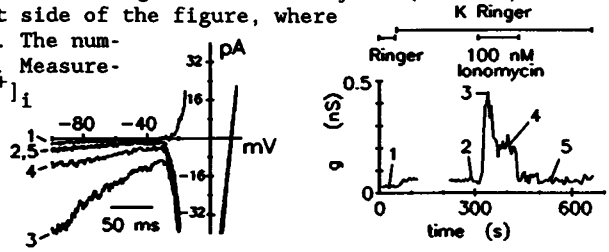

Tu-PM-E6 MECHANISMS FOR OPENING STRETCH-ACTIVATED ION CHANNELS.
R.D. MacGregor†, F. Sachs§ and C.A. Hunt†. †School of Pharmacy, University of California, San Francisco CA 94143 and §Department of Biophysical Sciences, State University of New York, Buffalo NY 14214

The energy required to open a stress-activated ion channel in chick skeletal muscle appears to be gathered from a large area ($>3x10^5 Å^2$) of the plasma membrane (Guharay and Sachs, J. Physiol. 352, 685,1984). However, the mechanism by which this energy is used to open the channel is not known. One model (*ibid*) has the channel protein at the hub of a cytoskeletal network, such that stress applied to the membrane is applied directly to the channel protein via the cytoskeletal elements.

Here we present an alternative model for the opening of stress-activated ion channels, where channel opening results from a movement of the channel protein either into or within the lipid bilayer. We assume 1) the membrane cytoskeleton inhibits the diffusion of lipid molecules on the inner membrane leaflet, 2) application of stress to a membrane causes the membrane to be stretched 3) with the energy of the stretched membrane being distributed between the cytoskeleton and the plasma membrane lipid, and 4) that the energy in the stretched lipid can be used to drive the movement of the channel protein. One type of movement was selected to model the process. We posit that the movement can be represented as the absorption of a membrane-spanning cylindrical protein segment into the bilayer (characterized by a radius and a free energy of transfer from the aqueous phase into the membrane lipid), and that this absorption switches the channel from a closed to an open state. We derive equations to predict the probability that a channel is in the open state as a function of the pressure applied to a patch clamp used to stress the membrane and monitor channel activity. We demonstrate that this theory adequately mimics experimental channel open probability versus pipette pressure data (*ibid*) and that the same model parameters mimic the response of cytochalasin B treated cells if it is hypothesized that this treatment prevents the cytoskeleton from sustaining membrane stress (i.e. all stress applied to the membrane is sustained by the lipid bilayer).

Tu-PM-E7 DRUG INDUCED SHIFTS IN MEASURES OF CHANNEL AVAILABILITY DO NOT NECESSARILY REFLECT MODIFIED GATING KINETICS. C. F. Starmer, F. R. Gilliam, V. V. Nesterenko and A. O. Grant. Duke University Medical Center, Durham, N. C. and Inst. of Exp. Cardiology, All Union Cardiology Research Center, Moscow, USSR. Intr. by J.M. Kootsey.

When channel blockade exhibits dependence on membrane potential, the "apparent" activation, m^*, and inactivation, h^*, appear modified. If blockade increases monotonically with potential, we show that m^* and/or h^* are obligated to shift in the hyperpolarizing direction in the absence of modified gate kinetics. Thus distinguishing between properties of the drug-channel interaction and possibly modified channel kinetics is ambiguous. Using Armstrong's TEA^+ model and voltage independent binding and unbinding rates, $m^* = [1+(1+D/k_D)\exp(V-V_m)/s]^{-1}$ with a midpoint shift of $s*\ln(1+D/k_D)$ where s is the slope factor of the drug-free Boltzmann characterization, k_D is the equilibrium dissociation constant and D is the drug concentration. For tertiary agents blocking inactivated channels where trapping of the charged moiety is assumed, the shift is similar but no longer parallel and $h^* = [1+[1+D/k_D(1+k_pH^+/l_p)]\exp(V-V_h)/s]^{-1}$ where k_p and l_p are rates of protonation and deprotonation. Studies of 80 μM lidocaine block found a k_D of 8.8 μM yielding a shift of 14 mV compared with a predicted shift of 15 mV. Approximating k_pH^+/l_p by an exponential, p exp(qV), and using control values for V_h, s and k_D, both the shift and shape of the lidocaine induced changes in h^* were accurated predicted. We conclude that constant affinity binding can lead to shifts in apparent m or h that do not reflect modified gating kinetics.

Tu-PM-E8 ADRENERGIC AGONISTS MODULATE THE MEMBRANE CONDUCTANCE OF PATCH-CLAMPED BROWN FAT CELLS. M.T. Lucero & P.A. Pappone, Department of Animal Physiology, University of California, Davis, CA 95616.

Microelectrode recordings from brown fat cells show that they respond to adrenergic stimulation with a triphasic membrane potential response that has been postulated to play a role in regulating the tissue's thermogenic activity. We had previously examined whole-cell patch-clamped cultured brown fat cells and had found no membrane responses to norepinephrine (NE) under a variety of conditions. We report here that cultured brown fat cells have membrane responses to adrenergic agonists when recordings are made using the "slow patch" technique (Horn & Marty, J. Gen. Physiol., 92:145, 1988). Current-clamped brown fat cells from 5-22 day primary cultures from neonatal rats had resting membrane potentials averaging -47±3 mV (n=17). Application of <500 nM NE resulted in a hyperpolarization of E_m which began within a few seconds of NE application, and increased E_m to maximal potentials 10 to 12 mV negative to the resting potential within 10 to 15 seconds. The membrane hyperpolarization was transitory, and recovery of the original resting potential was often followed by multiple hyperpolarizing oscillations in E_m occurring at a rate of 1-1.5/min. Application of NE to voltage-clamped cells showed that the hyperpolarizing response is due to an increase of 1 to 2 nS in the membrane conductance, probably due to opening of calcium-activated K channels based on the negative reversal potential of the NE-induced currents and the sensitivity of the conductance increase to block by apamin. Oscillations in the NE-induced outward currents were also present when the cells were voltage clamped at -60 mV, and had a similar frequency as that seen in current clamp experiments. Stimulation with specific agonists indicate that the NE-induced conductance is regulated by an α-adrenergic receptor. These results show that cultured brown fat cells are capable of membrane responses to NE and that these responses require some cytoplasmic constituent which is lost in conventional whole-cell experiments. This work was supported by NIH grant AR34766 and a Jastro Shields Fellowship.

Tu-PM-E9 ANGULAR DEPENDENT CIRCULAR DICHROISM OF ORIENTED α-HELICES

Glenn A. Olah and Huey W. Huang, Physics Dept., Rice University, Houston, TX 77251

The assignment of the 192nm and the 208nm circular dichroism (CD) bands of α-helices as exciton split components of the peptide ππ* transition has recently been cast in doubt [Yamaoka et al., J. Am Chem. Soc. 108, 4619 (1986)]. By measuring the linear dichroism of electric field oriented polypeptides they concluded that the 208nm band was not polarized parallel to the α helix axis which is contrary to the prediction of the exciton theory . We measured the CD of electric field oriented polypeptides and also showed an apparent disagreement with the exciton theory ; however, our data was reconciled with the theory when the bending flexibility of the long polypeptides was taken into account. To circumvent using long polypeptides we developed an elaborate method for measuring the CD of bulk oriented short α helices (alamethicin) by embedding them into a stacked defect-free lipid/H_2O multilayer system. This method basically involves tilting the helices at various angles with respect to the incident light. Most importantly, this method eliminates the linear dichroic and birefringent distortions on the CD spectra arising from the oriented nature of the multilayers themselves. In this way, we unequivocally showed the 208nm band to indeed be polarized parallel to the α helix axis. Since many interesting membrane proteins have α helical transmembrane sections, we suggest that knowing the angular dependence of their CD spectra would be useful for a conformation and/or orientation analysis of these proteins.

* Supported in part by ONR, NIH, and Welch Foundation.

Tu-PM-E10 **THE MECHANISM OF COLICIN E1 CHANNEL FORMATION: pH-DEPENDENT UNFOLDING AND MEMBRANE POTENTIAL-DEPENDENT INSERTION INTO THE LIPID BILAYER.** A. R. Merrill and W. A. Cramer (Intr. by C. Post), Dept. of Biological Sciences, Purdue University, West Lafayette, IN, 47907.

Channel formation in vitro by colicin E1 requires (I) acidic pH and (II) a trans-membrane potential. The pH dependence is expressed at several levels: (i) a pH-dependent conformational change, discussed here, (ii) charge neutralization required for binding to the membrane and initial insertion, and (iii) pH-dependent single channel conductance and ion selectivity of the inserted channel. Acidic pH causes (i) unfolding and exposure of a hydrophobic domain as indicated by greater partition of colicin E1 into Triton-X-114 at pH 3.5 relative to 6, and (ii) solvent exposure of Cys-505, the only cysteine in the molecule, near the COOH-end of the 35 residue hydrophobic segment. Cys-505 was labeled 1:1 under denaturing conditions with the cysteine-specific reagent, 5-[2-((iodoacetyl)amino)ethyl]aminonapthalene-1-sulfonic acid (IAEDANS). The resulting renatured peptide was fully active. The quenching of IAEDANS fluorescence by acrylamide was: pH 3.5 > 6.0, for peptide in solution; pH 6.0 < pH 3.5, for peptide inserted into liposomes. (II) Labeling of the peptide at pH 4.0 by the lipophilic reagent, [^{125}I]-TID, incorporated into membrane vesicles was 33 $\pm$ 14% (5 trials) larger in the presence of a K^+-diffusion potential of -100 mV compared to a 0 mV control. Labeling under similar conditions but at pH 6.0 (no channel formation), resulted in negligible labeling of the peptide in both the presence and absence of a membrane potential. This indicates that insertion of a significant fraction of the bound channel peptide into the bilayer is associated with voltage gating of the channel. [Supported by NIH GM-18457 (WAC) and a Canadian NSERC Fellowship (ARM).]

Tu-PM-F1 CHOLESTEROL MODIFIES SHORT-RANGE REPULSION BETWEEN PHOSPHATIDYLCHOLINE MEMBRANES. T.J. McIntosh, A.D. Magid, and S.A. Simon, Departments of Cell Biology, Neurobiology, and Anesthesiology, Duke University Medical Center, Durham, N. C. 27710.

Pressure (P) versus fluid separation (d_f) relations have been measured for egg phosphatidylcholine (EPC) bilayers containing 0 to 0.5 mole fraction cholesterol by x-ray diffraction analysis of bilayers squeezed together by osmotic pressures up to 2600 atmospheres. For this range of cholesterol concentrations, the pressure-distance curves are nearly the same for 5 Å < d_f < 15 Å, implying that cholesterol has a relatively small effect on the repulsive hydration pressure. However, for d_f < 5 Å, the incorporation of cholesterol has a marked effect on the pressure-distance relation. For pure EPC bilayers there is a distinct upward break in the plot of log P versus d_f at d_f = 5 Å, which we have attributed to the onset of steric hindrance between apposing PC head groups (McIntosh et al., Biochemistry 26, 7325). The incorporation of cholesterol reduces this upward break by an amount that depends on cholesterol concentration. For bilayers containing 0.5 mole fraction cholesterol there is no break in the log P vs d_f curve, and electron density maps show that the high density head group peaks from apposing bilayers merge at high applied pressures. We interpret these data in terms of a model where cholesterol spreads apart the PC molecules in the plane of each bilayer, reducing the volume fraction of PC head groups. This reduces the steric repulsion between head groups from apposing bilayers, and, at equimolar cholesterol concentrations, allows PC head groups from apposing bilayers to interpenetrate as the bilayers are forced together.

Tu-PM-F2 THE MAGNITUDE OF HYDRATION REPULSION BETWEEN NEUTRAL BILAYERS DEPENDS ON DIPOLE POTENTIAL. S. A. Simon, A. D. Magid, and T. J. McIntosh (Intr. by J. M. Corless), Departments of Neurobiology, Anesthesiology, and Cell Biology, Duke University Medical Center, Durham, N. C. 27710.

The close approach of adjacent neutral bilayers is resisted by the solvation (hydration) pressure, which arises from the polarization of solvent molecules by the membrane surface. It has been found empirically that the solvation pressure decays exponentially with increasing bilayer separations, d_f, such that $P = P_0 \exp(-d_f/\lambda)$, where λ is proportional to the cube root of the solvent's molecular weight, and is 1 to 2 Å for water. However, the physical and chemical factors that determine the magnitude and plane of origin of P are not well understood. We have hypothesized that the magnitude of the hydration potential is proportional to the dipole potential (V_d) and that the perpendicular component of the electric field polarizing the solvents is proportional to V_d/λ. We have tested this hypothesis by varying V_d in three ways: (1) by analyzing different lamellar phases of zwitterionic phosphatidylcholines (PC) and uncharged monoglycerides, (2) by using non-aqueous solvents between PC bilayers, and (3) by incorporating different amounts of cholesterol in the bilayer. P_o and λ were measured by x-ray diffraction analysis of bilayers squeezed together by osmotic pressure, and V_d was measured for monolayers in equilibrium with bilayers. For the range of 200 mV < V_d < 550 mV, P_o ranged from 9×10^7 to 5×10^9 dyn/cm^2 with the plane of origin defined as the physical edge of the bilayer. Our results indicate that P_o can be estimated from the relation $P_o = 2\chi (V_d/\lambda)^2$, where χ is the orientational susceptibility. These observations suggest a common mechanism for the action of a wide range of membrane fusogens that reduce V_d and would therefore be expected to reduce the repulsive solvation pressure between membranes.

Tu-PM-F3 NON-LAMELLAR PHASES AND CHAIN ORDER PROFILE IN MYRISTIC ACID/DIMYRISTOYL PHOSPHATIDYLCHOLINE 2:1 (MOLE/MOLE) MIXTURE. N.J.P. Ryba, T. Heimburg and D. Marsh, Max-Planck-Institut f. biophysikalische Chemie, Abt. Spektroskopie, D-3400 Goettingen, Fed. Rep. Germany.

Aqueous dispersions (pH 4.0) of a 2:1 mole/mole mixture of myristic acid (MA) with dimyristoyl phosphatidylcholine (DMPC) undergo a sharp calorimetric transition at 43°C from a lamellar gel phase to a fluid non-lamellar phase. The symmetry and dynamic properties of the fluid phase have been investigated with ^{31}P NMR of the DMPC component and with ^{2}H NMR of the specifically deuterated or perdeuterated MA and DMPC components. The NMR spectra consist of a mixture of two components with isotropic and cylindrical symmetry, respectively. Immediately above the phase transition the spectra are solely isotropic, and with increasing temperature the cylindrical component increases at the expense of the isotropic component. The isotropic component corresponds to a cubic phase, most probably with space group Pn3m, and the cylindrical component to an inverted hexagonal H_{II} phase. At any given temperature, the proportion of the H_{III} spectral component is greater for MA than for DMPC, indicating a compositional heterogeneity or phase separation in the fluid phase. The chain order parameter profile in the H_{II} phase of the mixture differs from that in the fluid lamellar phase of DMPC alone. At an equivalent temperature above the chain melting phase transition, the order parameter "plateau" region is shorter in the H_{II} phase. The chain order profile for MA is shifted relative to that of DMPC, demonstrating that the fatty acid is located deeper in the hydrophobic region of the H_{II} phase.

Tu-PM-F4 STRUCTURE AMD METASTABILITY OF N-PALMITOLEOYL GALACTOSYL-CEREBROSIDE BILAYERS.
N.S. Haas and G.G.Shipley, Biophysics Institute, Boston University School of Medicine, Boston, MA 02118.

Differential scanning calorimetry (DSC) and x-ray diffraction have been used to study hydrated N-palmitoleoyl galactosyl-cerebroside (NPGC) bilayers. DSC of fully hydrated NPGC shows endothermic transitions at 31, 39, and 51°C indicative of polymorphic or metastable phase behavior. Upon cooling there is a single exothermic transition at 18°C (ΔH = 7.2 kcal/mol). After heating NPGC from -10°C to 45°C and immediately recooling, the exothermic transition is no longer observed; immediate reheating shows only a high temperature transition at 53°C (ΔH = 12.8 kcal/mol). Incubation at low temperatures (e.g. -10°C) also promotes complete conversion to the high melting (Tm=53°C) form. Thus, the transitions at 31 and 39°C appear to be due to metastable phases of hydrated NPGC, whereas the high temperature transition (Tm=53°C, ΔH = 12.8 kcal/mol) is associated with the stable form of NPGC. X-ray diffraction data recorded at 0, 45, and 65°C show the presence of NPGC bilayers at all temperatures. At 65°C, lamellar reflections (h=1⇒4) corresponding to a bilayer periodicity d=48Å are observed, together with a diffuse wide angle reflection at 1/4.5Å characteristic of a melted chain L_α bilayer phase. Below Tm, bilayer phases (d=55Å) with crystalline chain packing modes are indicated by the presence of multiple reflections in the wide angle region. In some cases additional diffraction lines are observed in the low angle region suggesting either more complex lipid phase structures or the presence of the metastable bilayer phases.

Tu-PM-F5 SHAPES OF TWO-DIMENSIONAL LIPID DOMAINS NEAR A CRITICAL POINT,
Harden M. McConnell, Stauffer Laboratory for Physical Chemistry, Stanford, CA 94305

Evidence based on epifluorescence microscopy shows that a binary mixture of cholesterol and dipalmitoylphosphatidylcholine (DPPC) can exhibit two immiscible fluid phases in monolayers at the air-water interface (1). The abrupt appearance and disappearance of domains of these phases at pressures of the order of 10 dynes/cm and 30 mole% of cholesterol indicates that this is a mixing-demixing critical point. We discuss the shapes of these fluid domains as one approaches this critical point from the two-phase side of this point.The sizes, shapes and shape transitions of finite two-dimensional lipid domains can be characterized theoretically by distance parameters $d \sim \delta \exp(\lambda/\mu^2)$, where δ is an intermolecular distance (~ 10 Å), λ is the line tension separating the domains, and μ is the difference in the dipole densities in the two phases (2). Both λ and μ approach zero as the critical point is approached. For two-dimensional systems it can be shown that the ratio λ/μ^2 should also approach zero. For a helpful reference, see (3). The decreasing values of d are then theoreticaly expected to lead to distortions of domain shapes from circles, and to domain fission. These effects are observed experimentally (1). Domain widths in the parallel stripe phase (4,5) are predicted to become small and fall below optical resolution. I am indebted to B. Widom for helpful correspondence. This work was supported by National Science Foundation Grant DMB 8619320.
(1) S. Subramaniam & H. M. McConnell, J. Phys. Chem. 91, 1715-1718 (1987). (2) H.M. McConnell & V.T. Moy, J. Phys. Chem.92, 4520-4525 (1988). (3) Rowlinson & Widom, Molecular Theory of Capillarity, Oxford Press (1982). (4) Andelman et al. J. Chem. Phys. 86, 3673-3681 (1987). (5) D.J. Keller, H.M. McConnell & V.T. Moy J. Phys. Chem. 90, 2311-2315 (1986).

Tu-PM-F6 SPECTROSCOPIC STUDIES OF THE EFFECTS ON MOLECULAR ORDER AND DYNAMICS IN PHOSPHOLIPID MODEL MEMBRANES OF THE INTERACTION OF VITAMIN E WITH FATTY ACID ACYL CHAINS.
Stephen R. Wassall*, Timothy M. Phelps*, Lijuan Wang*, Regina C. Yang*, William Ehringer† and William Stillwell†, Departments of Physics* and Biology†, Indiana University-Purdue University at Indianapolis, Indianapolis, IN 46223.

Structural roles within the membrane, in addition to the generally accepted antioxidant function, have been hypothesized for α-tocopherol (the main constituent of vitamin E). Membrane stabilization via interactions between α-tocopherol and unsaturated fatty acyl chains form the basis of the proposals.

ESR of doxyl spin labelled stearic acids intercalated into DMPC (dimyristoyl (14:0) phosphatidylcholine), DOPC (dioleoyl (18:1) PC), dilinoleoyl (18:2) PC, dilinolenoyl (18:3) PC and diarachidonoyl (20:4) PC membranes shows that α-tocopherol increases order and decreases fluidity to a greater degree when the phospholipid chains are saturated than when there is unsaturation. Fluorescence polarization studies provide complementary measurements. Moment analysis of broadline ^2H NMR spectra for [$^2H_{62}$]DPPC and [$^2H_{62}$]DPPC/linoleic (18:2) acid (4:1 molar ratio) membranes indicates that the perturbing influence of α-tocopherol on membrane order and phase behaviour is substantially reduced in the presence of the unsaturated free fatty acid. The proposals of membrane stabilization by vitamin E are discussed in the light of these results.

Tu-PM-F7 X-RAY DIFFRACTION AND CALORIMETRIC STUDIES OF HYDRATED C(8):C(18)PHOSPHATIDYLCHOLINE (PC) and C(10):C(18)PC, J.Shah, P.K.Sripada and G.G.Shipley, Biophysics Institute, Boston University School of Medicine, Boston, MA 02118.

C(18):C(10)PC and C(18):(12)PC form mixed interdigitated bilayers. Here we report the thermotropic and structural behavior of C(8):C(18)PC and C(10):C(18)PC (which have the equivalent chain length ratio of C(18):C(10)PC and C(18):C(12)PC respectively). C(8):C(18)PC was studied as a function of hydration. For fully hydrated C(8):C(18)PC the reversible chain melting transition was observed at 8.1°C (H=6.8 Kcal/mol). X-ray diffraction at 0°C showed a small bilayer repeat distance d=50.2 A° and a sharp, symmetric wide angle reflection at 4.1 Å, characteristic of mixed interdigitated bilayer. At 30°C (above the chain melting transition) a diffuse reflection was observed at 4.5 Å with d=60.29 Å. The lipid bilayer thickness (d_{p-p}) determined from the electron density profiles shows that d_{p-p} increases as a consequence of chain melting ($d_{p-p}(0°C)=27A°$ and $d_{p-p}(30°C)=31A°$). However, fully hydrated C(10):C(18)PC shows an asymmetric transition at 11.8 °C. At 0 °C, the x-ray diffraction pattern shows two lamellar phases corresponding to co-existing interdigitated and non-interdigitated phases. Probably C(10):C(18)PC lies at the boundary; increasing sn-1 chain length gives stable non-interdigitated (2-chain) bilayers and decreasing sn-1 chain length leads to stable mixed interdigitated (3-chain) bilayers (see C(8):C(18)PC).

Tu-PM-F8 THEORY OF THERMAL ANOMALIES IN THE SPECIFIC HEAT OF LIPID BILAYERS CONTAINING CHOLESTEROL

J. H. Ibsen and O.G. Mouritsen, Technical University of Denmark, Lyngby, Denmark and M.J. Zuckermann, McGill University, Montreal, Canada

The presence of cholesterol in lipid multilayer systems leads to the occurence of thermal anomalies in the specific heat. In particular, the specific heat of lipid cholesterol bilayer systems is composed of a sharp componant with an associated entropy which decreases with increasing cholesterol concentration and a broad componant whose associated entropy exhibits a maximum as a function of cholesterol concentration. In a previous publication , we proposed a microscopic interaction model which took account of both the crystalline and chain conformation degrees of freedom plus the effects of cholesterol firstly as an "ice-breaker" for the crystal and, secondly, having a tendency to order neighbouring lipid acyl chains. Mean field calculations using this model gave a phase diagram which corresponded to the experimental phase diagram obtained from the nuclear magnetic resonance experiments of Davis. Here we present the results of a calculation for the specific heat of lipid-cholosterol bilayers using the model described above in the mean field approximation. The parameters use the same as those used to obtain the calculated phase diagram. The calculated specific heat exhibited both the sharp and broad components found experimentally. This implies that no special mechanisms such as complexing need be invoked.

Tu-PM-F9 Modification of Lipid Vesicles with Membrane Bound Carbohydrates: Stabilization During Freezing and Drying. Raymond P. Goodrich and John D. Baldeschwieler. California Institute of Technology, Department of Chemistry and Chemical Engineering, Noyes Lab, 127-72, Pasadena CA 91125.

The freeze drying of biological membranes is detrimental to the structural integrity of the membrane. This damage is induced in part by the removal of water from the phospholipid component of the membrane. The result is fusion, lipid phase transition, and leakage of vesicle contents. We have prepared a series of compounds which prevent this drying induced damage to liposomal membranes composed of Egg PC or POPC. Only 2-5% lipid mixing as measured by the RET assay and 0-10% leakage of the aqueous marker carboxyflourescein occurs when the ratio of protective agent to lipid reaches a value of 0.25 mole/mole. At this molar ratio, alterations in the phosphate, carbonyl, and choline moieties of the phospholipids are observed by Raman and FT-IR spectroscopies. Lipid phase behavior in the acyl chain region, as monitored by DSC, is also modified. Gel to liquid crystalline transition temperatures are driven downward by as much as 50-60 degrees Celsius. The membrane alterations can be associated with direct interaction of the protective agents with the membrane in the dry state. These interactions in turn induce effects which are normally associated with the presence of water. The extent of this interaction is dependent on specific structural requirements for the protective agent. Compounds deviating from these requirements are ineffective. This work was supported in part by a National Research Service Award (T32 GM07616) from the National Institute of General Medical Sciences, grant no. DAAG-29-83-K-0128 from the ARO, and a gift from Monsanto.

Tu-PM-F10 INFLUENCE OF DOMAINS OF INTERDIGITATED LIPID BILAYER ON THE STRUCTURAL ORGANIZATION OF SURROUNDING LIPIDS. **Joan M. Boggs, Biochemistry Dept., Research Institute, Hospital for Sick Children, Toronto, CANADA, M5G 1X8.**

The antibiotic Polymyxin B (PMB) is known to cause the acidic lipid dipalmitoylphosphatidylglycerol (DPPG) to form a fully interdigitated bilayer below its phase transition temperature, when added in a 1:5 mole ratio, where it saturates the lipid (1). If PMB-unbound lipids are also present, such as DPPG or dipalmitoyl phosphatidic acid (DPPA) at non-saturating concentrations of PMB, or neutral lipids which do not bind PMB, such as dipalmitoylphosphatidylcholine (DPPC) or dipalmitoylphosphatidylethanolamine (DPPE), they will tend to form a non-interdigitated bilayer. The structural incompatibility of interdigitated and non-interdigitated domains in the same bilayer suggests that the unbound lipids must either phase separate into a non-interdigitated structure or become interdigitated along with the PMB-bound lipid. In order to study the forces which determine which of these two possibilities occurs, the percentage interdigitated lipid in mixtures of PMB-bound lipid with unbound lipids was determined using long chain spin labels with the nitroxide group located near the terminal methyl of the chain. These spin labels are more motionally restricted in the interdigitated than in the non-interdigitated gel phase bilayer (2). This allows determination of the percentage interdigitated lipid by resolution of the spectrum into motionally restricted and more mobile components. The results indicated that unbound lipid can become interdigitated along with the PMB-bound lipid and that increasing negative charge of the unbound lipid increases its tendency to become interdigitated, participation of the unbound lipid in intermolecular hydrogen bonding inhibits its own interdigitation and also that of the PMB-bound lipid, and a decrease in fatty acid chain length of the unbound lipid relative to the PMB-bound lipid promotes its interdigitation.

1. *Ranck, J.L. and Tocanne, J.F. (1982) FEBS Lett. 143, 175-178;*
2. *Boggs, J.M. and Rangaraj, G. (1985) Biochim. Biophys. Acta 816, 221-233.*

Tu-PM-F11 FLUORESCENCE ENERGY TRANSFER AS A SPECTROSCOPIC GONIOMETER. TOWARDS A VECTORIAL THEORY OF TRANSFER POLARIZATION.

B. Wieb Van Der Meer, Department of Physics and Astronomy, Western Kentucky University, Bowling Green, KY 42101. (502) 745-5003

The orientation factor in Fluorescence Energy Transfer (FET) is usually considered to be a nuisance limiting the accuracy of FET as a spectroscopic ruler. Our point of view is that this factor is a source of orientational information which is most clearly seen in a FET polarization experiment. FET Polarization can be used as a spectroscopic goniometer. We consider two limits:

1. the orientational diffusion of Donor and Acceptor is slow compared to the fluorescence lifetime of the Donor and to 1/k, where k is the rate of transfer.
2. this diffusion process is fast.

In both limits we derive expressions for the fluorescence anisotropy (FA) in the case of exciting the Donor and looking at emission from the Acceptor. The analogy with single probe FA suggests an interpolation between these two limits. An application to membranes is a "double probe" FA method: Measuring in membranes 1) the FA from a Donor only 2) the FA from an Acceptor only 3) the transfer FA from a Donor to an Acceptor. The combination of results from 1, 2, and 3 gives information on orientational order and dynamics. Homotransfer and heterotransfer will be discussed.

We thank Joe Beechem for an illuminating discussion on time scales of diffusion and transfer.

Tu-PM-F12 ORDER AND HYDROGEN BONDING FOR MEMBRANE LIPIDS STUDIED BY FT-IR

G. Lindblom, A. Holmgren, L.B-Å Johansson, L. Rilfors, Å. Wieslander* and A. Nilsson.

Departments of Physical Chemistry and Biochemistry*, University of Umeå, S-901 87 Umeå, Sweden.

Fourier-transform infrared linear dichroism (FT-IR-LD) was measured for bilayers of 1,2-dioleoyl-δn-glycero-3-phosphocholine (DOPC), 1-octanoyl-δn-glycerol (monooctanoin), and 1-oleoyl-δn-glycerol (monoolein) in H_2O and D_2O. Order parameters were determined for vibrational modes in the acyl chain region of the bilayer, the backbone region and the head group region. The two acyl chains in DOPC are more ordered than the single chains in monooctanoin and monoolein. Intramolecular hydrogen bonding was shown to occur in the monoglycerides. FT-IR spectra of water in lamellar, cubic and reversed hexagonal phases formed by the DOPC/monoolein/water system indicate a pertubation of water molecules as compared with bulk water. Furthermore, the results suggest a hydrogen bonding interaction between DOPC and monoolein.

Monoglucosyldiglyceride (MGDG) and diglucosyldiglyceride (DGDG), isolated from membranes of *Acholeplasma laidlawii*, show strong lipid-lipid interactions in CCl_4 and $CHCl_3$. Even at high temperatures (55 °C) and low concentrations (10^{-3} M), the hydrogen bonding features of the spectra are retained.

Tu-PM-G1 BIOSYNTHETIC INCORPORATION OF L-[4-C13]-ASPARTIC ACID INTO BACTERIORHODOPSIN.
S. L. Siemsen, S. L. Helgerson and E. A. Dratz, Chemistry Department, Montana State University, Bozeman, MT 59717.

Bacteriorhodopsin (bR) is an integral membrane protein synthesized by H. halobium. A number of structure/function analysis techniques, including solid state NMR and FTIR difference spectroscopy, require bR enriched with isotopically labeled amino acids. We have investigated the incorporation of [U-C14] aspartic acid into bR when grown using synthetic media and normal aeration. Exogenous asp is not required for growth of H. halobium. There are conflicting results in the literature defining other essential and non-essential amino acids derived from asp (asparagine, isoleucine, methionine, lysine and threonine). The requirement for glutamate was also determined since asp metabolized via the TCA cycle can incorporate carbon into glu. Met, ile and lys are all essential and are not produced significantly from added asp. Thr, asp and glu are non-essential. The exogenous asp concentration needed for the most efficient incorporation of [4-C14] asp into bR was determined. Asp concentrations reported in the literature did not give the most efficient incorporation under our growth conditions. Amounts above and below our optimal concentration (.25 g/l) resulted in decreased efficiency. Reverse-phase HPLC of the phenylthiocarbamyl amino acid derivatives showed that 70% of the carbon 14 label remained in asp, while 20% was incorporated into glu and 10% into thr. When grown with [4-C13] asp the overall isotopic enrichment ranged from 23% to 83%. The higher and lower enrichment corresponded to a slower and faster biosynthetic rate of bR production, respectively. Solid state NMR spectra of [4-C13] asp enriched bR in purple membrane and blue membrane will be compared. (Supported by NIH 1 RO1 EY06913 and ONR N00014-87-K-0278.)

Tu-PM-G2 ASPARTIC ACID SUBSTITUTIONS AFFECT THE QUANTUM YIELD AND KINETICS OF PROTON RELEASE AND UPTAKE BY BACTERIORHODOPSIN.
T. Marinetti+, S. Subramaniam*, T. Mogi*, T. Marti* and H.G. Khorana*. +Rockefeller University, New York NY 10021 and *Depts. of Chemistry and Biology, MIT, Cambridge MA 02139.

We report time-resolved conductivity measurements of light-induced H^+ release and uptake for a series of bacteriorhodopsin mutants carrying Asn or Glu substitutions at one of the putative membrane-buried aspartic acid residues (85, 96, 115 and 212). For the Asp 96→Asn mutant, H^+ uptake was slowed 25-fold with no observable effect on the release step. For Asp 85→Asn, H^+ uptake occurred with normal kinetics but the yield was significantly lower compared to Asp 96→Asn or wild type, especially at pH 6. Substitution of Asp 85 or Asp 96 by Glu had smaller but detectable effects on the kinetics and quantum yield of H^+ movements. Both Asn and Glu substitutions at positions 115 and 212 lowered the quantum yields compared to wild type. Of these, only the Asp 115→Glu mutant showed an effect on the H^+ release step, and only the Asp 212→Glu mutation decreased the H^+ uptake rate. These experiments, which directly measure the H^+ transfers to and from the aqueous phase, imply an obligatory role for Asp 96 in H^+ uptake in the normal operation of the proton pump. Our results also indicate that the H^+ release and uptake steps occur independently of each other following initiation of the photocycle.

Supported by grants from O.N.R., N.I.H. and N.S.F. to H.G.K.*, D.R.G. 937 to S.S.* and from N.I.H. to T.M+.

Tu-PM-G3 **STRUCTURAL STABILITY OF BACTERIORHODOPSIN POINT MUTATIONS OF CHARGED RESIDUES IN HELIX C AND G**
1Christie G. Brouillette, 2Tatsushi Mogi, 2Lawrence J. Stern, and 2H. Gobind Khorana . 1 Dept. of Medicine, Univ. of Alabama Med. Ctr., Birmingham, AL. 35294; 2 Depts. of Biology and Chemistry, M.I.T., Cambridge, MA 02139)

Bacteriorhodopsin can refold to functional structure from a denatured and delipidated state after extraction from the purple membrane. Monomeric bacteriorhodopsin and single site mutants have been reconstituted into lauryl maltoside detergent micelles and studied by differential scanning calorimetry. These results have been compared to similar studies on the purple membrane (Brouillette, et al., *Biochemistry* 26:7431, 1987). Micellar bacteriorhodopsin is thermally less stable than purple membrane at every pH studied (2.4 to 9.6). The pH- and temperature-induced spectral changes of micellar bacteriorhodopsin are similar to those of purple membrane, suggesting they have similar tertiary structures. The stabilization free energy has been determined for the mutants D96E, D96N, D85E, R82Q and D212E. The D96 and D85 mutants are approximately as stable as the wt protein. Mutants R82Q and D212E are distinctly less stable. Implications for the structure and function of these mutants will be discussed. (Support: NIH GM-35474 (CGB), GM-28289 (HGK) and Navy N0014-82-K-068 (HGK).

Tu-PM-G4 GENETIC TRANSFER OF BACTERIORHODOPSIN TO AN EUKARYOTIC CELL.

Volker Hildebrandt, Massoud Ramezani Rad*, Ulrike Swida*, Paul Wrede, Stephan Grzesiek, Georg Büldt. Free University Berlin, Institute of Physics/Biophysics, Arnimallee 14, D-1000 Berlin 33, FRG. *Institute of Biochemistry and Molecular Biology, Ehrenbergstr. 26-28, D-1000 Berlin 33, FRG.

The retinal protein bacteriorhodopsin (BR) acts as a light-driven proton pump in the plasma membrane of the archaebacterium Halobacterium halobium. The gene encoding for the larger precursor of bacterioopsin (bop-gene) and a modified gene coding only for the mature protein were introduced in yeast expression vectors. After transformation of Schizosaccheromyces pombe, bacterioopsin is reconstituted to bacteriorhodopsin in vivo by addition of retinal to the cell cultures, which leads to a slight purple colour of yeast cells. Photocyclic activity was measured with flash spectroscopy on protoplasts and subcellular fractions (e.g. mitochondrial fraction), and found to be very similar to the BR photocycle in the purple membrane. The cleavage of the precursor protein of bacterioopsin found in S. pombe is similar to the cleavage of the precursor in H. halobium. Processing was made visible with antibodies. The archaebacterial bop-gene is expressed in the eukaryote without any modification of the codon usage. The expression of the α-helical integral membrane protein BR in eukaryotic yeast cells is of interest for further studies on protein transport and protein integration into membranes as well as for bioenergetics and genetics. In contrast to the expression of BR in E. coli, a membrane incorporated and functional active protein is found in yeast cells.

Tu-PM-G5 SOLID-STATE ^{13}C NMR MAS SPECTROSCOPY OF 4'-^{13}C-TYROSINE BACTERIORHODOPSIN,

R.G. Griffin[1], S.K. Das Gupta[1], M.R. Farrar[1,2], G.S. Harbison[1], J. Herzfeld[2], J. Lugtenburg[3], D.P. Raleigh[1], S.O. Smith[1], C. Winkel[3], Francis Bitter National Magnet Lab.[1], MIT, Cambridge, MA 02139, Department of Chemistry, Brandeis University[2], Waltham, MA 02254, and Department of Chemistry, Rijksuniversiteit te Leiden[3], 2300 RA Leiden, The Netherlands

Solid-State ^{13}C NMR MAS spectra were obtained for the membrane protein, bacteriorhodopsin (bR), labelled with 4'-^{13}C tyrosines, in the dark-adapted state. Difference spectra (labelled minus natural abundance) taken at pH values between 7 and 12 exhibit a single centerband/sideband pattern centered at 156.1 ppm which remains constant as a function of pH. In the pH 13 spectrum a second line appears with an isotropic shift 8.5 ppm downfield from the previously seen tyrosine peak. Comparison with solution spectra and with crystalline model compounds reveals that this second peak is due to the formation of tyrosinate. Integrated intensities indicate that about half of the tyrosines are deprotonated at pH 13. This result demonstrates the ability to detect deprotonated tyrosines in a protein with solid-state NMR. In addition, the spectra confirm our earlier reported results that bR_{568}, which comprises approximately 40 % of dark-adapted bR, does not contain a tyrosinate at pH values between 7 and 12. We estimate that deprotonation of a unique tyrosine in bR_{568} should account for 4% of the total tyrosine signal. This would be detectable with the current signal-to-noise ratio. We observe subtle linewidth changes in the tyrosine spectra between pH 7 and 12 which we interpret to be due to protein environmental affects.

Tu-PM-G6 LYSINE CONFORMATIONAL CHANGES DURING THE BACTERIORHODOPSIN PHOTOCYCLE AS STUDIED BY FTIR DIFFERENCE SPECTROSCOPY AND SCALED QUANTUM MECHANICAL FORCE CONSTANT CALCULATIONS

Earl McMaster*, Aaron Lewis+*, and Mordechai Sheves# *Dept. of Applied Physics, Cornell University, Ithaca, New York 14853 +Dept. of Applied Physics, Hebrew University, Jerusalem 93707, Israel #Dept. of Organic Chemistry, The Weizmann Institute of Science, Rehovot 76100, Israel

We have used FTIR difference spectroscopy to demonstrate that lysine conformational changes play an important role in the bacteriorhodopsin (BR) photocycle. K/BR and M/BR FTIR difference spectra were taken of BR containing various isotopically labeled lysine side-chains including $^{2}H_2$-LYS, $^{2}H_4$-LYS, $^{2}H_8$-LYS and ^{15}N-LYS. These studies have allowed us to further assign the observed vibrational frequencies of lysine to specific normal modes along the lysine side-chain.

To facilitate the assignment of the normal modes as well as the interpretation in terms of conformational changes in the lysine side-chain we have initiated a computational study. Ab initio as well as semiempirical molecular orbital calculations were done at the Cornell National Supercomputer Facility (CNSF). This involved calculation of the potential energy surface in the region of a local minimum of a given conformation. A normal mode analysis is then performed using scaled force constants to produce the vibrational frequencies.

Tu-PM-G7 LIGHT-INDUCED CHANGES IN THE DIAMAGNETIC SUSCEPTIBILITY ANISOTROPY OF BACTERIORHODOPSIN

D. Dresselhaus*, G. Maret+ and N.A. Dencher

Dept. Physics/Biophysics, Freie Universität, Arnimallee 14, D-1000 Berlin 33, FRG; *Hahn-Meitner Inst., D-1000 Berlin 39, FRG; +Hochfeld-Magnetlabor des Max-Planck-Institut, F-38042 Grenoble.

Purple membranes (PM) in aqueous suspensions orient with the membrane planes perpendicular to the magnetic field direction. This membrane alignment arises from the anisotropy of the diamagnetic susceptibility, which in bacteriorhodopsin (BR) could result from the oriented peptide bonds of the transmembrane α-helices and/or by a net orientation of aromatic amino acid side chains with their planes perpendicular to the membrane surface. We used optical birefringence and small-angle neutron scattering to determine the degree of magnetic field-induced orientational order of PM and to examine light-induced changes in the orientation. Magnetic field strength from 0 to 13 Tesla and of 20 Tesla were applied. In some of the experiments, the field-induced orientation of PM in the ground state BR-568 and in the photocycle intermediate M-410, respectively, was permanently fixed in a polyacrylamide gel matrix. Our results convincingly demonstrate that in the M state the anisotropy of the diamagnetic susceptibility is smaller than in the BR-568 state, leading to a reduced degree of orientational order of the PM in the field. A tilt of α-helices away from the membrane normal or turning of amino acid aromatic ring planes towards the membrane plane during the BR-568 to M transition can account for these changes. This is in agreement with the structural changes seen in our recent neutron diffraction experiments, which can be explained by a displacement of 4-5 amino acids or, more probably, by an approx. 1-2° tilt of 3 to 4 α-helices (Dencher et al. (1988) Biophys. J. 53, 380a).

Tu-PM-G8 TRANSMEMBRANE LOCATION OF THE CYCLOHEXENE RING OF THE CHROMOPHORE OF BACTERIORHODOPSIN BY NEUTRON DIFFRACTION.

T. Hauß, H. Otto, S. Grzesiek, J. Westerhausen and M.P. Heyn

Biophysics Group, Freie Universität Berlin, Arnimallee 14, D-1000 Berlin 33, FRG.

D_{11}- retinal, a synthetic retinal with 11 deuterons in the cyclohexyl ring (Seiff et al., PNAS 83 (1986)), was incorporated biosynthetically in bacteriorhodopsin by adding it to the growth medium of the retinal-minus mutant JW5. Deuteron-labelled and unlabelled purple membranes were used to make oriented multilayers at 86% relative humidity. These samples with a lamellar spacing of 53.1 Å and a mosaic spread of 9° (FWHH) were used for neutron diffraction experiments on the D16-diffractometer of the ILL in Grenoble. Five orders of lamellar reflections were observed. Phasing of the reflections was done by D_2O/H_2O exchange. From the non-linearity of the scattering amplitude with D_2O-content it was concluded that the membranes form asymmetric microdomains. The ring location perpendicular to the membrane is clearly asymmetric: about 10 Å from the polar headgroup region of one side of the membrane and approximately 25 Å from the headgroup region of the other side. Since the ring labelled with a photoaffinity label reacted mainly with ser 193 and glu 194 (Huang et al. (1982)), it is most likely located on the extra-cellular side of the membrane. Preliminary measurements using a retinal selectively deuterated near the Schiff base indicate that this end of the chromophore is located closer to the middle of the membrane.

Tu-PM-G9 CHROMOPHORE STRUCTURE OF BACTERIORHODOPSIN'S M_{412} INTERMEDIATE AND PHOTOCYCLE KINETICS FROM TIME-RESOLVED RESONANCE RAMAN SPECTROSCOPY: EVIDENCE SUPPORTING THE "C-T MODEL".

J.B. Ames, S.P.A. Fodor, and R.A. Mathies, Dept. of Chem., University of California, Berkeley, CA 94720; and R. Gebhard, E.M.M. van den Berg, J. Raap, and J. Lugtenburg, Dept. of Chem., Leiden University, 2300 RA Leiden, The Netherlands.

The structure of the chromophore in bacteriorhodopsin's M_{412} intermediate has been determined, and the kinetics of the photocycle intermediates have been analyzed using time-resolved resonance Raman. Raman spectra of ^2H- and ^{13}C-isotopic derivatives have been analyzed to determine the structure of M_{412} about the C=N and the C_{14}-C_{15} bonds. When the Schiff base geometry is *anti*, the C_{15}-D rock appears as a localized resonance Raman active mode at ~980 cm^{-1}. When the Schiff base geometry is *syn*, in-phase and out-of-phase combinations of the C_{15}-D rock and N-C_{1ys} stretch are predicted at ~1060 and ~910 cm^{-1}, respectively, and the in-phase mode carries the majority of the resonance Raman intensity. 15-D M_{412} exhibits a mode at 968 cm^{-1} which is a localized C_{15}-D rock. The frequency of this mode, its intensity, and its isotopic shifts all support the anti geometry for M_{412}. Time-resolved Raman experiments on M_{412} show that the various rise and decay components of M_{412} all contain C=N-*anti* chromophores. M_{412} exhibits a 14,15-D_2 rocking mode at 958 cm^{-1} which indicates that the chromophore has a 14-*s-trans* conformation. Consequently, M_{412} contains a 13-*cis*, 14-*s-trans*, 15-*anti* chromophore. This result supports the recently proposed "C-T Model" for the mechanism of the proton pump in bacteriorhodopsin [Fodor et al. (1988) *Biochem.* 27, 7079]. The kinetics of the L_{550}, M_{412}, N and O_{640} intermediates were determined by measuring the resonance Raman intensity of the ethylenic line of each intermediate as a function of time at pH 7, 3 M KCl and 30°C. These kinetic data can be fit to a sequential scheme which includes backreactions in the later part of the photocycle as expected from microscopic reversibility. This demonstrates that biphasic decay of M_{412} does not require two different M forms or branching.

Tu-PM-G10 STRUCTURE OF THE RETINAL CHROMOPHORE IN SENSORY RHODOPSIN FROM RESONANCE RAMAN SPECTROSCOPY AND RETINAL ANALOGUES. Stephen P.A. Fodor[+], David Baselt[+], Rob van der Steen[#], Johan Lugtenburg[#], Roberto A. Bogomolni[++] and Richard A. Mathies[+]. [+]Dept. of Chem., Univ. of Calif., Berkeley, CA 94720; [#]Dept. of Chem., State Univ. of Leiden, 2300 RA Leiden, The Netherlands; [++]Dept. of Biochem. & Biophys., Univ. of Calif., San Francisco, CA 94143.

Sensory rhodopsin (SR-I) mediates the phototactic response of *Halobacterium halobium* to orange light. To determine the chromophore structure in SR-I, we have obtained resonance Raman spectra of SR_{587} in native Flx-5R membranes. The dominant line in the vibrational spectrum is the ethylenic stretch at 1530 cm^{-1} whose frequency correlates well with the absorption maximum at 587 nm. The close frequency correspondence of the C-C single bond "fingerprint" modes at 1166, 1196 and 1206 cm^{-1} to those of BR_{568} and HR_{578} shows that the chromophore in SR_{587} is all-*trans*. The ~1630 cm^{-1} C=N stretching frequency indicates that the chromophore is attached to the protein via a protonated Schiff base linkage. The low frequency of the C=N stretch and the magnitude of its shift in D_2O suggests a weak hydrogen-bond to the protein. Regeneration of SR-I membranes with analogues locked in the 6-s-*cis* and 6-s-*trans* conformations indicates that SR-I binds retinal in the 6-s-*trans* conformation (Baselt et al., Biophys. J., *in press*). The opsin shift for the 6-s-*trans* analogue in SR is 1100 cm^{-1} less than that for the native chromophore (5700 cm^{-1}). This reduction indicates that ~20% of the opsin shift in SR-I is due to a protein-induced conformational change from twisted 6-s-*cis* in solution to planar 6-s-*trans*. The low frequency of the Schiff base stretching mode and the magnitude of its deuterium shift argue that there is a weakened hydrogen-bonding interaction between the Schiff base proton and its protein environment that is responsible for the increased opsin shift in SR (5700 cm^{-1}) compared to BR (5100 cm^{-1}).

Tu-PM-G11 HEAVY-ATOM LABELLED RETINAL LOCALIZED IN THE PLANE OF THE PURPLE MEMBRANE BY X-RAY DIFFRACTION.

G. Büldt, N.A. Dencher, K. Konno*,K. Nakanishi*,H.-J. Plöhn, B.N. Rao*
Dept. Physics/Biophysics, Freie Universität Berlin, Arnimallee 14, D-1000 Berlin 33, FRG; *Dept. Chemistry, Columbia University, New York, N.Y. 10027, USA.

The chromophore retinal of bacteriorhodopsin (BR) is the antenna for the absorption of light and triggers by its trans to 13-cis isomerization via conformational changes in the protein moiety (Dencher et al. (1988) Biophys. J. 53, 380a) the vectorial proton translocation across the purple membrane. We have determined by X-ray diffraction the location of the heavy-atom label of three different retinal analogs in the plane of the purple membrane. These three analogs, i.e., polyene chain labelled 9-bromo-retinal and 13-bromo-retinal as well as the ring labelled Hg-retinal, were incorporated in BR either biosynthetically using a retinal deficient mutant strain or with photochemically bleached bacterioopsin. The 9-bromo-BR and the 13-bromo-BR were tested and found to be functional active as a proton pump. The position and orientation of the retinal obtained by our experiments are in agreement with recent neutron diffraction data (Jubb et al. (1984) EMBO J. 3, 1455; Heyn et al. (1988) PNAS 85, 2146). This indicates that the heavy-atom labelled chromophores are isomorphously incorporated into BR. One advantage of X-ray studies is that only 1 mg purple membrane is required in contrast to about 100 mg in the case of neutron diffraction. This will be helpful for any investigation of light induced structural changes in the retinal binding pocket during BR's pumping cycle.

Tu-PM-G12 SYNTHETIC, RETINAL-MIMICKING PROBES FOR THE STUDY OF THE TERTIARY STRUCTURES OF RHODOPSIN BACTERIORHODOPSIN AND THEIR PHOTOACTIVATED FORMS.

Valeria Balogh-Nair, Liang Chen and Wei-Xing Li, Department of Chemistry, City College of New York, New York, N.Y. 10031.

Compounds of the type I, II and III bearing the photoaffinity labels, azide, trifluoromethyldiazirine, diazoacetoxy and trifluorodiazopropionate were synthesized to serve as retinal-mimicking probes for the investigation of the tertiary structures of bacteriorhodopsin (bR), rhodopsin (Rh) and their photoactivated M_{412} and Meta II forms. The trans isomers of probes I, II and III were used to form bR analogs, whereas the 9-cis or 11-cis isomers to regenerate artificial rhodopsins.

Binding studies with I, II and III showed that the ring binding sites in bR and Rh are flexible enough to fit even highly modified synthetic retinals, including those with spacer arms.

These studies were supported by NSF grants BNS 851363 and BNS 8812506, and the Petroleum Research Fund (ACS) grant 17797-AC1.

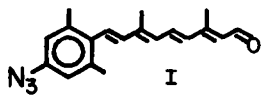

I

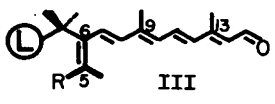

III

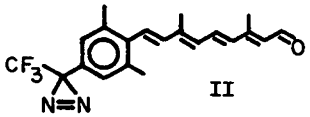

II

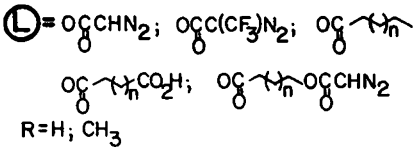

Tu-PM-H1 TRANSIENTS IN HILL'S CAP, NO CAP MODEL OF THE DYNAMIC INSTABILITY IN MICROTUBULE ASSEMBLY. Robert J. Rubin, Laboratory of Molecular Biology, NIDDK, National Institutes of Health, Bethesda, MD 20892.

Hill [Proc. Natl. Acad. Sci. USA 81 6728 (1984)] has proposed a simple two-phase (cap, no cap) macroscopic model describing the kinetic behavior at a labile tip of a microtubule (MT). In the model, an MT exists either in a slowly growing phase; or the same MT exists in a rapidly shrinking phase which is entered if/when the GTP-tubulin cap is lost through a fluctuation, thus exposing GDP-tubulin subunits, which constitute the main body of the MT. Transition between the two phases--loss of a cap or formation of a new cap--occurs very infrequently and in a stochastic manner. In this paper, we first use Hill's model to obtain an exact expression for $\langle m(t) \rangle$, the average length as a function of time for an MT nucleated on a centrosome (initial length equal to zero). Then we obtain some qualitative and quantitative results on the time-dependence of $\langle m(t) \rangle$. This initial value problem complements my recent calculation, within the frame-work of Hill's model, of the mean life-time of an N-unit long MT in the growing or shrinking phase [R. J. Rubin, Proc. Natl. Acad. Sci. USA 85 446 (1988)]. I have extended my analysis of mean life-times and will present two simple expressions for MT's in the growing phase which are N units long: (1) the mean life-time of the subset of MT's which disassemble completely without ever re-entering the growing phase; and (2) the mean number of times that the growing phase is re-entered before complete disassembly.

Tu-PM-H2 THE "LATERAL CAP" MODEL FOR DYNAMIC MICROTUBULES
Peter M. Bayley and Stephen R. Martin, N.I.M.R., Mill Hill, London NW7.

Direct observations of dynamic instability of microtubules close to steady-state in vitro show the coexistence and interconversion of growing (G) and shrinking (S) microtubules. These observations, plus measurements of T-GTP content during microtubule assembly, impose constraints on the mechanisms for the relationship between addition of T-GTP and GTP hydrolysis. We model this system using an approach essentially different from that of Hill and co-workers. The tubulin-GTP addition process takes into account the multiplicity inherent in the configuration of the microtubule end in terms of differences in kinetics and affinities due to the specific geometry and nucleotide content of the different potential sites for attachment of T-GTP. GTP hydrolysis occurs on a tubulin-GTP molecule only as it becomes embedded in the microtubule lattice; both lateral and longitudinal protein-protein interactions are thus involved. The extent of the tubulin-GTP in the microtubule then approximates to a single-layer (the "Lateral-Cap") in terminal positions of the lattice, both in microtubule elongation and at steady-state. Fluctuations occur mainly due to dissociation of T-GTP. The results show three well-differentiated states : growth, shrinkage, and pause; the elongation rate of a given microtubule is not completely uniform (cf. recent in vivo observations). Transitions G/S ("catastrophe") and S/G ("rescue") are functions of [T-GTP], as reported (Walker et al., J.Cell Biol. 1988, In Press). The model is applicable to dynamic processes at both ends of the microtubule.

Tu-PM-H3 DISASSEMBLY OF BROKEN MICROTUBULES: SIZE OF THE "GTP CAP".
Stephen R. Lynch and Robley C. Williams, Jr., Department of Molecular Biology, Vanderbilt University, Nashville, TN 37235.

The involvement of GTP hydrolysis in the assembly of microtubules from their tubulin subunits appears to give rise to a non-equilibrium situation described as "dynamic instability". Individual microtubules are observed to grow and shrink with remarkable rapidity even when the total mass of assembled microtubules is at steady state. This phenomenon apparently occurs because the presence of GTP-bearing subunits at their ends is required for stability. One would predict that when a microtubule is broken in the middle, the vast majority of the broken ends would have GDP-bearing subunits, would be unstable for that reason, and would depolymerize. We have observed this phenomenon by assembling microtubules in the drive syringe of a stopped-flow spectrophotometer. After a steady state is reached, the solution is driven rapidly through mixing jet, where the turbulence breaks the microtubules into pieces of a few microns in length. Disassembly ensues, followed by reassembly, measured by observation of the turbidity at 350 nm. The height of the minimum indicates that the GTP cap is small (less than 15% of the microtubule's length), and kinetic analyses show that the disassembly phase is markedly slowed by the presence of microtubule-associated proteins. Supported by NIH Grant GM25638.

Tu-PM-H4 **STEADY STATE NUCLEOTIDE BINDING BY KINESIN ATPase.** **D.D. Hackney and K. Wright, Depart. of Biological Sciences, Carnegie Mellon University, Pittsburgh, PA 15213.**

The rate limiting step in MgATP hydrolysis by bovine brain kinesin in the absence of microtubules is the slow release of ADP from the active site (Hackney, Proc. Natl. Acad. Sci. USA 85, 6314 (1988)). This results in a stoichiometric burst of product formation when ATP is added to nucleotide-free kinesin (Hackney, Malik & Wright, Fed. Proc. *In Press* (1989)). It was found that the net rate for bimolecular ATP binding determined from the variation of the burst rate with ATP concentration is 2.5 $\mu M^{-1}sec^{-1}$ and the rate of ADP release is 0.008-0.009 sec^{-1}. This predicts a Km for ATP of approximately 3.5 nM. To test this prediction, steady state titrations were performed with nucleotide-free kinesin in the presence of pyruvate kinase and phospho*enol*pyruvate to convert released ADP back to ATP. Conditions were choosen such that the only significant nucleotide pools were ATP free in solution and ADP bound at the active site of kinesin. At 23 nM 120 kDa peptide most of the nucleotide is present as bound ADP at substoichiometric nucleotide levels. A limiting amount of bound ADP equal to the concentration of 120 kDa peptide is reached at high nucleotide level. At 0.9 nM 120 kDa peptide most of the nucleotide is present as free ATP at substiochiometric levels. Theoretical modeling for such a mutual depletion case indicates that the Km is approximately 3.5 nM consistent with the predictions of the transient kinetic experiments.

Supported by U.S. Public Health Service grant AR25980.

Tu-PM-H5 SIMULATION OF SPORADIC STREAMING AND THE HYALINE CAP CYCLE IN *AMOEBA PROTEUS*

Micah Dembo; Theoretical Division, Los Alamos National Laboratory.

Many models of the cytoskeletal motility of *Amoeba proteus* can be formulated in terms of the theory of reactive interpenetrating flow (Dembo and Harlow, 1986, *Biophys. J.* 50:109-121). We have previously reported tests of such models against the phenomenon of steady axisymmetric fountain flow (Dembo, 1989, in press). The simplest workable scheme revealed by such tests (the minimal model) accounts for the self assembly of the cytoskeleton of *proteus*; for the formation and detailed morphology of the endoplasmic channel, the ectoplasmic tube, the uropod, the plasma gel sheet, and the hyaline cap. The model accounts for the kinematics of the cytoskeleton, the velocity field of the forward flow of the endoplasm, the contraction of the ectoplasmic tube, and the inversion of the flow in the fountain zone. The model also gives a satisfactory account of measurements of pressure gradients, measurements of heat dissipation, and measurements of the output of useful work by amoeba. We now show by direct numerical simulation that for slightly changed conditions the minimal model yields the oscillatory form of fountain flow (sporadic streaming).

Tu-PM-H6 THE CRYSTAL STRUCTURE OF PROFILIN-I: AN ACTIN-BINDING PROTEIN. FROM *ACANTHAMOEBA*. By K.A. Magnus and E.E. Lattman, Department of Biophysics, and T.D. Pollard, Department of Cell Biology and Anatomy, Johns Hopkins University School of Medicine, Baltimore, Maryland 21205 USA.

We have determined and are refining the three-dimensional structure of profilin at 2.4 A resolution using x-ray crystallographic techniques. Profilins are thought to regulate actin polymerization in various non-muscle cells primarily by sequestering actin monomers in non-polymerizable form. The profilin-I molecule from *Acanthamoeba castellanii* is about 25 A in diameter and comprises 125 amino acid residues folded into two domains. The amino terminal domain is largely antiparallel beta structure while the carboxyl domain is mostly alpha helical. Chemical cross-linking has established that lysine 115 of the helical domain of profilin is in contact with glutamate 364 of actin in the 1:1 profilin-actin complex. Similarities in parts of the primary sequences of other actin-binding proteins and of profilins in the contact region have recently been noted, suggesting the possibility of similar tertiary structural regions in this family of proteins.

This work supported by GM 35171 from the National Institutes of Health.

Tu-PM-H7 THE SEQUENCE OF THE DICTYOSTELIUM GELATION FACTOR, AN F-ACTIN CROSSLINKING PROTEIN, SHOWS A CONSERVED ACTIN-BINDING SITE AND A 100-RESIDUE CROSS-BETA MOTIF THAT REPEATS SIX-FOLD. Michael Schleicher, Angelika Noegel and Murray Stewart, (Intr. by T. Pollard); Max-Planck-Institute for Biochemistry, 8033 Martinsried, FRG, and MRC Laboratory of Molecular Biology, Cambridge, U.K.

The two major F-actin crosslinking activities in Dictyostelium discoideum are α-actinin and the 120K gelation factor. Both are homodimeric, rod-shaped molecules with contour lengths of 40nm and 35nm, respectively. Comparison of the sequences of α-actinin (Noegel et al., FEBS-Lett. 221:391-396, 1987) and the gelation factor shows that, at the N-terminus, both molecules have highly homologous regions thought to be involved in binding F-actin. This actin-binding site seems to be strongly conserved and is found, for example, in chicken fibroblast α-actinin and human dystrophin. The structural motifs which lead to the elongated shape of α-actinin and the gelation factor are quite different, although they are both of the order of 100 residues in length. Whereas the α-actinin rod has a repeating motif that is thought to be highly alpha-helical, the C-terminal 600 residues of the gelation factor molecule are rich in proline and glycine, and computer analysis predicts almost no alpha-helix forming domains. A model will be presented in which these repeating motifs are organized in a cross-beta conformation that can account for the rod-like structure, the flexibility of the molecule, and the mechanism of dimerization.

Tu-PM-H8 MOTION OF MAGNETOTACTIC BACTERIA IN A ROTATING MAGNETIC FIELD. Charles P. Bean, School of Science, Rensselaer Polytechnic Institute, Troy, NY 12180-3590.

Richard Blakemore[1] has shown that there exists a large class of bacteria that possess a magnetic moment and that are oriented by the magnetic field of the earth. Their motion is thus guided along the lines of magnetic field. BLakemore (private communication) has also noted that these magnetotactic bacteria will follow the rotating field of a laboratory magnetic stirrer and that this rotation may easily be seen by cyclic changes of the scattering of light. A theory of this rotation for non-motile bacteria may be made by assuming that the total torque on a bacterium is zero. (Inertial terms in the equation of motion may be neglected in this region of low Reynolds number.) The torque from the magnetic field is $\mu B \sin\theta$, where μ is the magnetic field, B is the magnetic field strength and θ is the angle between μ and B. The torque from viscous drag at low Reynolds number is $-8\pi\eta a^3 d\theta/dt$ where η is the viscosity and a is the equivalent spherical radius of the bacterium. For a uniform rotating field, $d\theta/dt = 2\pi f$ where f is the frequency. Equating these terms, $\sin\theta = 16\pi^2\eta a^3 f/\mu B$. The bacteria will follow the field up to a critical frequency, f_c, given by $f_c = \mu B/16\pi^2\eta a^3$. Thus measurement of this frequency gives a measure of μ/a^3. For motile bacteria of linear velocity v the same theory applies but they will swim in circles of radius r where $v = 2\pi f r$. Thus, measurement of circle size gives a measure of v.

[1]R.P. Blakemore, Science 190, 377 (1975).

Tu-PM-H9 **INVESTIGATIONS OF THE BACTERIAL ROTARY MOTOR USING OPTICAL TWEEZERS.**

Steven M. Block †‡, David F. Blair ‡, and Howard C. Berg †‡.
† Rowland Institute for Science, 100 Cambridge Parkway, Cambridge MA 02142 and
‡ Department of Cellular and Developmental Biology, Harvard University, 16 Divinity Avenue, Cambridge MA 02138.

A single-beam gradient force optical particle trap ('optical tweezers') has been built into a conventional light microscope. The device uses a moderate-power infrared laser to trap particles using radiation pressure, and is based upon recent developments by A. Ashkin and colleagues (*Science* 235: 1517-1520 (1987) and *Nature* 330: 769-771 (1987)). It can manipulate a range of biological materials without overt damage, readily producing microdyne forces on small assemblies of proteins, organelles, and even intact cells. Among other applications, optical tweezers offers an elegant means of studying the mechanical properties of biological motors. Data will be presented from the first quantitative experiments employing light traps on bacteria. These measurements have revealed new information about the properties of the rotary motor in *Streptococcus* strain V4051, including a novel 'lock-up' phase that can occur at extremely low protonmotive force. A videotape demonstrating optical tweezers will be shown.

Tu-PM-H10 **ION TRANSFERS LIMIT THE SWIMMING SPEED OF BACTERIA.**

Jenny Z. Liu, Michaela Dapice, Shahid Khan
Departments of Anatomy and Structural Biology & Physiology and Biophysics, Albert Einstein College of Medicine, Bronx, N.Y.10461, U.S.A.

Motility in the monoflagellated, marine bacterium V. alginolyticus is powered by sodium gradients(1986 B. B. A. 850:449). We have found that lithium will also drive motility in these bacteria. The sodium and lithium dependence of swimming speeds in this bacterium has been investigated in solutions of varying viscosity. The concentration dependence is a function of the drag on the cell. At high viscosity, swimming speeds are relatively insensitive to changes of ion type or concentration. These results will be presented and their implications for the events limiting mechanochemical cycling in this motor discussed.

Tu-Pos1 **2,3-BUTANEDIONE MONOXIME (BDM) SUPPRESSES CROSS-BRIDGE REATTACHMENT FOLLOWING LASER PHOTOLYSIS OF CAGED ATP.** Thomas D. Lenart+, Jonathan W. Tanner*, and Yale E. Goldman*. Dep'ts of Biochemistry-Biophysics+ and Physiology*, Univ. of Pennsylvania, Philadelphia, PA 19104.

BDM suppresses muscle tension, reportedly by membrane or myofibrillar actions or both (Horiuti et al., J. Musc. Res. and Cell Mot. 9:156, 1988). We tested whether BDM affects cross-bridge detachment and reattachment during relaxation from rigor of single glycerol-extracted rabbit psoas muscle fibers following laser pulse photolysis of caged ATP in the absence of Ca^{2+}. BDM (20 mM) suppressed the transient rise in tension that normally precedes final relaxation (fig.) by 67.3 ± 1.4 %, s.e.m., n=12, measured at the time of the peak tension rise at 20°C and 0.6-1.1 mM liberated ATP. When fibers were stretched or released (< 1% of length) 1 sec prior to photolysis, the tension trace converged to the isometric control within 20 msec (fig., s=stretch, i=isometric), and the difference trace (s-i) decayed to zero before final relaxation. Assuming this convergence indicates the initial detachment of rigor cross-bridges (Goldman et al., J. Physiol. 354:577, 1984), the apparent second-order rate constant for cross-bridge detachment by ATP was 5-20 x 10^5 $M^{-1}s^{-1}$ at 20 mM BDM. In paired comparisons, the half-time for decay of the tension difference trace (fig.) was 26.7 ± 2.6 % shorter in the presence of 20 mM BDM than in controls. The results support the hypothesis that BDM inhibits the contractile apparatus by suppressing cross-bridge attachment. Supported by the MDA and NIH grant HL15835 to the Penna. Muscle Inst.

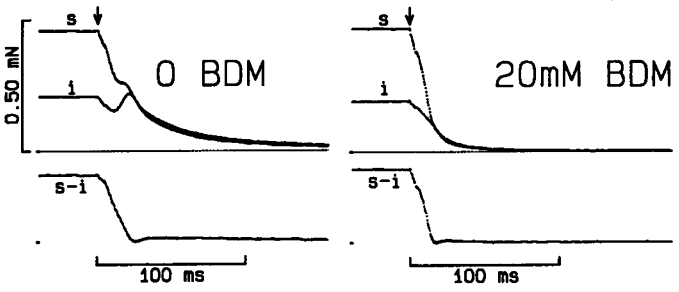

Tu-Pos2 **PHOTOLYSIS OF CAGED ATP IN MUSCLE FIBERS WITH NEGATIVELY STRAINED CROSS-BRIDGES INDICATES THAT RELAXATION IN THE PRESENCE OF MgADP IS HIGHLY STRAIN DEPENDENT.** J.A.Dantzig & Y.E.Goldman, Dept. of Physiology, Univ. of Penna., Phila., PA 19104

To explain the Fenn effect (extra energy liberation during shortening), A.F. Huxley (1957) assumed that negative strain accelerates cross-bridge detachment. To test for strain-dependence of cross-bridge detachment we measured relaxation from rigor with positively and negatively strained cross-bridges using laser pulse photolysis of caged ATP within glycerol-extracted single fibers from rabbit psoas muscle. To obtain negative strain, a relaxed single fiber was stretched to 3.0-3.35 μm sarcomere length, put into rigor with 10 mM caged ATP and released just prior to photolysis so that tension fell below the resting level but above zero (Goldman et al., J. Physiol. 398:72P, 1988). 20 mM 2,3-butanedione monoxime (BDM; Lenart, Tanner & Goldman, this volume) or 25 mM P_i was used to suppress cross-bridge reattachment. Photolysis, in the absence of Ca^{2+} caused an increase in tension (fig. lowest trace; 100 μM MgADP) as negatively strained cross-bridges detached. Steady levels of MgADP from 0.1-1 mM had little effect on the rate of relaxation from negative tension (at ~770 μM liberated ATP, $t_{1/2}$ ≅ 10ms), whereas MgADP markedly slowed relaxation from positive tension ($t_{1/2}$ = 12.3±.8 ms (s.e.m., n=6) in the absence of ADP; $t_{1/2}$ increased up to 115 ms at 1 mM MgADP). Even with BDM or P_i, cross-bridge reattachment seemed to influence the overall relaxation. In the presence of MgADP, the markedly faster relaxation of negatively strained cross-bridges is in the direction expected from the Huxley (1957) model. The present strain-dependence of relaxation, however, does not fully explain the Fenn effect. Support: MDA and NIH grant HL15835 to the Penna. Muscle Institute.

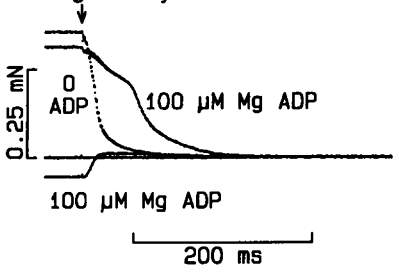

Tu-Pos3 **A CROSSBRIDGE SCHEME IN SKINNED RABBIT PSOAS FIBERS DEDUCED FROM RELAXATION KINETICS AND SINUSOIDAL LENGTH PERTURBATION ANALYSES.** Masataka Kawai# and Herbert R. Halvorson*. #Department of Anatomy, University of Iowa, Iowa City, IA 52242, and *Division of Physical Biochemistry, Henry Ford Hospital, Detroit, MI 48202.

Two exponential processes (B) and (C), deduced from sinusoidal analysis, are interpreted in terms of a crossbridge scheme which utilizes relaxation kinetics applied to a non-equilibrium steady state condition. A minimum of 4 states (X_0 - X_3) are needed to account for the MgATP (S) and MgADP (D) effects of the rate constant $2\pi c$ (equivalent to phase 2 of step analysis). In this crossbridge scheme, D or S are in rapid equiliblium with rigor-like state X_1, and transitions between X_2 and X_3 (actomyosin dissociation and its reversal) are sensed by $2\pi c$. The fitting of the data to the scheme is satisfactory and yields the association constant for D to be 2.8 mM^{-1}, and for S to be 1.0 mM^{-1}. The rate constants for the dissociation and the reverse dissociation are 520 s^{-1} and 63 s^{-1}, respectively. The scheme is extended to include X_5 (force-generating state), and this extension accounts for S and D sensitivities of the rate constant $2\pi b$. This extension also explains the phosphate (P) sensitivity of $2\pi b$, but approximately. In order to have more satisfactory fit, an additional state X_4 is needed. In this scheme, P is in rapid equiliblium with X_5 to form X_4, and the transition $X_3 \rightarrow X_4$ (power stroke) is sensed by $2\pi b$. The association constant for P is 0.1 mM^{-1}, and the rate constants for the power stroke and back stroke are 120 s^{-1} and 140 s^{-1}, respectively. This crossbridge scheme is consistent with the hypothesis that the transition $X_5 \rightarrow X_1$ (ADP desorption) rate limits the crossbridge cycle. We find this to be ~3 s^{-1} based on the ATP hydrolysis rate.

Tu-Pos4 THE EFFECT OF CALCIUM CONCENTRATION ON THE PHOSPHATE RELEASE STEP OF THE ACTOMYOSIN ATPase MECHANISM. E. Homsher and J. Lacktis. Physiol. Dept. School of Medicine, UCLA, Los Angeles, Ca. 90024.

Hibberd et al (Science, 228,1317, 1985) have suggested that the release of inorganic phosphate (Pi) from the AM** ADP Pi crossbridge is associated with force production. Dantzig et al (Biophys.J. 51, 3a, 1987) found that rapid photogeneration of Pi in isometrically contracting glycerinated muscle fibers produces an exponential decline in force (the Pi transient), whose rate (λ) increases with Pi concentration. This suggests that λ is proportional to the sum of the forward (force producing) and backward (loss of force) rate constants for Pi release. Chalovich et al (J.B.C. 257, 2432, 1982) have suggested that calcium binding to the troponin-tropomyosin complex may regulate the kinetics of the Pi release step. To test this hypothesis we measured the Pi transient (induced photogeneration of 1mM Pi from caged-Pi) rate in glycerinated rabbit psoas fibers at 10°C at pCa 4.5, 6.1, and 6.5 . The amplitude and rate of the Pi transient at both pCa 4.5 and 6.1 (where force is 0.8 of that at pCa 4.5) were 15% Po and 36 s^{-1} respectively. At pCa 6.5, where force is 0.4 of that at 4.5, the Pi transient became biphasic: a first phase, whose amplitude and rate were the same as those at pCa 4.5 was followed by a second phase whose amplitude was 15% Po and whose rate was 5 s^{-1}. We interpret this data as indicating that the rates of Pi release from and binding to crossbridges in isometric contractions are independent of pCa. The appearance of a second phase at pCa 6.5 may represent the loss of cooperativity in thin filament activation following the Pi induced dissociation of strongly attached crossbridges. (Supported by NIH grant AM30988-07).

Tu-Pos5 A MODEL OF CROSS-BRIDGE ACTION: THE EFFECTS OF ATP, ADP, AND Pi. E. Pate and R. Cooke. Dept. of Pure and Applied Math., WSU, Pullman, WA 99164; Dept. of Biochem. and Biophys. and the CVRI, UCSF, San Francisco, CA 94143.

We have explored a model of cross-bridge kinetics that explains many of the effects on steady-state muscle contraction of ligands that bind to the nucleotide site on myosin. The model follows the basic mathematical framework previously investigated by Huxley, and by Eisenberg, Hill and Chen. In the model, detached cross-bridges initially bind in a weakly-attached A.M.D.Pi state at the beginning of a cross-bridge powerstroke. Pi release then results in transition to a strongly-bound A.M.D. state as has been suggested by the experimental work of a number of investigators. ADP release and subsequent cross-bridge detachment due to ATP binding occur at the end of the power stroke. Work in a number of laboratories has defined the effects on contraction of variations in concentrations of ATP, ADP, and Pi. The maximum shortening velocity (Vmax) and ATPase of fibers exhibit classical, Michaelian behavior with respect to [ATP]. Isometric tension (Po) decreases for [ATP] above 20 uM with significantly different values of Km for the changes in Po and ATPase. ADP acts as a competitive inhibitor of Vmax and ATPase while potentiating Po. As [Pi] is raised, Po decreases linearly with log[Pi]. There is a smaller decrease in the ATPase activity and very little change in Vmax. The model can explain the somewhat contradictory effects on Vmax, Po, and ATPase of ATP, ADP, and Pi. The model also demonstrates that the connection between the parameters of contraction and the free energy of hydrolysis of ATP can be quite complex. Supported by NSF DCB8811470 and USPHS AM30868.

Tu-Pos6 MYOSIN HEAD ORIENTATION IN THE PRESENCE OF ADP. P. G. Fajer, E. A. Fajer, J. J. Matta and D. D. Thomas, Biochemistry, University of Minnesota, Minneapolis MN 55455.

We have previously reported that ADP does not induce more than 10° axial rotation of the myosin heads in rigor muscle (Thomas et al., Biophys J. 47, 380a, 1985). In the present study, we have increased the orientational resolution by using perdeuterated maleimide spin label (d-MSL), which has a considerably narrower linewidth than that of the standard protonated spin label. Subfragment 1 (S1) was labelled with d-MSL and infused into unlabelled rabbit psoas fibers in the absence of ADP, and its EPR spectrum was compared to that obtained in 5mM ADP. As previously reported, the changes were very small, excluding the possibility of a large scale rotation. These small effects were not significantly temperature dependent (4° to 22°C), and were observed in intrinsically labelled muscle fibers also. The increased spectral resolution produced more clear evidence that the orientational distribution in rigor is complex. Using a simplex fitting routine, we have analyzed the spectra in terms of two Gaussian orientational populations. In rigor, the two (roughly equal) populations are centered at approximately the same angle, but the degrees of disorder of the two components is different (10° and 40° full width). The main effect of ADP was to increase the broader component by about 10°. We have also analyzed the spectra by an alternative method (Burghardt and Thompson, Biophys J. 46, 729, 1984), with consistent results.

Tu-Pos7 MECHANISM OF PPDM AND PHENYLMALEIMIDE INHIBITION OF RIGOR STIFFNESS OF SKINNED RABBIT PSOAS FIBERS. V.A. Barnett and M. Schoenberg, NIAMS, NIH, Bethesda, MD 20892.

Last year at this meeting we reported that incubation of resting skinned psoas fibers (μ = 170 mM, 5°C) with para-phenylenedimaleimide (pPDM) or phenylmaleimide (PM) results in the reduction of rigor stiffness (μ = 170 mM). A 60 minute treatment reduces the rigor stiffness to < 10% of its original value. It is known that pPDM crosslinking of the essential sulfhdryls of myosin (SH_1 and SH_2) in the presence of ATP preserves a myosin conformation that has a low actin affinity. PM effects are presumably not due to crosslinking. Crossbridge dynamics in pPDM- or PM-modified single psoas fibers were compared with that in unmodified fibers by measuring the force response to a rapid (0.5 ms) step stretch in low ionic strength (μ = 40 mM) rigor and relaxing solutions. PM-modified fibers in the presence of ATP, and pPDM-modified fibers in the presence or absence of ATP, show initial stiffness (~35% unmodified rigor) followed by a rapid decay. This is indicative of rapid crossbridge detachment. However, in rigor, PM-modified fibers demonstrate significant stiffness (~50% unmodified rigor) that does not decay. This indicates that the PM-fibers retain nucleotide sensitivity of their detachment rate constants even though their ability to bind actin has been reduced. Therefore, the mechanism by which these two reagents inhibit acto-myosin interaction is fundamentally different, pPDM-treatment produces a crossbridge similar to the myosin·ATP crossbridge. Regardless of nucleotide, it has rapid detachment rate constants. PM modification of muscle fibers weakens crossbridge binding apparently by reducing the attachment rate constants since the detachment rate constants, in the absence of ATP are similar to those observed for unmodified rigor fibers.

Tu-Pos8 EFFECT OF PARTIAL EXTRACTION OF LC_2 ON THE DYNAMIC STIFFNESS OF SKINNED SKELETAL MUSCLE FIBERS. P.A. Hofmann, J.M. Metzger, M.L. Greaser and R.L. Moss. Department of Physiology and Muscle Biology Lab., U. of Wisconsin, Madison, WI 53706.

We previously demonstrated that partial extraction of LC_2 from rabbit skinned muscle fibers causes: (1) a left-shift of the tension-pCa relationship and (2) a 25-30% decrease in V_{max} during the high velocity phase of shortening (Biophys. J. 53:567a, 1988). To account for these changes, we hypothesized that partial extraction of LC_2 may change the mechanical properties of the cross-bridges. To investigate this possibility, in-phase stiffness was measured at 10°C by applying small amplitude (< 0.1% L_0) sinusoidal length changes (3.3 KHz) at one end of the fiber and measuring the resultant changes in tension and sarcomere length (by laser diffraction). Tension and stiffness were measured at various pCa's: (1) prior to LC_2 extraction, (2) after partial extraction of LC_2 and (3) after LC_2 recombination. Extraction resulted in an increase in stiffness at pCa > 4.5 and this increase was proportional to the increases in tension observed in the same pCa range. Readdition of LC_2 resulted in a return of tension and stiffness to control values. The maximum tension (1.14×10^5 N/m^2), stiffness (28.4 N/m) and elastic modulus (2.18×10^7 N/m^2) at pCa 4.5 were unaffected by extraction of LC_2. These findings strongly support the idea that there is an increase in the number of cross-bridges formed during Ca^{2+} activation of LC_2 deficient fibers, which in turn increases the cooperative activation of the thin filament. Since no change in stiffness per cross-bridge was observed, it is likely that the previously observed decrease in V_{max} with LC_2 extraction represents a slowing of the kinetics of cross-bridge cycling. However, it is still possible that for greater extents of shortening cross-bridge stiffness is increased by LC_2 extraction. Supported by NIH and the AHA.

Tu-Pos9 FURTHER EVIDENCE THAT LC_2 MODULATES THE CALCIUM SENSITIVITY OF THE RATE OF CROSS-BRIDGE ATTACHMENT IN SKINNED SKELETAL MUSCLE FIBERS. Joseph M. Metzger and Richard L. Moss. Department of Physiology, University of Wisconsin, Madison, WI 53706.

Last year we reported (Biophys. J. 53:566a) an increase in the Ca^{2+} sensitivity of the rate constant of tension redevelopment (k_{tr}; Brenner and Eisenberg PNAS 83: 3542, 1986) following partial extraction of myosin LC_2 from rabbit psoas fibers. Initial extraction was done in solution containing, in mM, 20 EDTA, 20 KCl, 5 Imidazole at 30°C for 3 hrs, which resulted in removal of ~50% endogenous LC_2. Following extraction, k_{tr} was unchanged at pCa 4.5; however, at submaximal [Ca^{2+}] k_{tr} increased relative to control. At pCa 6.0 k_{tr} was 3.8±0.7 s^{-1} in controls and 9.3±1.0 s^{-1} following extraction. Attempts to restore the k_{tr}-pCa relation by adding back exogenous LC_2 to the extracted fibers met with limited success. In an attempt to facilitate the recombination of LC_2 with myosin, less harsh conditions (20 EDTA, 50 KCl, 5 PO_4, pH 7.00, 0.5 mg/ml TnC, 20°C for 2 hrs) were developed for the extraction of LC_2. In fibers extracted in this way, LC_2 readdition returned k_{tr} to near control values. In the figure, k_{tr} was 3.0 s^{-1} in control, 4.5 s^{-1} following extraction, and 3.0 after recombination of exogenous LC_2. The reversibility of the effects of LC_2 extraction supports our hypothesis that LC_2 modulates the Ca^{2+} sensitivity of cross-bridge cycling in mammalian skeletal muscle. Supported by NIH.

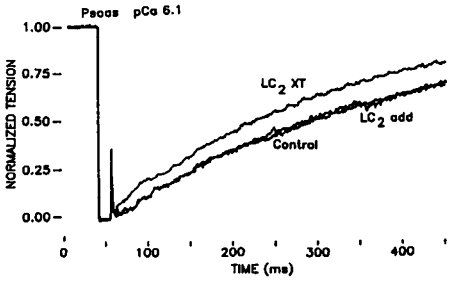

Tu-Pos10 MAXIMUM RATE CONSTANT OF CROSS-BRIDGE ATTACHMENT IS SEVEN-FOLD GREATER IN FAST- THAN SLOW-TWITCH SKINNED SKELETAL MUSCLE FIBERS. Joseph M. Metzger and Richard L. Moss. Department of Physiology, University of Wisconsin, Madison, WI 53706.

The Ca^{2+} sensitivity of the rate constant of tension redevelopment (k_{tr}), was examined in rat and rabbit slow- and fast-twitch skinned single fibers at 15°C, pH 7.00, and an ionic strength of 180 mM. Variations in k_{tr} due to [Ca^{2+}] have been related to a direct effect of Ca^{2+} upon f, the rate constant of cross-bridge attachment in A.F. Huxley's model of contraction (Brenner PNAS 85:3265, 1988). At maximum levels of Ca^{2+} activation (pCa 4.5), k_{tr} was more than seven-fold greater in fast compared to slow fibers (Figure). In rat superficial vastus lateralis (svl) fibers, which contained fast isoforms of the contractile and regulatory proteins, maximum k_{tr} obtained at pCa 4.5 was 22.9±0.5 s^{-1} (n=20). In contrast, maximum k_{tr} in rat slow-twitch soleus fibers was 3.0±0.1 s^{-1} (n=12). Interestingly, the maximum k_{tr} in rabbit fast psoas fibers (17.0±1.3 s^{-1}; n=6) was significantly lower than the value obtained in rat fast svl fibers. The greater than seven-fold difference in apparent f between slow and fast fibers contrasts with the three-fold difference observed in V_{max}, thought to be limited by the detachment rate constant for negatively strained cross-bridges. Supported by NIH.

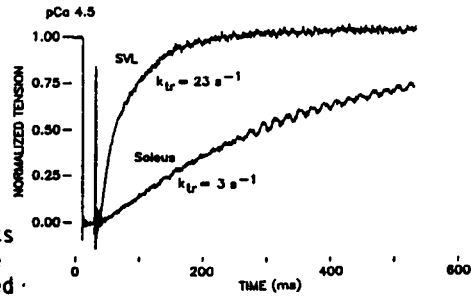

Tu-Pos11 A MODEL OF THE AUGMENTATION OF ISOMETRIC TENSION DUE TO P-LIGHT CHAIN PHOSPHORYLATION IN MAMMALIAN SKELETAL MUSCLE. **Bradley M. Palmer and Russell L. Moore,** The Departments of Medicine and Physiology, The Pennsylvania State University, Hershey, PA 17033.

There are data supportive of the hypothesis that isometric tension potentiation (ITP) in skeletal muscle is the physiological consequence of myosin P-light chain (PLC) phosphorylation via a mechanism whereby PLC phophorylation increases the sensitivity of the contractile element to activation by Ca^{2+}. In order to examine this hypothesis more closely, a simple mathematical model of isometric tension dependence on pCa and PLC phosphorylation was constructed for a contractile system in which PLC phosphorylation does not affect P_o nor v_o. The model is based on the equation T = exp[-a exp[b pCa]], where T is the fraction of P_o, 'a' is a constant rendering the general shape to the pCa vs. T relationship, and 'b' is a function of PLC phosphorylation. The values for 'a' and 'b' were found by fitting the equation to data reported by Sweeney and Stull (Am. J. Physiol. 250(19): C657, 1988) regarding the effect of PLC phosphorylation on the pCa vs. T relationship. The value of 'a' was established as 2.035×10^{-18}, and the relation of 'b' to PLC phosphorylation was assumed to be linear and was determined presuming that PLC phosphate content for Sweeney and Stull's reported potentiated state was equivalent to a 0.75 mol P/mol PLC condition. The result is the relation b = 7.4634 - 0.0548(mol P/mol PLC). Using this model, the effect of PLC phosphorylation on isometric tension was examined by analyzing the increase in tension resulting from PLC phosphorylation at many different pCa values. Inspection of the resulting 'PLC phosphate vs. tension augmentation' relationships indicated that (i) a very subtle change in the pCa vs. T relationship can have a large effect on tension augmentation, and (ii) the slope of the relationship increases dramatically as pCa decreases.

Tu-Pos12 MANIPULATION OF THE 'P-LIGHT CHAIN PHOSPHATE VS. ISOMETRIC TENSION POTENTIATION' RELATIONSHIP IN MOUSE EDL MUSCLE. R.L. Moore, B.M. Palmer, E. Snell, B. Stauffer, R. Grange, and M.E. Houston. The Depts. of Medicine and Physiology, The Penn State University, Hershey, PA

A model of a muscle system in which myosin P-light chain (PLC) phosphorylation increases the sensitivity of the contractile element to activation by Ca^{2+} predicts that the slope of PLC phosphate vs isometric tension potentiation (ITP) relationship should increase when the basal extent of contractile element activation is decreased. To test this hypothesis, extensor digitorum longus muscles were isolated from female Balb/c mice, mounted in muscle baths (30°C), and treated with (DANT) or without (C) 17.6 uM dantrolene, an agent known to partially inhibit Ca^{2+} release from the SR. DANT produced 49±2 and 73±1% decreases in P_o and P (unpotentiated), respectively. The DANT induced decrease in P occurred at a rate =-0.238±0.004 min^{-1}. Basal PLC phosphate contents in C and DANT muscles were 0.02±0.01 and 0.01±0.01 mol P/mol PLC, respectively. The effects of conditioning stimuli of various duration (0.35-1.5 s) and frequency (110-150Hz) on subsequent twitch tension (P*) and PLC phosphate content were examined. Regression lines describing the PLC phosphate vs. P*/P-1 relationships in C and DANT muscles were y=0.815x -0.029 and y=2.244x +0.281, respectively (i.e. DANT caused a significant 2.7 fold increase in slope). In C and DANT muscles, peak tension (and PLC phosphate content in mol P/mol PLC) of fused tetanic contractions of 0.94, 0.72 and 0.52 Po increased following conditioning stimuli by 0(.46±.04), 8±1 (.34±.03), and 21±2% (.18±.02), respectively. These data are consistent with the hypothesis that ITP in intact skeletal muscle is the result of a PLC phosphate induced increase in the sensitivity of the contractile element to activation by Ca^{2+}.

Tu-Pos13 CONTRACTION-INDUCED INJURY TO EDL MUSCLES IN YOUNG AND OLD MICE. Susan V. Brooks and John A. Faulkner, Department of Physiology and Bioengineering Program University of Michigan, Ann Arbor, Michigan 48109.

Lengthening contractions cause injury to skeletal muscles as evidenced by decreases in the maximum force developed and in the number of fibers present. Fibers that are severely injured degenerate and then regenerate. In young mice, the regeneration process is so effective that thirty days after injury maximum force and fiber number has returned to control values. With free transplantation of whole skeletal muscles, the muscle transplants in old animals regenerate less well than those in young animals. We tested the hypothesis that following the same degree of contraction-induced injury, skeletal muscles in old mice regenerate less well than skeletal muscles in young mice. Extensor digitorum longus (EDL) muscles from young (2-3 months) and old (26-27 months) mice were injured by a 15 minute protocol of repeated lengthening contractions. The extent of injury was evaluated by the decrement in maximum isometric force measured in situ 3, 7, 14, and 28 days after injury. Three days after contraction-induced injury maximum forces were 39% and 41% of control values for muscles from young and old mice respectively. These values were not different from each other. The maximum forces of muscles from young and old mice were also not different 7 days after injury, recovering to 56% and 58% of control values. Twenty-eight days after injury, muscles from young mice show no significant deficit in maximum force while muscles from old mice recovered to 80% of control values. We conclude that when injured to the same degree, skeletal muscles in old animals regenerate less well than muscles in young animals. Supported by NIH grant AG 06157.

Tu-Pos14 SKELETAL MUSCLE DAMAGE INDUCED BY LENGTHENING-CONTRACTIONS. Eileen Zerba, Thomas E. Komorowski and John A. Faulkner. Departments of Physiology and Anatomy & Cell Biology, The University of Michigan, Ann Arbor, MI 48109.

Lengthening contractions cause histological and ultrastructual damage to fibers and a decrease in maximum force of extensor digitorum longus (EDL) muscles in young and old mice. We tested the hypothesis that following lengthening contractions the action of free radicals results in ultrastructural damage to individual fibers. Muscles in old mice were expected to be more susceptible to free radical damage than muscles in young mice. EDL muscles of young and old mice were injured in situ by 5 min of lengthening contractions 20% of fiber length (L_f) at 0.5 L_f/s. Experimental animals were injected intraperitoneally with 1000 units/kg of polyethyleneglycol superoxide dismutase (PEG-SOD), an enzyme that quenches superoxide radicals, 24 hrs pre-injury and 24 and 48 hrs post-injury. The degree of damage to muscles was assessed at 1 hr and at 3 days after the injury by measurements of maximum force and by light (LM) and electron (EM) microscopical techniques. Compared to control values, maximum force was 61% and 46% for injured muscles in young and old mice respectively. In mice treated with PEG-SOD, injured muscles recovered 95% and 75% in young and old respectively. Quantification by LM indicated the decrease in force developed by injured muscles was proportional to the number of damaged fibers. Damaged myofibers could be distinguished by LM by their rounded appearance, pale staining reaction, and absence of sarcoplasmic elements. With EM, damaged myofibers had very few nuclei, irregularities of mitochondria and membrane systems, and disruption of myofibrils. Some myofibers had phagocytes within a continuous basal lamina. Supported by NIH grant AG 06157.

Tu-Pos15 **EFFECT OF EXTERNAL CALCIUM AND NIFEDIPINE ON TWITCH POTENTIATION IN SKELETAL MUSCLE.** Gamboa-Aldeco, R.*, Picones, A.# & Stefani, E. *Ctro. Invest. Ciencias de la Salud-UJAT, Tabasco, Mexico. #Depto. de Fisiol. CINVESTAV-IPN, Mexico. D.F. & Dept. Physiol. Mol. Biophys. Baylor College of Medicine. Houston, TX.

We report the effect of external Ca withdrawal and nifedipine on the contracile response of twitch fibres. Tension was isometricaly recorded from isolated EDL muscle fibres. Voltage pulses of 3 ms and 1.2 times threshold intensity were applied with electrodes parallel to the fibre. Solution without Ca (0 mM-Ca; 3 mM-Mg and 1 mM-EGTA) did not alter resting potential, membrane resistance or I_{Na} threshold. However this condition reduced the degree of twitch observed after tetanus or K contracture. Reduction of external Ca produce a reduction in postetanic (PTP) and postcontracture potentiations up to 78±3% (17) and 70±8% (8) of normal values respectively. Solution without Ca did not affect twitch or the raising phase of tetanus, but reduced the area of the tension-time curve of tetanus up to 70±14% (5) of normal. Nifedipine 1 μM in Ringer solution did not affect the development of twitch or the raising phase of tetanus, but reduced PTP (82±6%) (4) and the area of tension-time curve of 100 mM-K contractures (25±9%) (4). These results support the idea that external Ca and nifedipine modulate Ca release from the SR. Myoplasmic calcium transients measured in cut fibers have a fast and slow component. We suggest the fast one is related to twitch, the slow to witch potentiation and contracture.

Tu-Pos16 ***EFFECT OF ACIDOSIS ON FORCE-CALCIUM RELATION IN CARDIAC MUSCLE WITH SKELETAL TROPONIN-C EXCHANGE: IMPLICATIONS FOR THE MECHANISMS OF MYOCARDIAL ISCHEMIA AND MUSCLE FATIGUE***

A. Babu, S. Scordilis and J. Gulati, Albert Einstein College of Medicine, Bronx, NY and Smith College, Northampton, MA.

Acidosis has a bigger effect on pCa-force relation in cardiac muscle than in fast-twitch fibers. Because the TnC moiety determines the Ca^{2+}-sensitivity in both tissues, and TnCs differ in their primary structures and Ca^{2+}-binding properties, we investigated the effects of TnC exchange in cardiac muscle with acidosis. Thin trabeculae from the right ventricle of hamster were skinned and TnC was extracted. The pCa-force relations were determined at pH 7.0 and 6.5 after loading the trabecula with skeletal TnC. These results were compared with cardiac TnC loaded trabeculae. The force relation was shifted towards lower pCa values with pH 6.5, but the net decrease in sensitivity with pH was nearly the same for cardiac-TnC- and skeletal-TnC-loaded preparations. The mean shifts were (in pCa units) 0.59 ± 0.04 (8) for native, 0.59 ± 0.08 (3) for CTnC-loaded and 0.52 ± 0.07 (5) for STnC-loaded trabeculae. In native fast-twitch fibers from psoas muscle acidosis produced a shift in Ca^{2+} sensitivity of 0.24 ± 0.02 (4) pCa unit, a value less than half on cardiac muscle. These results provide the most direct evidence that the shifts in Ca^{2+}-sensitivity induced by pH changes, similar to those accompanying myocardial ischemia and muscle fatigue, are independent of the TnC moiety. Slow-twitch fibers (from soleus muscle) gave a shift like fast-twitch fiber, providing additional support for this idea.

[Support: NIH & NY Heart Association; and Blakeslee fund to Dr. Scordilis.]

Tu-Pos17 THE EFFECTS OF LACTIC ACID ON THE DEVELOPMENT OF TETANIC FORCE BY FROG SARTORIUS MUSCLE. J.M. Renaud. Dept. of Biological Sciences, Univ. of Calgary, Alberta, Canada T2N 1N4.

The effects of lactic acid on the intracellular pH and the development of tetanic force of frog sartorius muscles was studied to determine quantitatively the role of lactic acid in muscle fatigue. Lactacidosis was obtained by exposing unfatigued muscles one hour to 40 mM l-lactic acid and an extracellular pH of 6.4 or 7.2. During lactacidosis at pHo 6.4, the intracellular pH decreased from 7.13 to 6.58 and the intracellular concentration of lactic acid increased from 6.5 to 26.7 mM. During that time tetanic force decreased by 9.7%. The effect of lactic acid were reversible: removal of l-lactic acid resulted in a recovery of both the intracellular pH and tetanic force. At pHo 7.2, the intracellular pH decreased from 6.95 to 6.75 and lactic acid concentration increased form 6.8 to 23.7 mM. The change in tetanic tension was transient. It intitially decreased by about 6% for 15 min, then returned to its original value. The relaxation phase was prolonged during lactacidosis at both 7.2 and 6.4. It is concluded that the effect of lactic acid on the tetanic force of frog sartorius muscle is too small to be a major factor in muscle fatigue.

Tu-Pos18 THE MECHANICAL PROPERTIES OF FLATTENED MUSCLE. Henry H. Gale, Dept. of Physiology, Creighton University Medical School, Omaha, NE 68178.

Along with the effect of length, the mechanical output of muscle is sensitive to the lateral spacing of the myofilaments as shown by osmotic compression tests. However, osmotic compression acts on all sides of a muscle which is not the biological case. Muscles working in-situ encounter uniaxial lateral forces. This occurs in skeletal muscles in which the fibers run obliquely to the working axis, pennate muscles or where the muscle curves between origin and insertion. Oblique fiber angles and curved fiber paths result in force components acting sideways across the fiber and the filament lattice within it. The muscles of hollow internal organs follow curved paths in the organ walls. Muscular pumps create pressure differences across their walls; the force gradient acts sideways, uniaxially, on the filament array in the cells. During pumping movements the fibers are deformed laterally by uniaxial forces as the walls change thickness.

Osmotic compression experiments necessarily change muscle volume with deformation of the filament lattice occurring in all sidewards directions. In the physiologic case, muscle volume is constant, thus uniaxial compression causes flattening with narrowing occurring in the direction of compression and expansion occurring perpendicular to the direction of compression. Therefore, in a flattened cell, the filament lattice may be compacted in one direction and may spread apart in another with opposing effects on mechanical output. But if fiber flattening is not accompanied by lattice spreading and causes only compaction, the unopposed effect on mechanical output may be greater.

Barnacle giant muscle fibers were length clamped and laterally flattened during rest or during contraction. Electron microscopy was used to determine myofilament spacing. The results will be analyzed in terms of previous mechanical experiments on compressed muscle.

Tu-Pos19 **WARNING: CERTAIN ANIONS MAY BE HAZARDOUS TO YOUR SKINNED RABBIT PSOAS MUSCLE FIBERS.** Mark A. Andrews*, David W. Maughan# and Robert E. Godt*. *Dept. of Physiology & Endocrinology, Medical College of Georgia, Augusta, GA 30912, and #Dept. of Physiology & Biophysics, University of Vermont, Burlington, VT 05405.

We found that salts used to adjust ionic strength in skinned skeletal fiber solutions inhibit maximal calcium-activated force (F_{Max}) in an order that approximates the Hofmeister lyotropic series for destabilization of protein structure (Andrews et al., Biophys J. 53:570a, 1988). In these solutions potassium salts cause swelling of chemically skinned fibers in a similar order: methanesulfonate (Ms) < acetate ≈ lactate < propionate < Cl < nitrate. If, however, Dextran T 500 (a long-chain polymer) was added to maintain constant fiber diameter, F_{Max} increased slightly, yet these salts still decreased F_{Max} in the same order. Thus, we conclude that anion-dependent swelling of fibers does not explain the ordering of salt effects on F_{Max}, but, more likely, protein destabilization may be responsible. Supporting this notion, SDS-PAGE (with silver staining) of single fibers revealed significant extraction of myosin heavy and light chains in relaxing solutions with Cl, even at physiological ionic strength (165 mM). Extraction was exacerbated at high ionic strength (390 mM). Such extraction was not seen in Ms solutions, even at 390 mM ionic strength. Protein extraction from fibers in propionate or acetate solutions was intermediate between that with Cl and Ms. These data strengthen our aversion to Cl and confirm our preference for Ms in skinned fiber bathing solutions. (Support: NIH AR 31636 and DK 33833)

Tu-Pos20 CONCENTRATIONS OF GLYCOLYTIC PROTEINS IN RABBIT PSOAS MUSCLE FIBERS. David Maughan and Elisabeth Wegner, Dept. of Physiology & Biophysics, Univ. of Vermont, Burlington, VT 05405

Studies of glycolytic enzyme localization in muscle have advanced the idea of multi-enzyme complexes (cf. Clarke & Masters, Int. J. Biochem. 7:359-365, 1976). To examine the stoichiometry of these enzymes, we measured their concentrations in segments of muscle fibers. Fibers were isolated under oil, their volumes measured, and the fibers transferred to vials containing relaxing solution with 0.02% saponin. After 20 min, the chemically skinned fibers were removed. The amount of each enzyme remaining in the fibers (non-diffusible fraction) and in the solution vials (diffusible fraction) was measured by quantitative SDS-PAGE (calibrated with protein standards). Concentrations of glycolytic enzymes in the diffusible fraction were (in ng/nl fiber, mean±S.D.): phosphofructokinase (PFK), 8.4±4.8; phosphoglucose isomerase, 2.2±0.9; enolase, 7.2±1.5; triose-phosphate isomerase, 3.1±1.5; glyceraldehyde-3-P dehydrogenase, 7.6±2.0; phosophoglycerate mutase, 2.8±0.7; pyruvate kinase, 12.8±5.2. Their concentrations in the non-diffusible fraction were negligible, except for PFK (about 0.07 of the diffusible fraction). Aldolase, phosphoglycerate kinase and lactate dehydrogenase diffused out, but their amounts could not be measured because their bands overlapped with each other or with others on the SDS-gels. The molar concentrations of phosphoglucose isomerase and enolase were, respectively, 0.7 and 3.6 times that of the PFK total (24 μmol/l fiber), while the molar concentrations of the others were about twice (2.2±0.2) that of the PFK total . The relative molar concentrations of each may be indicative of their stoichiometry in a multi-enzyme complex, should it exist. [Funded by NIH R01 DK33833]

Tu-Pos21 **PARVALBUMIN CONCENTRATION CORRELATES WITH MAGNITUDE OF RECOVERY OF RELAXATION RATE AFTER A PROLONGED TETANUS IN FROG SKELETAL MUSCLE FIBERS.** Tien-tzu Hou, Leo J. D'Anniballe and Jack A. Rall. Department of Physiology, Ohio State University, Columbus, OH 43210.

Calcium-binding protein parvalbumin (PV) may function to promote relaxation in fast contracting skeletal muscles. If so, its effect would diminish progressively with increasing tetanus duration as PV fills with calcium during contraction. Relaxation rate as a function of tetanus duration, determined in fibers isolated from tibialis anterior muscles of the frog, R. temporaria, at 0° C, decreased exponentially to a steady value with a rate constant of 1.4 s^{-1} (Hou and Rall. Biophys. J. 51: 475a, 1987). Recovery of relaxation rate with rest after a prolonged tetanus (4 s duration) should be controlled by rate of calcium dissociation from PV. Relaxation rate recovers exponentially with a rate constant of 0.14 ± 0.02 s^{-1} (N = 14). Thus time course of recovery is 10 fold slower than time course of slowing of relaxation rate. According to this reasoning, magnitude of recovery of relaxation rate should correlate with total [PV] in fibers. [PV] was measured according to Hou et. al. Biophys. J. 53: 569a, 1988. Linear regression analysis of magnitude of recovery of relaxation rate versus [PV] showed a significant positive correlation (r = 0.8, N = 7). Thus fibers with higher [PV] exhibit greater magnitudes of recovery of relaxation rate after a prolonged tetanus. (Supported by NIH and AHA, Central Ohio Heart Chapter.)

Tu-Pos22 CALCIUM DEPENDENCE OF STATIC AND DYNAMIC MECHANICAL PROPERTIES OF SINGLE SKINNED CARDIAC MYOCYTES. N.K. Sweitzer, P.A. Hofmann, J.M. Graham and R.L. Moss. Department of Physiology, University of Wisconsin, Madison, WI 53706.

We have developed techniques for the measurement of static and dynamic mechanical properties of single skinned cardiac myocytes. Rat myocytes were obtained by brief homogenization in a Waring blender and attached with a commercially available adhesive to a force transducer and piezo-electric translator. Frog myocytes were enzymatically dissociated and attached using the method of Warshaw and Fay (J. Gen. Phys. 82:157, 1983). Measurements were made at 22°C. Tension-pCa curves obtained at similar sarcomere lengths demonstrated that the calcium sensitivity of tension development is greater in frog than in rat myocytes. The pCa_{50}'s were approximately 6.2 for frog and 5.7 for rat myocytes. In frog atrial myocytes mean shortening velocities, measured using the slack test method, were 5.08 muscle lengths per second (ML/s) at pCa 4.5 and 2.13 ML/s at pCa 6.0. SDS-PAGE analysis of the single myocytes on which mechanical measurements were made showed the presence of a single myosin isozyme in frog atrial myocytes; rat ventricular myocytes contained two isozymes. Rat myocytes also showed a decrease in velocity when the concentration of Ca^{2+} was reduced, however the velocity data from rat exhibited a greater variability between cells, possibly due to variations in the proportions of the two myosin isozymes. Several conclusions may be drawn: (1) the regulatory proteins of frog atrial myocytes appear to have a greater affinity for Ca^{2+} than those in rat ventricle; (2) unloaded shortening velocity may vary with the myosin isozyme content of the myocyte; and (3) the demonstrated Ca^{2+} sensitivity of V_{max} is qualitatively similar to earlier results from skeletal muscle and may have important functional consequences on a beat-to-beat basis in the heart. Supported by NIH and the AHA of Wisconsin.

Tu-Pos23 ENERGY-DEPRIVATION CONTRACTURE IN RAT HEART: ROLE OF ATP

C.G. Nichols & W.J. Lederer. Dept. of Physiology, University of Maryland, School of Medicine. Baltimore, MD 21201.

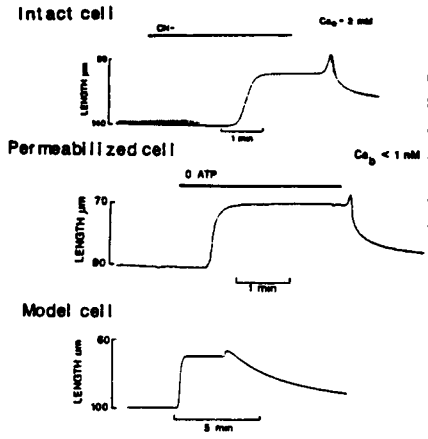

On exposure to complete metabolic blockade (2 mM cyanide, 10 mM 2-deoxyglucose) unloaded rat ventricular myocytes shortened ("contracture") to a constant length of 69 ± 1.6 % of control length. On removal of cyanide, cells shortened again ("recontracture") to 57 ± 2.0 % before relaxing. Similar contractures and recontractures were observed in saponin-permeabilized cells on removal of bath ATP (ATP_b) and subsequent readdition of ATP_b, even at pCa > 9. When $[ATP]_b$ was lowered to zero, shortening stopped at ~ 70 % control length. However, when $[ATP]_b$ was lowered to 4 - 20 µM, shortening continued to 30 % control length. When $[ATP]_b$ was restored from zero to 4 - 20 µM, recontracture shortening continued without relaxation. The results can be explained by a simple model that assumes Ca^{2+}-independent cross-bridge cycling occurs as [ATP] falls through a "window" range (0.1 - 100 µM; Fabiato and Fabiato, 1975, J. Physiol., 249, 497-517). As [ATP] falls below 1 µM, shortening ceases as cross-bridge cycling declines and stiffness increases due to rigor-bridge formation. Recontracture occurs on restoring ATP production, because stiffness falls and cross-bridge cycling increases. As [ATP] rises above 100 uM cross-bridge cycling ceases and the cell relaxes.

Supported by the N.I.H. and A.H.A. (Maryland Affiliate).

Tu-Pos24 METABOLIC AND FUNCTIONAL CONSEQUENCES OF BARIUM CONTRACTURE IN RABBIT MYOCARDIUM

WC Hunter, MR Berman, T Shibata, & WE Jacobus. Johns Hopkins University, Baltimore MD

Barium contracture is a convenient method for tonically activating myocardium while preserving cellular integrity. We studied both the metabolic and mechanical consequences of the duration of barium contracture in heart muscle. For the metabolic studies, we used ^{31}P NMR measurements to determine the time course of changes in phosphocreatine, ATP, Pi, total phosphate, and intracellular pH in isolated, perfused isovolumic rabbit hearts. For mechanical studies we measured force transients and dynamic stiffness in isolated rabbit right ventricular papillary muscles at different elapsed times in barium contracture. In the perfused hearts, phosphocreatine declined steadily, falling to 20% of control after 60 min of barium contracture, while ATP levels remained constant for approximately 25 min, then fell to 25% of control by 60 min. Pi rose to 200% of control within 15 min and remained unchanged thereafter, whereas total phosphate dropped steadily to 50% of control by 60 min. Intracellular pH fell from 7.24 to 6.96 within the first 5 min, but was unchanged thereafter. Myocardial oxygen consumption remained at control level for 30 minutes, then declined to 50% of control at 60 minutes. Consistent with the ATP and oxygen consumption measurements, mechanical performance of excised papillary muscles was unchanged for approximately the first 25 minutes. Thereafter, mechanical behavior progressively altered toward more rigor-like characteristics. In summary, these data show that myocardium in barium contracture represents a high energy demand state in which the active contractile processes are intimately involved in maintaining contractile force, rather than being a rigor state. This state is metabolically and mechanically stable for approximately 30 min, but begins to degrade thereafter.

Tu-Pos25 RESOLUTION AND EVALUATION OF ASYNCHRONOUS MOTIONS BETWEEN SARCOMERES IN CARDIAC MUSCLE CELLS. J.W. Krueger, A. Denton, G. Siciliano, Albert Einstein College of Medicine, Bronx, N.Y. 10461 & R.C. Tiberio, National Nanofabrication Facility, Cornell University, Ithaca, NY. 14583

We observed the motions that occur between the sarcomeres in the isolated cardiac muscle cell to learn more about the mechanical nature of their interconnections. The cell is observed with modulation-contrast microscopy, and the image of its striations is detected by a self-scanned photodiode array. Sarcomere length is measured >500/s from the local frequency content of the array's video signal (Myers et al. 1982) in two separate regions of the cell. The method also maps the spatial pattern of sarcomere shortening and lengthening by automatically advancing the point of sampling of one region along the length of the cell in 1.2 μm steps. A precision test grating, with a deviation of <30nm, was fabricated by electron beam lithography at the NNF. It indicates that the method accurately resolves a step change of 0.1 μm in the spacing of contiguous striations to ±0.01 μm for a 2.4 μm displacement of the sampling window, a surprising value well in excess of both the 0.5 μm resolution of the microscope and the ultrastructural regularity of the sarcomere. In the asynchronously contracting, unattached cell, sarcomeres can lengthen ~0.1 μm beyond their rest length prior to the arrival of the propagated wave of contraction. Such prelengthening extends nonuniformly for 10 to 15 μm in the cell and occurs also when the cell is lifted from the substrate by a micropipet. The sarcomere's dynamics differ in synchronous and asynchronous contraction, indicating that asynchrony imposes an additional internal restoring force in the unattached cell. The extra intracellular force estimated to account for sarcomere prelengthening (~0.3-0.4 $mN/mm2$) depresses the velocity of shortening and speeds the velocity of relengthening by only ~10-15%, and so the true sarcomeric restoring force must be *correspondingly larger* than that estimated from the asynchronous lengthening of the sarcomeres. The level of this internal force accounts easily for the diastolic recoil of the heart. Supported, in part, by HL 21325 (JWK) and NSF Grant ECS-8619049 (NNF).

Tu-Pos26 REGIONAL DIFFERENCES DURING UNLOADED CONTRACTION OF ISOLATED RAT CARDIAC MYOCYTES. Kenneth P. Roos*, A. Christyne Bliton, Mark J. Patton, and Stuart R. Taylor.
*Cardiovascular Research Laboratory, UCLA School of Medicine, Los Angeles, CA. 90024-1760, and Department of Pharmacology, Mayo Foundation, Rochester, MN. 55905.

Patterns of shortening and re-extension during unloaded twitches of adult rat cardiac myocytes were determined by comparing longitudinally and laterally contiguous striated regions. Differences that presumably reflect heterogeneous behavior among closely associated sarcomeres were measured across a cell's full width and along segments 6 to 14 striations long. Complete contractions were captured at high speed (120-400 Hz) with an integrated digital imaging system. Cells bathed in 2-5 mM Ca^{2+} saline were electrically stimulated after periods of rest or paced at 1-3 Hz. Striation periodicity was measured in many, small, longitudinally oriented regions of contiguous striations after image processing. The overall pattern of shortening and re-extension was uniform in a given region of the same cell. The onset of contraction was synchronous within the entire imaged area. But laterally adjacent regions across the width of the cell often differed in striation periodicity in the same contraction. There usually were differences in initial average striation periodicity (up to 70 nm), extent of shortening (up to 31%), and the onset of re-extension (up to 25 ms). Any shearing forces caused by different regional dynamics had no detectable consequences. These findings suggest that (i) cytoskeletal inter-connections between functional regions are weak or very elastic and (ii) the pattern of contraction determined from the average behavior of large numbers of sarcomeres does not reflect the characteristics of individual contractile units in a single twitch of the same cell. Supported by USPHS HL-29671 (KPR), and NS-22369, & NSF DMB-8503964 (SRT).

Tu-Pos27 BIFUNCTIONAL SPIN-LABELS: AN APPROACH TO OBTAINING SPECFIC AND IMMOBOLIZED LABELS ON MUSCLE PROTEINS. N. Naber and R. Cooke. Dept. of Biochemistry and CVRI, University of California, San Francisco, CA 94143. (Introduced by S. Akeson)

The traditional approach to spin-labeling proteins has been to use labels that are selective for a particular type of residue, e.g. lysines, and to attempt to place them on the most reactive residue of this class. Several problems arise in this approach: it is unusual for one residue to be much more reactive than other residues, and the labels are often not immobilized on the protein surface. We have attacked both of these problems by using bifunctional labels that have a reactive group on one side of the spin label ring and a large hydrophobic ring on the other side. The hydrophobic nature of the ring helps place the label on hydrophobic regions of the protein surface, providing greater reactivity with residues that are in the vicinity of these regions. Once the label has reacted with a residue the ring helps keep the label immobilized on the protein surface. One label that we have investigated has a succinimide group that reacts with lysines on one side and a fluorene ring on the other side both coupled to the 4 position of a TEMPO spin label. This label is found to react with many fewer groups than does a label containing only the reactive succinimide group. In addition the bifunctional labels are all immobilized with rotational correlation times in excess of 0.05 usec, while the majority of the corresponding monofunctional labels have correlation times less than 0.01 usec. Thus the bifunctional label has achieved both better specificity and greater immobilization than the monofunctional label. Supported by a grant from the USPHS, AM30868.

Tu-Pos28 MEASUREMENT OF THE RATE OF PRESTEADY STATE HYDROLYSIS OF NUCLEOSIDE TRIPHOSPHATES BY CARDIAC ACTOMYOSIN-S1 AND MYOSIN, Betty Belknap, Jeanne MacDowell, and Howard White, Dept. of Biochemistry, E. Virginia Medical School, Norfolk, Va. 23507.

We have measured the presteady state hydrolysis of ATP, GTP and 1,N^6-etheno-2-aza-ATP (aza-ATP) by bovine cardiac myosin-S1 and actomyosin-S1 using quenched-flow methods. 'Burst' measurements can be used to measure the rate and equilibrium constants of the hydrolytic steps for myosin and actomyosin. In the absence of actin the rate of the burst increases from 6.8 s^{-1} at 10 uM ATP to 15.7 s^{-1} at 25 uM ATP and is very similar to the rate constants measured for the fluorescence enhancement observed upon mixing ATP with myosin-S1 in the stopped-flow fluorimeter, 7.3 and 17.5 s^{-1}. In the presence of 24 uM actin (Km for actin activation of steady state ATP hydrolysis is ~5 uM under these conditions) a burst of 0.6 mole-pi/mole- S1 occurs with a rate constant of 60 s^{-1}. The rate of the fluorescence enhancement observed upon mixing 25 uM ATP with bovine cardiac actomyosin-S1 under identical conditions is 53 s^{-1}. The maximum rate of the fluorescence enhancement measured at saturating ATP is 80 s^{-1} for actomyosin-S1 compared to 40 s^{-1} for myosin-S1. The size of the phosphate burst was the same within experimental error for myosin-S1 and actomyosin-S1 ~0.6mole/mole-S1. These results indicate that the hydrolytic step on the attached cross bridge is too rapid, ~80 s^{-1} to be the rate limiting step of the ATP hydrolysis mechanism (Vmax = 1.2 s^{-1}), which must therefore either be phosphate release or a step preceeding phosphate release. No rapid burst of phosphate hydrolysis by either myosin-S1 or acto myosin-S1 could be measured using either GTP or aza-ATP as substrates. This work was supported by grants from the American Heart Association and the Muscular Dystrophy Association.

Tu-Pos29 PRELIMINARY RESULTS FROM NEUTRON DIFFRACTION OF MUSCLE BEARING DEUTERATED LIGHT CHAINS. R.A. Mendelson, D.B. Stone and D.B. Bivin, Cardiovascular Research Institute and Dept. Biochem./Biophys., Univ. of California, San Francisco, CA 94143

In order to have a non-perturbative probe of muscle crossbridges, we have labeled desensitized scallop muscle fibers and myofibrils with deuterated chicken light chain two (LC2). By contrast-matching in a 42% D_2O buffer, the neutron diffraction of protonated protein is strongly suppressed and diffraction arising from the deuterated LC2 alone is seen. The layer lines are sensitive to intra- and inter-myosin chords between LC2s at low resolution. Thus this technique senses the position and separation of LC2- bearing portions of the crossbridges.

An LC2 fusion protein was synthesized in *E. coli* grown on deuterated algal hydrolysate (Mendelson *et al.*, Biophys. J. *53*, 177a, 1988). Deuterated LC2 was isolated by modification of the method of Reinach *et al.* [Nature *322*, 80-83 (1986)]. In data from glycerinated myofibrils in rigor at full overlap we have identified several known equatorial and meridional or near-meridional peaks. Upon addition of $MgPP_i$, we observe a significant increase of intensity in the 14.5 nm region indicating that the light chain is more ordered with the thick filament periodicity in relaxation. Labeled fibers in contrast-matching buffer show a 14.5 nm meridional reflection which is not seen in unlabeled fibers. Supported by NIH (HL-16683) and Univ. of Calif. (CALCOR).

Tu-Pos30 INTERACTION OF SKELETAL MYOSIN-S-1 WITH A NON-POLYMERIZABLE MONOMERIC ACTIN FORM.
N. Bettache, R. Bertrand and R. Kassab.
Centre de Recherches de Biochimie Macromoléculaire. CNRS-INSERM Montpellier (France)

For the knowledge of the tertiary structure of S-1 when associated to actin, we have designed an actin derivative whose salts and S-1 induced polymerization ability were abolished by reaction with m-maleimidobenzoyl-N-hydroxysuccinimide ester (MBS). The presence of a free maleimido group in the MBS-actin permitted its specific covalent coupling to the S-1 heavy chain. This conjugaison did not involve the reactive SH1 or SH2 thiols ; it did not occur with G-or F-actin and it led to the blocking of the rigor recognition site of F-actin on S-1. MBS-actin and S-1 can form a tight, reversible complex that is stable during gel filtration and can be dissociated by Mg-PPi. In this complex, the two proteins were crosslinked by EDC with the formation of a soluble adduct similar to the 170K doublet generated by crosslinked F-actin-S-1. The tryptic digestion of the reversible complex showed that MBS-actin protects the 27K-50K junction, but, unlike F-actin, not the 50K-20K connector segment. These new MBS-actin-S-1 complexes which behave as "analogues" of the F-actin-S-1 system may be valuable for further understanding of the acto-S-1 interaction ; their eventual cristallization would initiate X-ray diffraction studies on the associated structures of S-1 and actin. Supported by grants from CNRS, INSERM and NATO.

Tu-Pos31 CHARACTERIZATION OF AN ACTO-MYOSIN HEAD INTERFACE IN THE 40-113 REGION OF ACTIN BY USING SPECIFIC ANTIGENIC PROBES. J.P. Labbé, C. Méjean, Y. Benyamin, C. Roustan (Intr. by D. Mornet). LP 8402 (CNRS) - U 249 (INSERM) (EPHE) PB 5051 - 34033 Montpellier Cedex France.

We observed by using R.I.A. or E.L.I.S.A. approaches that the myosin head (S1) is able to interact not only with coated filamentous actin but also with coated monomeric one. These interaction are reversed by ATP-Mg^{++}. Antibodies directed to the 18-28 region of actin compete with S1 to actin. In contrast, another population of antibodies directed to 1-7 sequence is unable to prevent S1-actin interaction. These results suggest a first region, near or at the 18-28 sequence, involved in the acto-S1 interface.

The occurence for a second site for S1 binding is based upon the following data :
- chemical crosslinking of S1 to actin implicates acidic residues in the 40-113 sequence,
- amino acid substitution at position 89 in various isoactins correlates the differences in K_D observed in S1 associations with the actin isoforms,
- the antibodies specific for the C-terminal part of the thrombic fragment (40-113) are in partial competition with S1 binding,
- at least, we observe a direct binding of myosin head to purified 40-113 fragment as obtained for filamentous or monomeric actins.

All these results suggest two independent regions involved in S1 interface, one of these being near the 95-113 sequence and including the residue 89.

Tu-Pos32 DIFFERENTIAL EFFECTS OF VANADATE ON ATP-INDUCED AND ITP-INDUCED CONTRACTIONS OF SKINNED RABBIT PSOAS MUSCLE FIBERS. Franklin Fuchs and Michael Hu, Department of Physiology, University of Pittsburgh School of Medicine, Pittsburgh, PA 15261.

The vanadate anion (Vi) is a phosphate analog which inhibits MgATP-induced myofibrillar contraction by forming a relatively inert M·ADP·Vi complex (Goodno, 1979; Dantzig and Goldman, 1985). MgITP can also provide energy for contraction but it is less effective in dissociating actin and myosin and in maintaining relaxation at high pCa (Finlayson, et al, 1969; Weber, 1969; Fuchs, 1985). Vanadate was found to have strikingly different effects on contraction of detergent-extracted psoas fibers in the presence of MgATP and Mg ITP. At concentrations of 0.5-1.0 mM, vanadate produced 90-95% inhibition of force development in the presence of 5mM MgATP, pCa 5.0. Substituting MgITP for MgATP under the same conditions, vanadate was totally ineffective in producing inhibition of contraction. Such fibers could be fully relaxed by addition of EGTA. Either vanadate is incapable of forming a stable M·IDP·Vi complex, or this complex binds more strongly to actin than the M·ADP·Vi complex. Supported by grants from the NIH (AR 10551) and American Heart Association.

Tu-Pos33 INTRAMOLECULAR CROSS-LINKING OF ACTIN ENHANCES ITS ATPase ACTIVATION OF SCALLOP MYOSIN.
H. Kwon, P.M.D. Hardwicke*, and A.G. Szent-Gyorgyi. Dept. of Biology, Brandeis University, Waltham, Mass. 02254 and *Dept. Chemistry & Biochemistry, Southern Illinois University, Carbondale, IL 62901.

Rabbit skeletal muscle F-actin was modified by lysine-directed photolabile cross-linkers (N-5-Azido-2-nitrobenzoyloxysuccinimide, 4-Benzoylbenzoic Acid N-Hydroxysuccinimide) in approximately a 1:1 molar ratio. Actin that was photolyzed either in the monomeric or the filamentous form moved as monomeric actin on SDS polyacrylamide gels, and also depolymerized and repolymerized readily, indicating that the cross-linking was intramolecular in both cases. The cross-linked actin enhanced the actin-activated MgATPase of the scallop myosin 3-4 times more than untreated actin, without altering the calcium sensitivity. Modified actin that was not photolyzed behaved as untreated actin. These results indicate that conformational changes in actin can alter its interactions with myosin.

This work has been supported by USPHS AR15963 and MDA.

Tu-Pos34 THE N-TERMINAL SEGMENT ON ACTIN AND ACTO S-1 INTERACTIONS IN THE PRESENCE OF ATP.
G. Das Gupta and E. Reisler, Department of Chemistry and Biochemistry, and the Molecular Biology Institute, University of California, Los Angeles, CA 90024-1569.

Immunochemical and solution studies employing site-specific antibodies directed against the N-terminal acidic residues on skeletal α-actin revealed that this segment of the protein could not be the main determinant of rigor actomyosin binding. [Miller, et al., Biochemistry 26, 6064-6070 (1987) and Mejean, Biochem. J. 244, 57-577 (1987)] However. subsequent work has shown that the same antibodies inhibit actomyosin ATPase activity and the binding of S-1 to actin in the presence of MgATP [Das Gupta, et al. Biophys J 53, 574a, (1988)]. In this study the acto-S-1 interactions in the presence of ATP and F_{ab} fragments of antibodies were studied at 5°C over a range of S-1 and F_{ab} concentrations. It is shown that at various levels of actin saturation by F_{ab} (between 0.15 and 0.9 F_{ab}/actin) the inhibited acto S-1 ATPase can be "switched-on" by tritrations with S-1. The activity transitions are cooperative, and as revealed in airfuge binding experiments, are accompanied by cooperative increases in the binding of S-1 to actin with the increase in S-1 concentration. The binding of S-1 to actin leads to only minor displacement of F_{ab} but the total combined occupancy of actin by F_{ab} and S-1 does not exceed 1.0 protein/ actin. The switched-on ATPase activities of acto-S-1 depend on the amount of F_{ab} co-bound to actin. At the binding of 0.15 S-1/actin, the co-binding of 0.85 F_{ab}/actin leads to an 80% inhibition of the acto-S-1 ATPase reaction. These results are discussed in terms of regulation of acto-S-1 interactions by antibodies against the N-terminus of actin.

Tu-Pos35 INTERACTIONS BETWEEN THE N-TERMINAL REGION OF ACTIN AND MYOSIN SUBFRAGMENT 1
J.E. Van Eyk and R.S. Hodges, Department of Biochemistry, University of Alberta, Edmonton, Alberta.

In order to delineate the amino acid sequence of the amino terminus of actin involved in the acto-myosin interaction, we synthesized four actin peptides, consisting of residues 1-7, 1-14, 18-28 and 1-28 by solid-phase peptide synthesis. The interaction between S1 and the actin peptides 1-14, 18-28 and 1-28 resulted in the precipitation of the S1-peptide complex. After centrifugation of mixtures comprised of varying mole ratios of peptide to S1, SDS urea gels and ATPase assays of the supernatant demonstrated that the mole ratio of the peptide-S1 complexes was 1:1. The presence of F-actin eliminated aggregation of the S1-peptide complex until a high concentration of peptide was reached. This suggests that the peptides and F-actin are in competition for a binding site on S1, and the presence of F-actin lowers the concentration of peptide-S1 complex free in solution thereby decreasing the chance for aggregation to occur. The actin peptides 1-14, 18-28 and 1-28 potentiated the acto-S1 ATPase in a manner similar to F-actin, while the actin peptide 1-7 did not affect either S1 or acto-S1 ATPase activity. The actin peptide 1-14 was the least effective at binding and potentiating the acto-S1 or acto-S1-TM ATPase activity, followed by peptide 18-28 which binds tighter to S1. The actin peptide 1-28 was by far the most potent and efficient peptide, indicating that at least part of the binding site for S1 lies within this sequence. The addition of other thin filament proteins such as TM, altered the ATPase rate induced upon addition of the peptide 1-28. This change in ATPase activity is an indirect reflection of the status of the F-actin filament and its interaction with S1. In the presence of TM, less peptide 1-28 was required to increase the maximum potentiation of the ATPase activity. This indicates that S1 does not interact as well with the actin-TM filament as when TM is absent. AS well, the presence of Tn or the synthetic TnI inhibitory peptide altered the concentration of peptide required for potentiation. This indicates that changes occur in the S1 interaction with F-actin filament depending on the state of the thin filament. It is clear that the synthetic actin peptide 1-28 competes with F-actin for S1 and probably this region in actin binds S1 and exerts some control over the S1 activity.

Tu-Pos36 CREATINE KINASE ACTIVITY IN SKINNED FAST- AND SLOW-TWITCH, AND CARDIAC MUSCLE FIBERS. Edith Chen, W. Glenn L. Kerrick and Phyllis E. Hoar, (Intr. by W. Nonner) Dept. of Physiology and Biophysics, Univ. of Miami, School of Medicine, Miami, FL 33101

Maximal Ca^{2+}-activated MgATPase activity was measured in single skinned fast- and slow-twitch fibers, and bundles of skinned cardiac fibers from the rabbit. This ATPase activity was determined by measuring the rate of oxidation of NADH to NAD which was coupled to the ATP regenerating system phosphoenol pyruvate (PEP) and pyruvate kinase (PK). The rate of oxidation of NADH was determined by measuring associated changes in NADH fluorescence. By allowing the exogenous ATP regenerating system PEP and PK to compete with the endogenous creatine phosphokinase (CPK) in the presence of creatine phosphate (CP) before and after inhibition of the endogenous CPK with iodoacetamide it was possible to determine the endogenous creatine kinase activity of the skinned fibers. These studies showed that the activity of creatine kinase was highest in skinned slow-twitch fibers and the lowest in fast-twitch fibers. The relative CPK concentration was also determined using two dimemsional gel electrophoresis. In addition it was determined that at a concentration of CP above 4.0 mM the rate at which ATP is regenerated was not limited by the CP concentration, but the concentration of CPK. Supported by grants from the NIH (AR 37447), American Heart Association and Florida Affiliate, and the Muscular Dystrophy Association.

Tu-Pos37 Ca^{2+}-ACTIVATION OF ATPase ACTIVITY AND CHANGES IN TnC_{DANZ} FLUORESCENCE PRECEDE FORCE DEVELOPMENT. W. Glenn L. Kerrick*+, Konrad Guth+, James D. Potter+, and Phyllis E. Hoar*, Dept. of Physiology and Biophysics* and Dept of Pharmacology+, Univ. of Miami, School of Medicine, Miami FL 33101.

ATPase activity, TnC_{DANZ} fluorescence, isometric force, and stiffness were measured in skinned fast-twitch fibers of the rabbit. In the presence of 2 mM MgATP and an ATP regenerating system Ca^{2+}-activated increases in ATPase activity and skeletal TnC_{DANZ} fluorescence preceded isometric tension development and muscle stiffness. These findings suggest that Ca^{2+}-binding to troponin is associated with the activation of actomyosin ATPase activity. Furthermore these findings suggest that only after myosin cross-bridge interactions have reached a critical level (as judged by ATPase activity) do force generating cross-bridges begin to form. Similar results were found for rat cardiac muscle using cardiac TnC_{IAANS}. If the ATP analogue ATPγS is substituted for ATP in fast-twitch fibers, then the muscle develops 80% of the stiffness, 65% of the ATPase activity, and 20% of the force relative to that found with ATP. In addition the Ca^{2+}-dependence of the ATPase activity, muscle stiffness, and tension are similar. In contrast to the findings for ATP, these findings suggest that in the presence of ATPγS Ca^{2+}-binding to TnC causes the simultaneous activation of force-generating myosin cross-bridges and actomyosin ATPase activity. In addition these data show that ATPγS is hydrolyzed at a significant rate in skinned muscle fibers even though little force is developed relative to ATP. Supported by NIH grants (AR37447, AR37701), the American Heart Association and Florida Affiliate, and the Muscular Dystrophy Association.

Tu-Pos38 THE KINETICS OF THE INTERACTION OF MYOSIN SUBFRAGMENT 1 WITH REGULATED ACTIN. Shwu-Hwa Lin[1], Frank Garland[2], and Herbert C. Cheung[1]. [1]Graduate Program in Biophysical Sciences and Department of Biochemistry, University of Alamaba at Birmingham, Birmingham, AL 35294 and [2]Department of Natural Sciences, University of Michigan-Dearborn, Dearborn, MI 48128

The kinetics of the interaction of actin(A) with myosin subfragment 1(S1) was previously studied in stopped-flow experiments with S1 that was fluorescently modified at SH_1 with 5-(iodoacetamido)-fluorescein(IAF). The kinetic traces of the association reaction were resolved into two first-order steps (S.-S. Lin and H.C. Cheung (1988) Biophs. J. 53(#2, pt. 2): 183a). We have extended the previous work by using regulated actin to monitor the association and dissociation kinetics. When 1.5 μM of labeled S1 (S1-AF) was mixed with regulated actin in the range 3-9 μM in 60 mM KCl, 30 mM TES, pH 7.0, 1 mM $MgCl_2$, 1 mM EGTA and at 20°C, the kinetic traces were resolved into two first-order steps with rate constants k_1 (fast) and k_2 (slow). At each of the actin concentration k_1 was about 2-fold slower than the fast rate constant observed with pure actin and k_2 was about the same as the slow rate constant observed with unregulated actin. In the presence of Ca^{2+} k_1 and k_2 increased by 40-50%. The dissociation of A•S1-AF was monitored by displacement of the labeled S1 with native S1. The observed single first-order rate constant was 0.01-0.02 s^{-1}. With regulated actin the dissociation rate constant was found to be about a factor of 5 slower than with pure actin. The two observed first-order steps observed in the association reaction occurred after the formation of the encounter complex between actin and S1 and were not greatly affected by the presence of tropomyosin and troponin on the actin filament. The regulatory proteins, however, had a large effect on the dissociation rate. (Supported in part by NIH AR31239).

Tu-Pos39 FLUORESCENCE STUDIES OF THE INTERACTION OF TROPONIN C AND I FROM BOVINE CARDIAC MUSCLE. Ronglih Liao, Chien-Kao Wang, and Herbert C. Cheung. Graduate Program in Biophysical Sciences, and Department of Biochemistry, University of Alabama at Birmingham, Birmingham, AL 35294

The interaction of bovine cardiac troponin C (CTnC) with cardiac troponin I (CTnI) was studied using CTnC that was modified at Cys 35 and Cys 84 with the fluorescent probe 2-(4'-iodoacetamidoaniline)-naphthalene-6-sulfonic acid (IAANS). The studies were carried out at 20°C in a medium containing 0.3 M KCl, 50 mM Tris, 0.1 mM DTT, pH 7.5 and 1 mM EGTA. The free energy of formation of the binary complex (CTnC-IAANS)·CTnI was -9.4 kcal/mol in the absence of divalent cations. It decreased to -10.0 kcal/mol in the presence of Mg^{2+} and -12.1 kcal/mol in the presence of Ca^{2+}. The complex was stabilized by only -0.6 kcal when the two Ca/Mg sites of CTnC were saturated by Mg^{2+}, and was further stabilized by -2.1 kcal when the single Ca specific site was filled. This large negative coupling free energy is comparable to that previously reported for the troponin C·troponin I complex from skeletal muscle when the two Ca specific sites of skeletal TnC were saturated.

The (CTnC-IAANS)·CTnI complex was further characterized by measuring the efficiency of fluorescence energy transfer (FRET) from Trp 192 of CTnI to the fluorophore attached to the two thiols of CTnC. The distance R(2/3) between donor and acceptor determined in the absence of divalent cations and in the presence of Ca^{2+} were 21 and 28 Å, respectively. The effects of phosphorylation of CTnI on the energetics of its complex formation with CTnC and on the intermolecular FRET distance will be discussed (Supported in part by NIH AR25193).

Tu-Pos40 TIME-RESOLVED FLUORESCENCE STUDIES OF BOVINE CARDIAC TROPONIN C AND I COMPLEX. Ronglih Liao, Chien-Kao Wang, and Herbert C. Cheung. Graduate Program in Biophysical Sciences, and Department of Biochemistry, University of Alabama at Birmingham, Birmingham, AL 35294

Using nanosecond fluoresecnce spectroscopy, we have investigated the interactions of cardiac troponin C (CTnC) and cardiac troponin I (CTnI). The results for isolated CTnC were recently reported (Wang, et al., 1988. Proc. SPIE, 909, 139). The emission decay of the fluorescence probe IAANS (2-(4'-iodoacetamidoanilino)naphthalene-6-sulfonic acid) in the binary complex (CTNC-IAANS)·CTnI was well characterized by a sum of two exponentials. At 20°C and in the absence of cations the two decay times were 2.0 and 6.9 ns. The long lived component of the emission comprised 43% of the observed amplitude. A decrease in temperature shifted the distributions of the decay components in favor of the long-component. In the prescence of Ca^{2+}, both lifetimes became longer.

The fluorescence anisotropy decay of (CTNC-IAANS)·CTnI exhibited two rotational correlation times. In the absence of Ca^{2+} and at 20°C ϕ_1~ 1.2 ns and ϕ_2~ 29.2 ns. A decrease in temperature led to a substantial increase of both correlation times and a decrease of the angular range(θ) for the rotational motion of the probes. Upon addition of Ca^{2+} to saturate all three Ca^{2+}-binding sites of CTnC in the binary complex, ϕ_1 was reduced by ~ 8%, while ϕ_2 was increased by ~ 15% with a substantial decrease in the angular amplitude (θ). In comparison with isolated CTnC, the motional freedom of the attached probe in the binary complex was more restricted. This motion was further reduced by the addition of Ca^{2+} (Supported in part by NIH AR25193).

Tu-Pos41 FLUORESCENCE PROPERTIES OF CHICKEN TROPONIN C, RECOMBINANT TROPONIN C, AND A DELETION MUTANT. Chien-Kao Wang[1], Gong-Qiao Xu[2], Sarah E. Hitchcock-DeGregori[2], Z. Dobrowolski[2], and Herbert C. Cheung[1]. [1]Dept. of Biochemistry, Univ. of Alabama at Birmingham, Birmingham, AL 35294 and [2]Dept. of Anatomy, UMDNJ-Robert Wood Johnson Medical School, Piscataway, NJ 08854

We have used fluorescent probes to compare the properties of chicken troponin C(C-TnC), recombinant TnC(R-TnC), and a mutant TnC(dKGK) in which residues 91-93 (LysGlyLys) in the helical linker were deleted (G.Q. Xu and S.E. Hitchcock-DeGregori (1988) J. Biol. Chem. 263, 13962). At pH 7.5 the relative quantum yield of dansylaziridine (DNZ) attached to Met 28 was enhanced in the presence of Ca^{2+} by a factor of 1.4 for C-TnC and R-TnC and 2.4 for the mutant protein. The fluorescence resonance energy transfer (FRET) distance, R(2/3), between DNZ at Met 28 and 5-(iodoacetamido)eosin linked to Cys 101 was 33 Å for C-TnC and 31 Å for both R-TnC and mutant dKGK. Addition of Ca^{2+} changed the respective FRET distnaces to 31, 29, and 32 Å. The probe 1,5I-AEDANS was attached to the single thiol of all three proteins and the solvent accessibility of the attached probe was determined by the steady-state method. AEDANS attached to C-TnC and R-TnC was more accessible to collisional quenching in the presence of Ca^{2+} than in its absence, whereas the opposite results were observed with the mutant protein. The anisotropy decay of the labeled proteins were resolved into two rotational correlation times. In the absence of Ca^{2+} the long correlation time of C-TnC and R-TnC was about 10 ns, and the correlation time of the mutant was 8 ns. The angular range (θ) of probe movement was 48-49° for C-TnC and R-TnC and only 39° for the deletion mutant. Ca^{2+} decreased the θ of C-TnC and R-TnC by 3-5° and that of the mutant by 1.5°. The FRET distance of R-TnC and the mutant is the same in the absence of Ca^{2+} even though the deletion of 3 residues of the central helix may shorten the molecule by 3 Å. (Supported by NIH AR25193, GM36326 and MDA).

Tu-Pos42 INTERACTIONS BETWEEN Ca^{2+} AND RIGOR CROSSBRIDGES DURING THIN FILAMENT REGULATORY STRAND ACTIVATION IN SINGLE FIBERS OF RABBIT PSOAS. PW Brandt, D Roemer and FH Schachat, Columbia U. NYC. and Duke U. Durham NC.

All 26 of the troponin-tropomyosin (Tn-Tm) complexes of a regulatory strand undergo a concerted transition from the "off" to the "on" position; this holds true whether the activating ligand is Ca^{2+} in physiological concentrations of MgATP or rigor crossbridges in the absence of Ca^{2+} (Brandt et al, JMB, 1984, 1987; Biophysical J, 1988). Evidence for the cooperative interactions between Tn-Tm complexes of the regulatory strand is found in the progressive decline of the slopes of both the pCa/tension and pS/tension curves, concurrent with troponin C (TnC) extraction (pCa = -log[Ca], pS=-log[MgATP]). To investigate the relationship between these two activating ligands, we have undertaken experiments in which skinned single rabbit psoas fibers are activated by rigor crossbridges in the presence of sub-maximally (pCa>5.5) activating Ca^{2+}. We have performed a pS/tension series in which the pCa was fixed between 6 and 6.5 while the pS was varied between 7 (rigor) and 2. To quantify the slope (n_s) and midpoint (pK_2) of the right side (pS<5) of the curve, we fit the pS/tension data to an empirical equation. Unextracted fibers activated by rigor crossbridges in the absence of Ca^{2+} (pCa>=8) have a pK_2 of 4.6, and n_s of 4.2. Both the n_s and the pK_2 progressively decrease with increasing Ca^{2+}; by pCa 6, n_s is 1 and pK_2 is 2.6. It fails to relax fully even at pS 2; to obtain full relaxation the pCa must be reduced to 8. As expected, with extraction of TnC the n_s in pCa 6 increases to values obtained at pCa 8.

Tu-Pos43 IS THE TROPONIN C CENTRAL HELIX ESSENTIAL? Z. Dobrowolski, G.-Q. Xu, and S. E. Hitchcock-DeGregori (Intr. by S. Malamed). Department of Anatomy, UMDNJ-Robert Wood Johnson Medical School, Piscataway, N.J. 08854.
A central helix connecting the two Ca binding domains is conserved in the X-ray structures of four-site Ca binding regulatory proteins. In avian troponin C (TnC) the sequence of the helical linker (res. 87-97) is KEDAKGKSEEE. To learn the functional significance of this structure we used oligonucleotide-directed mutagenesis to change its length (dEDA, dKGK, dKG, dSEEE, dKEDAKGK, and inEELAKSE at res. 95; d=deletion, in=insertion). The mutants proteins were expressed in E. coli, and purified for functional analysis (Xu and Hitchcock-DeGregori, 1988, J. Biol. Chem. 263, 13962-13969). All mutants show Ca dependent changes in electrophoretic mobility, though certain mutants differ from wildtype in the extent. The Ca dependence of the fluorescence intensity of TnC modified at Cys 101 with eosin-5-iodoacetamide (IAE) showed two transitions with midpoints ~$6x10^{-8}$M and ~$2x10^{-5}$M Ca^{2+} reflecting Ca binding to the high and low affinity sites of the protein. The fluorescence response of all the mutants was generally the same as wildtype with the exception of the insertion mutant in which the second transition was small relative to the wildtype. All mutants show Ca dependent binding to TnI as measured in urea gels and a Ca dependent increase in the monomer/excimer fluorescence ratio of pyrene-TnI as a function of Ca^{2+}. The midpoint of the transition is ~$1x10^{-6}$M Ca^{2+} and reflects Ca^{2+} binding to the Ca specific sites. The ratios in the absence of calcium of dKGK and dKEDAKGK are greater than the wildtype. The total increase in the ratios of dSEEE and insertion mutants are greater than wildtype. All mutants relieve inhibition of the actomyosin ATPase by TnI in the absence of calcium. dKGK and dKEDAKGK are more effective than wildtype, consistent with the fluorescence results. All mutants can form functional complexes with TnI and TnT though all are not equally effective. We conclude that TnC mutants with large changes in the length of the central helix (shorter or longer by two turns) or changes in the orientation of the two halves of the molecule with respect to each other retain the fundamental properties of TnC. Supported by NIH-GM36326, MDA, AHA NJ Affiliate.

Tu-Pos44 THE EFFECT OF pH ON THE Ca^{2+} AFFINITY OF THE Ca^{2+} REGULATORY SITES OF TnC IN SKINNED MUSCLE FIBERS. James D. Potter[1] and Saleh El-Saleh[2]. [1]Department of Pharmacology, University of Miami School of Medicine, Miami, FL 33101. [2]Department of Physiology, University of Cincinnati College of Medicine, Cincinnati, Oh.

The effects of pH on muscle function are well known. Lowering pH has been shown to shift the Ca^{2+} dependence of force development and ATPase activity to higher Ca^{2+} concentrations, and to lower the maximal force generated by skinned muscle fibers. The site(s) of action of protons in altering these processes is unknown. It has been proposed that the changes in Ca^{2+} dependence, brought about by pH changes, result from alterations in the affinity of the Ca^{2+} binding subunit of Tn, TnC, for Ca^{2+}. In spite of many attempts to prove this, the results on this are still equivocal and may be due to the inadequacies of the techniques used previously. To measure this directly we have selectively extracted TnC from rabbit psoas muscle skinned fibers (Zot and Potter (1982) J. Biol. Chem.) and replaced it with TnC_{DANZ}. When TnC_{DANZ} is incorporated into skinned muscle fibers, Ca^{2+} binding to the two Ca^{2+}-specific regulatory sites increases its fluorescence and this can be used as a measure of Ca^{2+} affinity. Previous studies (Robertson et al., (1978) Biophys. J., El-Saleh & Solaro (1988) J. Biol. Chem.) have shown that pH alters the Ca^{2+} affinity of these sites on TnC in solution, but the question still remained whether this also occurred when TnC was incorporated into fibers and whether this would correspond to the known changes in the force-pCa relationship. In the skinned fiber experiments reported here we show that lowering the pH from 7.0 to 6.5 shifts the force-pCa relationship as previously demonstrated and that there is a proportional shift in the affinity of the regulatory sites for Ca^{2+}. Thus these results clearly show that these sites on TnC are responsible for at least part of the changes seen in the Ca^{2+} dependence of force development. Supported by grants from the NIH, MDA and AHA-Ohio affiliate.

Tu-Pos45 INHIBITION OF TnI-TnC INTERACTION AND CONTRACTION OF SKINNED MUSCLE FIBRES BY THE SYNTHETIC PEPTIDE TnI [104-115]. J.C. Ruegg, C. Zeugner, J.E. Van Eyk, C.M. Kay and R.S. Hodges, Physiologisches Institut, Universitat Heidelberg, Heidelberg, Federal Republic of Germany and Dept. of Biochemistry, University of Alberta, Edmonton, Alberta, Canada.

Circular dichroism was used to study the induction of helix in TnC or TnI-TnC by the TnI peptide [104-115] at various Ca^{2+} concentrations. The increase in negative ellipticity and pCa^{2+} values for the peptide-TnC complex, indicates that binding of the peptide to TnC, induces a small helical conformational change in TnC which results in an increase in the Ca^{2+} binding constant and the pCa_{50} value required to induce 50% of Ca^{2+}-dependent helix in TnC. The introduction of the peptide to a preformed mixture of TnI-TnC resulted in an increase in negative ellipticity and a decrease in the pCa_{50} and the apparent Ca^{2+} binding constant towards the values obtained for the TnI peptide -TnC complex and away form those of TnI-TnC. This demonstrates that the TnI peptide can successfully compete with TnI for TnC and thereby inhibit the TnI-TnC interaction. The addition of the TnI peptide to skinned rabbit psoas or porcine cardiac fibres resulted in the inhibition of the force development and a decrease in the pCa_{50} values required for 50% Ca activation. The magnitude of the inhibition of tension development and the shift in the Ca^{2+} sensitivity for skinned cardiac muscle fibres was approximately half that observed with skeletal muscle fibres. In view of the CD findings, these skinned fibre results can be accounted for by the peptide inhibiting the TnI interaction with TnC. However, it is possible that the TnI peptide has a direct inhibitory effect on TM-actin. Mastoparan, another TnC binding peptide, also inhibited the tension development in skinned skeletal and cardiac muscle fibres, but was much less efficient than the TnI peptide, suggesting the the TnI peptide can better adopt the specific conformation required to bind to TnC.

Tu-Pos46 REACTIVITY OF CYSTEINE-84 IN CARDIAC TROPONIN C IS MODULATED BY Ca^{2+}. F. Fuchs[1] and Z. Grabarek[2]. [1]Dept. of Physiol., University of Pittsburgh Sch. Med. Pittsburgh PA 15261 and [2]Dept. Muscle Res. Boston Biomed. Res. Inst., Boston MA 02114.

Bovine heart troponin C (cTnC) contains two cysteine residues, Cys-35 located in the nonfunctional Ca^{2+}-binding loop I and Cys-84 in the N-terminal segment of the central helix. We have studied reactivity of Cys residues in cTnC with 5,5'-dithiobis(2-nitrobenzoic acid) (DTNB), the SH specific crosslinker 4,4'-dimaleimidylstilbene (DMS) and 7-diethylamino-3-(4'-maleimidylphenyl) -4-methylcoumarin (CPM). The latter two compounds fluoresce only when reacted with the protein. A relatively slow rate of reaction in the native state as compared to the urea-denatured state indicates that both Cys residues are partly buried in the 3D structure of the protein. The reactivity with all three probes is increased in the presence of Ca^{2+}. To identify the Cys residues that are affected by Ca^{2+} we have analyzed the distribution of CPM in CNBr fragments of cTnC modified in the presence and absence of Ca^{2+}. Both Cys residues are labeled at similar rates in the absence of Ca^{2+}. In the presence of Ca^{2+} the reactivity of Cys-84 is increased while that of Cys-35 slightly decreased. Our findings are consistent with the model of Herzberg et al. (J. Biol. Chem. 261,2638,1986) and the data of Ingraham and Hodges (Biochemistry 27,5891,1988) which suggest that the Ca^{2+}-induced conformational change in the N-terminal half of troponin C involves separation of the helix C from the central helix, thereby increasing the accessibility of Cys-84. Supported by grants from NIH (AM-10551, HL-05949) and American Heart Association.

Tu-Pos47 EFFECTS OF INORGANIC PHOSPHATE (Pi) ON Ca^{2+}-BINDING TO TROPONIN-C: Saleh C. El-Saleh, Dept. of Physiology and Biophysics, Univ. of Cincinnati College of Medicine, Cincinnati, OH 45267-0576.

The Pi and Proton accumulation occuring during fatigue, hypoxia or ischemia seems to correlate to a good extent with the reduction of muscle performance. Pi does not only inhibit maximal force production in muscle fibers, but it can also decrease the Ca-sensitivity of striated muscle (Kerrick and Hoar (1985) Biophys. J. 47, 296a; Kentich (1986) J. Physiol. 352, 353) and smooth muscle (Gagelman and Guth (1987) Biophys. J. 51, 457) skinned fibers. Of particular importance to this investigator is the question whether this decrease in the Ca-sensitivity of force development in striated muscle can be related to a competition between Pi and Ca-binding to Troponin-C in the thin filaments of striated muscle or whether Pi can decrease the Ca-binding to TnC via an indirect approach. Therefore, the direct effects of Pi on Ca-binding to the regulatory Ca-site(s) of skeletal (S) and cardiac (C) TnC were investigated using the fluorescently labelled derivatives of TnC: $STnC_{dans}$ and $CTnC_{iaans}$. The results show that Pi (28.5 mM) slightly desensitized the Ca-dependent binding to STnC causing a rightward shift in the pCa_{50} of 0.105 pCa units (μ = 135, pH 7.0). However with CTnC, Pi caused a rightward shift of 0.438 pCa units. This is the first reported evidence for direct influence of Pi on the regulatory Ca-binding sites of striated muscle TnC. On the other hand it seems that the degree of influence of Pi seems to depend upon interactions of TnC with other troponin subunits, mainly TnI. Preliminary data shows that STnI can amplify the Pi-induced depression of Ca-binding to the regulatory sites of STnC. Further experiments aimed at understanding the role of thin filaments in relation to the Pi effects on TnC-Ca binding is underway. Supported by a grant from the American Heart Association-Ohio.

Tu-Pos48 ***CA^{2+}-REGULATION IN RABBIT FAST TWITCH FIBERS BY LIMULUS TNC: INSIGHTS INTO THE MECHANISMS OF CA^{2+}-SPECIFIC AND CA^{2+}-MG^{2+} SITES IN VERTEBRATE MUSCLE.***

A. Babu, J. Gulati and W. Lehman, Albert Einstein College of Medicine, Bronx, NY and Boston University School of Medicine, Boston, MA.

The Ca^{2+}-specific sites in the N-terminus half of TnC trigger the contraction in vertebrate muscle, but functions of the Ca^{2+}-Mg^{2+} sites in the C-terminus half are less well defined. To gain insights into this in the fiber, recent studies have utilized the techniques whereby TnC is exchanged for calmodulin or cardiac TnC with varying properties. Since limulus TnC binds only one Ca^{2+} (Lehman et al, BBA, 434, 215, 1976), the fiber studies are extended to include this protein. Two protocols were used: (a) With approximately 70% TnC extraction (Babu et al, JBC, 262, 5815, 1987), limulus TnC was found to be completely ineffective for force recovery in 190mM salt, although it was taken up by the denuded sites in the presence of Ca^{2+}. (b) With 100% extraction (Gulati & Babu, BBRC, 151, 170, 1988), limulus TnC (with Ca^{2+}) produced a maximum of 62% force recovery in 40mM salt. On the one hand, limulus TnC behaved like calmodulin (4 total sites, all Ca^{2+}-specific) for the uptake in the fiber in that both are released in the absence of Ca^{2+}. On the other hand, it behaved as CTnC (1 trigger site and 2 Ca^{2+}-Mg^{2+} sites) in that low salt was essential to express the regulatory function. The results indicate that TnC-TnI interaction in vertebrate fiber occurs with limulus TnC despite the loss of Ca^{2+}-binding to the putative Ca^{2+}-Mg^{2+} sites. Further, the studies suggest that altered (low salt) milieu is essential to compensate for a nonfunctional trigger site. *[Supported by NIH and Heart Association.]*

Tu-Pos49 STRETCH OF ACTIVE MUSCLE DURING THE DECLINING PHASE OF THE CA TRANSIENT CAUSES BOTH INCREASED AND DECREASED CA BINDING TO INTRACELLULAR CA BINDING SITES. A.M. Gordon and E.B. Ridgway, Dept. of Physiology and Biophysics, Univ. of Washington, Seattle, WA, 98199 and Dept. of Physiology and Biophysics, Medical College of Virginia, Richmond, VA, 23298. (Intr. by D.A. Martyn)

In barnacle single muscle fibers, voltage clamped and micro-injected with the Ca specific photoprotein aequorin, muscle shortening during the declining phase of the Ca transient cause extra Ca to appear. This extra Ca is probably from the activating sites released by the change in affinity accompanying breaking of cross-bridges (Gordon and Ridgway, 1987). We now show that muscle stretches made at similar times cause a more complex, biphasic response, a positive phase consisting of a rapid increase in intracellular Ca followed by a negative phase consisting of a transient decrease in Ca. The amplitudes of both phases increase with increased stretch amplitude for stretches up to 4-5% of muscle length. Stretches performed at different times during the Ca transient produce differing ratios of the two phases. Later stretches show an enhanced positive phase, earlier stretches show an enhanced negative phase. The time course of the amplitude of the positive phase parallels the extra light seen on shortening which may sample a pool of bound Ca (Ridgway and Gordon, 1985). In fact, the amplitude of the positive phase on stretch is nearly the same as the extra light on shortening by the same distance. The time course of the negative phase of free Ca parallels the Ca transient itself. All this data is consistent with stretch increasing Ca affinity at some sites while simultaneously decreasing Ca affinity at other sites possibly due to the effects of strained versus detached cross-bridges respectively. (Supported by NIH grants NS08384 and AM35597.)

Tu-Pos50 HYBRIDIZATION OF REGULATORY PROTEINS (TROPONIN-TROPOMYOSIN) WITH CARDIAC MYOFIBRILS FROM DYSTROPHIC HAMSTERS. Ashwani Malhotra, Kirit Patel, M. Cecilia Lopez and James Scheuer, Montefiore Medical Center/Albert Einstein College of Medicine, Bronx, New York.

Studies on purified cardiac myofibrils (MF) from myopathic Syrian hamsters (M) (7-8 mo. old) suggest altered regulatory control by the troponin-tropomyosin (Tn.Tm). To investigate the control of Ca^{2+}-Mg^{2+} myofibrillar ATPase by Tn.Tm complex in M, MF and Tn.Tm were extracted from control C and M hamster hearts and also dog cardiac tissue (D). Cross hybridization studies were conducted using C or M MF with M, C or D cold or iodinated (^{125}I) Tn.Tm under soluble conditions at 0°C. Myofibrillar ATPase was determined in the absence (2.5 mM EGTA) and presence of different concentrations of free Ca^{2+} ion. Mean results of 4-6 studies for Ca^{2+}-Mg^{2+} ATPase (μ mole Pi/min/mg) and % Inhibition by EGTA are:

	C_{Mf}	M_{Mf}	M_{Mf}+C(Tn.Tm)	M_{Mf}+D(Tn.Tm)
Ca^{2+}-Mg^{2+}ATPase	0.173	0.144	0.105	0.114
EGTA ATPase	0.021	0.070	0.030	0.024
%Inhibition (EGTA)	82	52	72	79

MF from M hamsters when incubated with Tn.Tm isolated from C hamsters or from canine hearts (D) reversed the loss in calcium sensitivity. MF mixed with ^{125}I[Tn.Tm] confirmed binding of Tn.Tm in hybridized MF. Enzymatic data suggest that Tn.Tm from M has less inhibitory effect than Tn.Tm from C, diminishing the degree of calcium control MF ATPase in the hearts of cardiomyopathic hamsters.

Tu-Pos51 INTERACTION OF DNASE I WITH ACRYLODAN-LABELLED CARDIAC AND PLATELET TROPOMYOSINS.
I.D. Clark and L.D. Burtnick, Department of Chemistry, University of British Columbia, Vancouver, B.C., Canada, V6T 1Y6.

Tropomyosin (TM) from rabbit cardiac muscle and equine platelets, and a carboxypeptidase A - truncated platelet TM were labelled with the sulfhydryl-selective fluorescent reagent Acrylodan, AD [Clark & Burtnick, Arch. Biochem. Biophys. 260 (1988) 595-600]. In response to a report [Payne et al., Biochim. Biophys. Acta 883 (1986) 454-459] that DNase I can form a precipitable 2:1 complex with muscle TM, we decided to examine the effects of addition of DNase I to solutions of fluorescently labelled TM. In the presence of a 2:1 molar excess of DNase I, the emission maximum of each of the AD-labelled TMs was red-shifted about 8 nm to 522-525 nm and emission intensities at the maxima dropped about 15%. Addition of KI to each of the AD-TM samples in the presence of DNase I resulted in an increase in quenching efficiency over that observed for each AD-TM alone. Slopes of Stern-Volmer plots were 15-25% higher in the presence of DNase I. Addition of DNase I produced a 25-35% decrease in fluorescence polarization for the AD probe bound to TM. Each of these observations suggests that the fluorescent probe on each TM species studied becomes more exposed to the solvent environment upon interaction between DNase I and TM. Preliminary circular dichroism measurements in the vicinity of 220 nm are in accord with a net loss in helicity of both AD-TM and unlabelled TM samples on addition of DNase I.

Supported by the B.C. Heart Foundation and NSERC Canada.

Tu-Pos52

WITHDRAWN

Tu-Pos53 A TROPOMYOSIN FUSION PROTEIN AND ITS FACTOR X_a CLEAVAGE PRODUCT REGULATE ACTO-S1 MgATPase IN THE PRESENCE OF TROPONIN.
D. B. Stone and R. A. Mendelson, Cardiovascular Research Institute and Dept. Biochem./Biophys., University of California, San Francisco, CA 94143

A fusion protein of tropomyosin (TMFP) consisting of the N-terminal 31 amino acid residues of λ cII protein, the four amino acid recognition site for blood coagulation factor X_a and the complete chicken fast leg muscle α-tropomyosin sequence has been expressed in *E. coli* MZ1 (generously provided by A. R. MacLeod and F. Reinach) and purified by a modification of procedures for TM purification (L. B. Smillie and J. R. Pearlstone, personal communication). Characterization has been carried out in the presence of 10 mM Tris (pH 8), 25-125 mM NaCl and 2 mM $MgCl_2$. Falling-ball viscometry measurements indicate that TMFP does not polymerize in the presence of troponin (TN); however, sedimentation studies demonstrate that TMFP binds to F-actin in the presence or absence of TN. These properties resemble those of a fusion tropomyosin containing 80 amino acids of a non-structural influenza virus protein (Hitchcock-DeGregori and Heald, JBC *262*: 9730, 1987). However, in contrast to the longer fusion tropomyosin, TMFP inhibits the MgATPase of acto-S1 in a Ca^{++}-dependent manner in the presence of TN. This indicates that regulation is not prevented by an additional 35 amino acid N-terminal chain on tropomyosin. Cleavage of TMFP with factor X_a yields a product with properties similar to those of the unacetylated TM of Hitchcock-DeGregori and Heald (1987): i.e., it does not polymerize in the presence of TN, binds to F-actin only in the presence of TN, but does inhibit the MgATPase of TN-acto-S1 in a Ca^{++}-dependent manner. [Supported by grants from NIH (HL-16683) and NSF (DMB-8716091)].

Tu-Pos54 IMPORTANCE OF THE AMINO TERMINUS OF TROPOMYOSIN FOR REGULATION. Y.-J. Cho and S.E. Hitchcock-DeGregori (Intr. by F. Matsumura). Department of Anatomy,UMDNJ-Robert Wood Johnson Medical School, Piscataway, NJ 08854

Striated and smooth rat muscle α tropomyosins(TMs) were expressed in E. coli using two expression systems that produce fusion(f) and nonfusion(nf) TMs (Hitchcock-DeGregori and Heald, 1987, JBC, 262, 9730). The recombinant TMs were compared to chicken breast αα- and gizzard αβ-TMs in actin binding and ATPase activity. Fusion striated and smooth TMs showed no magnesium dependence in actin binding. They both bound well to actin at low free magnesium concentrations at which chicken breast and gizzard TMs failed to bind. The extent of the binding changed little at all magnesium concentrations tested (0.1-5.0 mM free Mg^{2+} at 10 mM NaCl). Both fTMs differed from the muscle TMs in the ATPase activity measured as a function of myosin S-1 concentrations. Unlike chicken breast and gizzard TMs, the fTMs showed slight, if any, cooperativity and were unable to activate the ATPase at any S-1 concentration tested (up to 8 μM of S-1 at 3.2 μM actin). Neither nonfusion(nf) smooth nor striated TMs had any effect on the ATPase activity, even though smooth nfTM binds well to actin, in contrast to striated nfTM. In the presence of troponin regulation of the ATPase activity by nfTMs is indistinguishable from the muscle protein. Together these results indicate that the structure of the amino terminus is crucial for the cooperative interaction of myosin S-1 with actin. The unacetylated nf smooth TM can neither inhibit nor activate the ATPase. The presence of the 80 amino acids fusion peptide on the amino terminus of the fTMs prevents myosin from switching the thin filament from the inhibited to the activated state. Supported by NIH-HL35726 and the American Heart Association.

Tu-Pos55 REMOVAL OF TROPOMYOSIN OVERLAP MODIFIES THE COOPERATIVITY OF MYOSIN S-1 BINDING TO RECONSTITUTED THIN FILAMENTS IN THE PRESENCE OF ADP. B. Pan, A.M. Gordon and Z. Luo, Department of Physiology and Biophysics, SJ-40, University of Washington, Seattle, WA 98195

It was established by Greene and Eisenberg (1980) that binding of S-1.ADP to regulated F-actin is cooperative, especially in the absence of Ca^{2+}. Hill et al (1980) demonstrated that the observations could be accounted for by a model in which the cooperativity arises from two sources: 1) simultaneous change of state of all the actins in a functional unit consisting of 7 actins and one tropomyosin(TM)-troponin(TN) complex, 2)nearest-neighbor interactions between functional units. It has been hypothesized that the end-to-end overlap between adjacent TM molecules is the structural basis of the nearest-neighbor interactions. however, experimental evidence for the proposal has been lacking. We tested the hypothesis by examining S-1.ADP binding to reconstituted regulated F-actin containing TM from which the C-terminal 11 amino acid residues were enzymatically removed (NPTM). S-1 binding was studied in the presence of 4 μM actin, 0-4.4 μM S-1, 3 mM ADP, 5 mM Mg, 50 mM KCl, 10 mM imidazole (pH 7.0), 1 mM DTT, 0.5 mM Ca^{2+} or 1 mM EGTA, at 23°C, with a procedure including ultracentrifugation and assay of S-1 NH_4/EDTA ATPase activity in supernatant. Removal of TM overlap had very little effect on S-1 binding isotherm at saturating Ca^{2+}(0.5 mM). In the absence of Ca^{2+}, substituting NPTM for TM reduced significantly the slope of the steep rising phase of the S-shaped binding curve. However, considerable residual cooperativity remained. Analysis of the binding data using the model of Hill et al(1980) suggested that removal of TM overlap abolished nearest neighbor interactions, whereas, the simultaneous change of state of 7 actins in a functional unit can account for the residual cooperativity.(Supported by NIH grants HL07403, NS07097, NS08384 and HL31962.)

Tu-Pos56 IMMUNOCYTOLOCALIZATION OF TITIN AND NEBULIN IN THE SARCOMERE OF RABBIT PSOAS CHEMICALLY-SKINNED FIBERS.

S. Pierobon Bormioli, R. Betto and G. Salviati.C.N.R.-C.S. Biologia e Fisiopatologia Muscolare,Istituto di Patologia Generale, Università di Padova - Padova, Italy.

Titin and nebulin are two gigantic proteins (M.W. 2,600 and 500 kDa) that have been suggested to form an endosarcomeric, elastic filament. In an attempt to localize the two proteins in the sarcomere we have produced monospecific polyclonal antibodies. Incubation of rabbit psoas chemically-skinned fibers at resting length either with anti-titin or anti-nebulin antibodies showed several lines of electron density in the A-band and at the A-I transition. A line in the I-band was also seen in fibers incubated with anti-nebulin antibody. In fibers that had been passively stretched to different sarcomere lengths the lines of density formed by anti-titin antibody remained at the same distance from the M line until the sarcomere length was 2.8 um. Beyond 2.8 um, the lines moved apart from the M line, but maintained constant their relative distance from M and Z lines. On the other hand, anti-nebulin labelled bands that are near the M disk in short sarcomeres seemed to move coordinately with the Z line when the sarcomere length was increased. These results indicate that titin is a component of the elastic filament which, at short sarcomere lengths,is bound to structures of the A band. On the other hand, the behavior of nebulin epitopes under stretching seems to rule out the hypothesis that nebulin is a component of the elastic filament. Work supported by Institutional funds from the Consiglio Nazionale delle Ricerche and by grant from MDA.

Tu-Pos57 RAT ATRIAL LIPID (LI) AND H_2O SOLUBLE (HI) INOSITOL (I) PHOSPHORYLATED ISOMERS: 1) MAY ORIGINATE FROM ISOMERS OF I, PLUS, 2) HAVE PHOSPHATE GROUPS (P) WITH DIFFERENT TURNOVER RATES. R. Rubio, University of Virginia, Department of Physiology, Charlottesville, VA 22908.

Double labeled LI and HI [^{3}H-myoinositol (^{3}H-MI) and ^{32}P) with increasing levels of phosphorylation were sequentially chromatographed by 5 successive steps in salt concentration. In all elution steps (1-5) there were two overlapping distinct peaks (2 "isomers"). Fraction 4 an 5 show peaks more polar than IP_3 and PIP_2. The elution patterns of ^{3}H- and ^{32}P-labeled LI and HI varied parallely. Unexpectedly, the P/H ratio (R): 1) for the "isomers" of the same fraction; one value was "low" and the other "high", 2) the R values remained constant throughout different phosphorylation levels, and 3) the R values of HI were almost 100-fold greater than R of "corresponding" LI. To test if the "isomers" may result from isomerization of ^{3}H-MI (through NAD/NADP dependent oxydo-reductases). Separate tissues were incubated with ^{3}H-acetate plus ^{3}H-glutamate or ^{3}H-MI. The chromatographic patterns obtained from ^{3}H-labeled "LI" and "IP" closely parallel those obtained with ^{3}H-MI. Sugar analysis demonstrated the production of ^{3}H-Scyllo inositol. Furthermore incubation with ^{3}H-Scylloinositol resulted in chromatographic pattern similar to those generated using ^{3}H-MI (supported by grants AHA/VA G880022 and HI 19242).

Tu-Pos58 THE REGULATION OF $[Mg^{2+}]$ IN SKELETAL MUSCLE; A ^{31}P NMR STUDY. BB. ROMAN, S.S. INGKANISORN, M.J. DAWSON, *Dept. of Physiology & Biophysics, University of Illinois, Urbana, IL 61801.*

Free intracellular magnesium concentration ($[Mg^{2+}]_i$) is maintained much lower than its thermodynamic equilibrium value, and is important in a wide variety of functional and metabolic processes. Variations in this quantity could have profound physiological or pathological consequences. $[Mg^{2+}]_i$ can be determined, after appropriate calibration and estimation of binding constants, from the position of the ß-nucleotide triphosphate peak (ß-NTP) position. While apparent variations in $[Mg^{2+}]_i$ from one tissue to another have often been reported using ^{31}P NMR, we know of no previous reports of changes in the ß-NTP position during the course of an NMR experiment. We have found that changing the $MgCl_2$ content of the bathing solution ($[Mg^{2+}]_o$) has no effect on concentrations of phosphorus metabolites or intracellular pH in isolated frog gastrocnemius muscle, but it does have a marked effect on the ß-NTP position. Apparent $[Mg^{2+}]_i$ decreased when the bathing solution Mg^{2+} was changed from 1mM to zero added magnesium, and it then increased when the $[Mg^{2+}]_o$ was raised to 25 mM. The calculated steady-state $[Mg^{2+}]_i$ varied by over 1mM, depending upon variations in $[Mg^{2+}]_o$ between 0 and 25 mM. As the $[Mg^{2+}]_o$ is raised, $[Mg^{2+}]_i$ tends to remain constant at the expense of greater osmotic work.